ED 251 317                                          SE 045 271

AUTHOR          Clark, Lenwood G., Ed.; And Others
TITLE           The Long Duration Exposure Facility (LDEF). Mission 1
                Experiments.
INSTITUTION     National Aeronautics and Space Administration,
                Hampton, Va. Langley Research Center.
REPORT NO       NASA-SP-473
PUB DATE        84
NOTE            197p.
PUB TYPE        Reports - General (140)

EDRS PRICE      MF01/PC08 Plus Postage.
DESCRIPTORS     Astronomy; *Biological Sciences; Earth Science;
                *Electronics; Lunar Research; Optics; *Physical
                Sciences; Research Methodology; *Science Experiments;
                *Scientific Research; Space Exploration; *Space
                Sciences
IDENTIFIERS     *Long Duration Exposure Facility

ABSTRACT
        The Long Duration Exposure Facility (LDEF) has been
designed to take advantage of the two-way transportation capability
of the space shuttle by providing a large number of economical
opportunities for science and technology experiments that require
modest electrical power and data processing while in space and which
benefit from postflight laboratory investigations with the retrieved
hardware. Many of the experiments are completely passive and depend
on postflight laboratory investigations for the experimental results.
The LDEF is essentially a free-flying cylindrical structure which can
accommodate 86 experimental trays mounted on its exterior; like the
space shuttle, the LDEF is reusable. This book provides descriptions
of 57 experiments from the United States and eight other countries
scheduled for the first LDEF mission on STS-13 (Space Transportation
System). Each description includes background information,
objective(s), and experimental approaches used. The disciplines
covered include materials, coatings, thermal systems, power,
propulsion, astrophysics, lunar and planetary sciences, biological
sciences, electronics, and optics. (Author/JN)

NASA SP-473

N

# THE LONG DURATION EXPOSURE FACILITY (LDEF)
## Mission 1 Experiments

## NATIONAL AERONAUTICS AND SPACE ADMINISTRATION

# THE LONG DURATION EXPOSURE FACILITY (LDEF)

## Mission 1 Experiments

Edited by

LENWOOD G. CLARK, WILLIAM H. KINARD,
DAVID J. CARTER, JR., AND JAMES L. JONES, JR.

*NASA Langley Research Center*

The use of trade names or names of manufacturers in this report does not constitute an official endorsement of such products or manufacturers, either expressed or implied, by the National Aeronautics and Space Administration.

# Foreword

The Long Duration Exposure Facility (LDEF) has been designed to take advantage of the two-way transportation capability of the Space Shuttle. Specifically, the LDEF is designed to provide a large number of economical opportunities for science and technology experiments that require modest electrical power and data processing while in space and which benefit from postflight laboratory investigations with the retrieved experiment hardware. The first LDEF mission (approximately 12 months duration) is currently scheduled for STS-13 in early April 1984, and subsequent missions are envisioned, possibly every 18 months.

The editors would like to acknowledge the contributions of all the Long Duration Exposure Facility experiment investigators who furnished the descriptive material used in preparing this document. Special thanks is also due Mrs. Glenna D. Martin of the LDEF Project Office staff for her invaluable assistance.

# Contents

)

## Science

## Electronics and Optics

# Introduction

The Space Shuttle brings a new dimension to space research, as was first demonstrated dramatically on April 14, 1981, when the gleaming black and white craft landed and rolled to a stop at Edwards Air Force Base. The Shuttle can transport payloads with ease not only to space but also from space, and the Long-Duration Exposure Facility (LDEF) has been tailored to utilize this two-way transportation capability.

Specifically, the LDEF has been designed to provide a large number of economical opportunities for science and technology experiments that require modest electrical power and data processing while in space and which benefit from postflight laboratory investigations with the retrieved experiment hardware. In fact, many of the experiments developed for the first LDEF–STS mission are completely passive and will depend entirely on postflight laboratory investigations for the experiment results.

Like the Shuttle, the LDEF is reusable, and repeat missions are planned, each with a new complement of experiments. The first LDEF mission is currently scheduled for early 1984 and subsequent missions are envisioned, possibly every 18 months.

## Description of LDEF

The LDEF is essentially a free-flying cylindrical structure. The experiments on LDEF are totally self contained in trays mounted on the exterior of the structure. LDEF can accommodate 86 experiment trays, 72 around the circumference and 14 on the two ends.

The LDEF is delivered to Earth orbit by the Shuttle. In orbit, the Shuttle remote manipulator system (RMS) removes the LDEF from the Shuttle payload bay and places it in a gravity-gradient-stabilized attitude. After an extended period in orbit, which is set by experiment requirements, the LDEF is retrieved on a subsequent Shuttle flight. The Shuttle RMS is used again during the retrieval to capture the LDEF and return it to the payload bay. (See fig. 1.)

The LDEF operation focuses on experimenters in the user community who conceive, build, and mount their respective experiments in trays for attachment to the LDEF. As LDEF has no central power or data systems, the primary interface with the LDEF which is of concern to the experimenters is the mechanical and thermal interface of the experiment to the tray. The LDEF
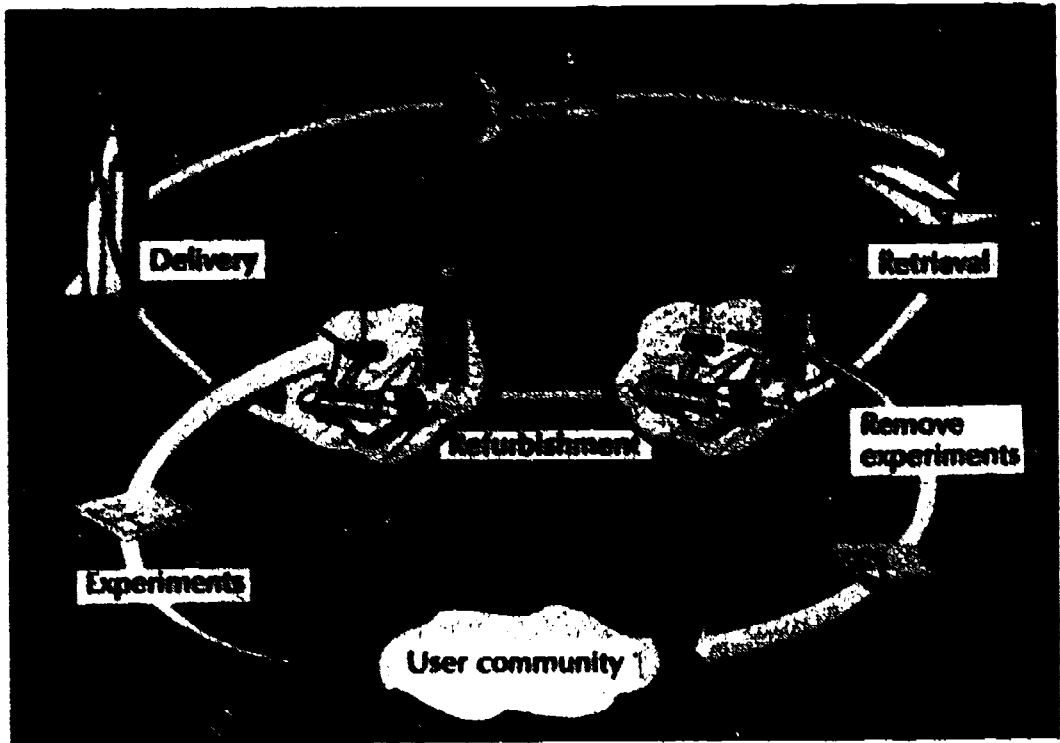
*Figure 1.—Shuttle-LDEF operations.*

does provide initiation and termination signals to experiments at the start and end of the mission. Any power and/or data systems required by the experiments are included by the experimenter in his respective tray.

Fifty-seven science and technology experiments involving investigators from the United States and nine other countries are planned for flight on the first LDEF mission. These experiments, a number of which include additional subexperiments, have been organized into four categories: (1) materials, coatings, and thermal systems; (2) power and propulsion; (3) science; and (4) electronics and optics. Each of the experiments is discussed in this document. The arrangement of these experiments on the LDEF structure is illustrated in figure 2.

Structure

The LDEF, which was built at NASA Langley Research Center, is a 12-sided open-grid structure made of aluminum rings and longerons (fore and aft framing members). (See fig. 3.) The LDEF is 30 ft long and 14 ft in diameter and weighs 8000 lb. The aluminum (6061-T6) center ring frame and end frames are of welded and bolted construction. The longerons are bolted to both frames, and intercostals (crosspieces positioned between the main rings) are bolted to the longerons to form intermediate rings. The main load of the

| Bay/Row | A | B | C | | D | E | F |
|---|---|---|---|---|---|---|---|
| 1 | A0175 | S0001 | Grapple | | A0178 | S0001 | S0001 |
| 2 | A0178 | S0001 | A0015 A0187 M0006 | | A0189 A0172 S0001 | A0178 | P0004 P0006 |
| 3 | A0187 | A0138 | A0023 A0034 A0114 A0201 | | M0003 M0002 | A0187 S1002 | S0001 |
| 4 | A0178 | A0054 | S0001 | | M0003 | S0001 | A0178 |
| 5 | S0001 | A0178 | A0178 | P0003 P0006 | A0178 | S0050 A0044 A0135 | S0001 |
| 6 | S0001 | S0001 | A0178 | | A0201 S0001 | A0023 S1006 S1003 M0002 | A0038 |
| 7 | A0175 | A0178 | S0001 | | A0178 | S0001 | S0001 |
| 8 | A0171 | S0001 A0056 A0147 | A0178 | | M0003 | A0187 | M0004 |
| 9 | S0069 | S0010 | A0134 A0023 A0034 A0114 A0201 | | M0003 M0002 | S0014 | A0076 |
| 10 | A0178 | S1005 | Grapple | | A0054 | A0178 | S0001 |
| 11 | A0187 | S0001 | A0178 | | A0178 | S0001 | S0001 |
| 12 | S0001 | A0201 | S0109 | | A0023 A0019 A0180 | A0038 | S1001 |

Trailing edge

Leading edge



Earth end (G)

A0056 A0172
A0201 A0015
M0002 A0147
S0001 A0139-A S0001

Space end (H)

S1001 M0001 A0201 A0023
M0001 A0038
S0001 A0038 A0133
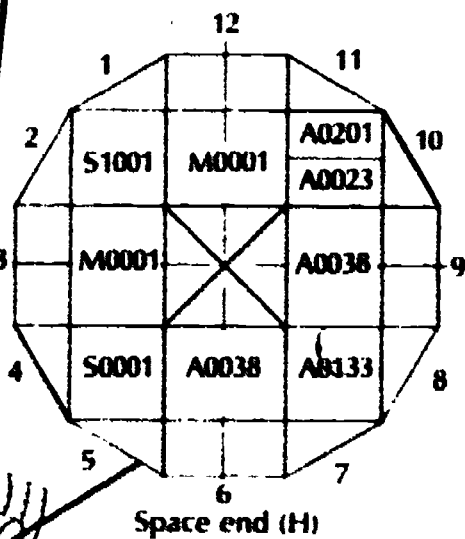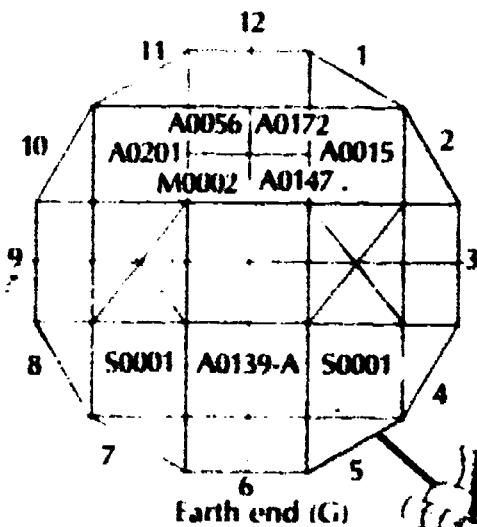
Figure 2.—LDEF experiment integration model.

11

3
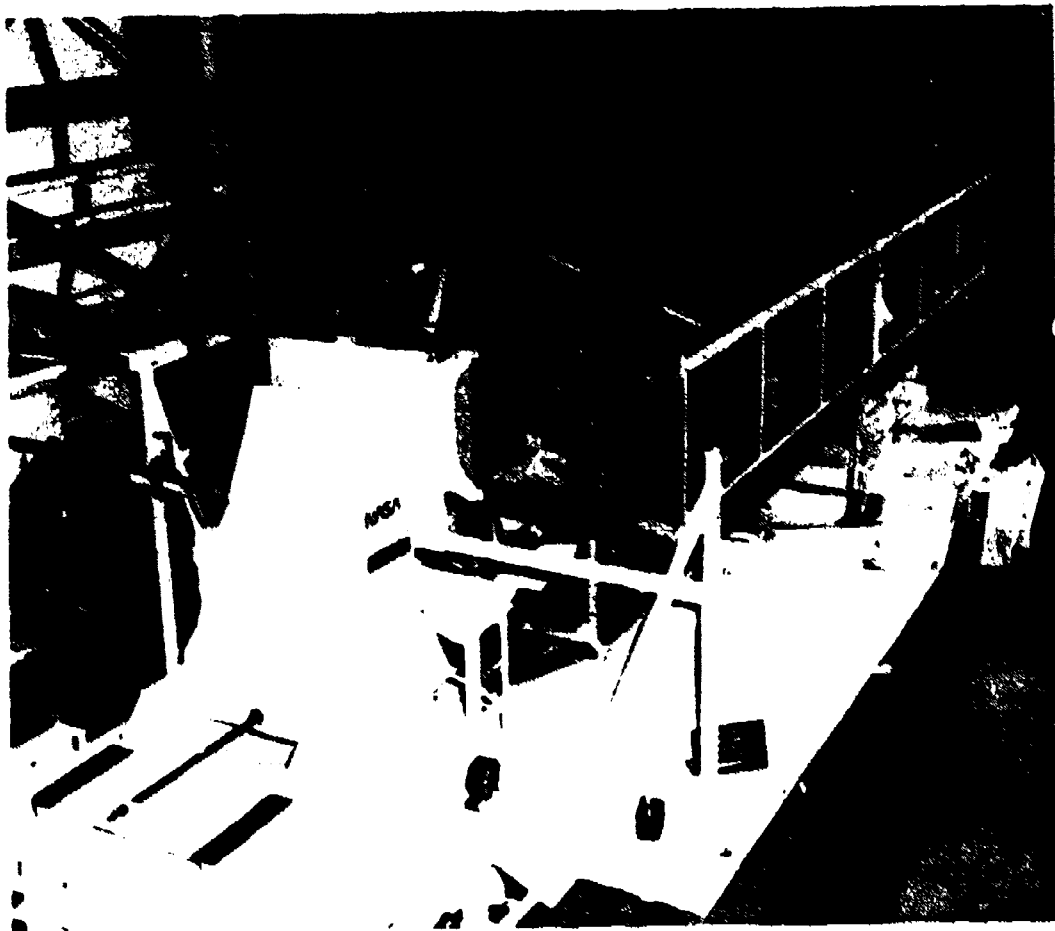
Figure 3   LDEF shown on ground transporter during final checkout before
shipment to NASA KSC

LDEF is transmitted to the orbiter through two side support trunnions on the center ring. A keel fitting on the center ring gives lateral support

The end support beam, attached by a pin joint to one end frame, will take vertical loads and ensure that loads through the attachment fittings are static The end support beam also reduces the effects of thermal distortion and other misalignments when LDEF is redeployed into the orbiter's payload bay. A fitting to allow attachment of the orbiter's remote manipulator system is located in a tray near the center ring frame.

## Experiment Trays

Typical trays for mounting experiment hardware to the periphery of the LDEF structure are 34 in. wide and 50 in. long. (See fig. 4). Trays for mounting hardware on the end frames are smaller (34 in square). The depths of the trays vary as required by the experiments. Tray depths being used on the first LDEF mission are 3, 6, and 12 in. Typical experiment weights that can be
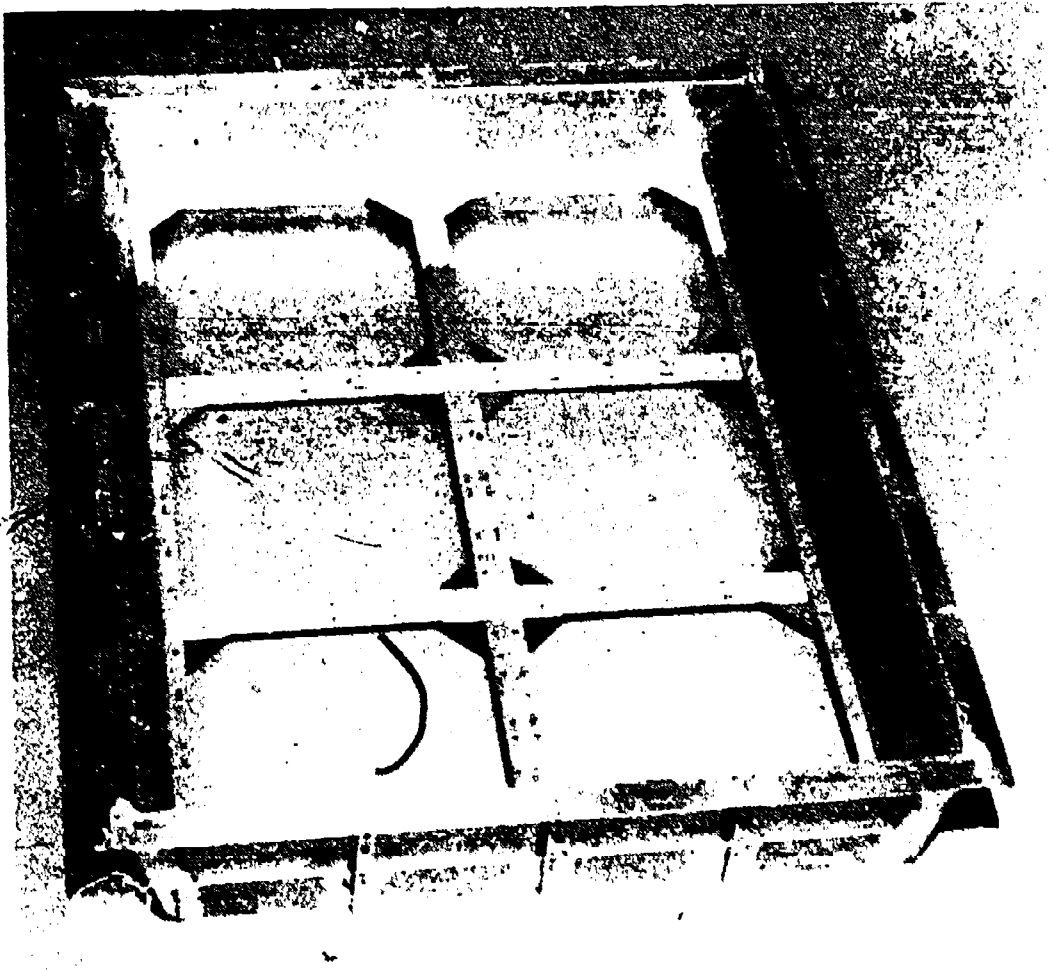
*Figure 4.—Typical LDEF experiment tray.*

accommodated in the trays range from 180 to 200 lb for the peripheral and end trays, respectively. The combined weight of the LDEF and the experiments for the first mission is approximately 21 400 lb.

## Information

For additional information regarding LDEF capability and operations, or future opportunities to fly experiments on LDEF, please contact:

William H. Kinard
LDEF Chief Scientist
Mail Stop 258
NASA Langley Research Center
Hampton, Virginia 23665
(804) 865-3704 or FTS 928-3704

5

*Materials, Coatings, and Thermal Systems*

# Growth of Crystals From Solutions in Low Gravity (A0139A)

M. David Lind
Rockwell International Science Center
Thousand Oaks, California

Kjeld F. Nielsen
Technical University of Denmark
Lyngby, Denmark

## Background

These crystal growth experiments are an extension of preliminary experiments performed during the Apollo-Soyuz Test Project flight and similar experiments being developed for a Spacelab flight. The crystal growth method to be used consists of allowing two or more reactant solutions to diffuse slowly toward each other into a region of pure solvent, in which they react chemically to form single crystals of a desired substance. This method depends on suppression of convection and sedimentation. Suppression of convection should also eliminate the microscopic compositional fluctuations often caused by time-dependent convection in crystal growth systems. In many cases, convection and sedimentation can be completely eliminated only under the conditions of continuous low gravity attained during orbital space flights. Ideally, this type of crystal growth process requires that a low level of gravity (less than $10^{-4}$ g) be maintained for a period of weeks or months. At present the LDEF flights are the only space flights planned which can fully satisfy this requirement.

## Objective

The objective of these experiments is to develop a novel solute diffusion method for growing single crystals. Crystals to be investigated are PbS, $CaCO_3$, and TTF-TCNQ. Each of these materials has current research and technological importance. PbS is a semiconductor, and $CaCO_3$ has useful optical properties; both would have many applications if they could be synthesized as large, highly perfect single crystals. The important property of TTF-TCNQ is its one-dimensional electrical conductivity. The conductivity is strongly dependent on crystal perfection; crystal growth in low gravity is expected to yield larger and more perfect crystals, which may have unique electrical properties.

The experiments are expected to yield crystals of each of the materials which are superior in size, structural perfection, and compositional homogeneity to those heretofore obtainable. The availability of such crystals

should make possible better determinations of their physical properties and, perhaps, investigations of possible device applications. The experiments should also contribute to a better understanding of the theory and mechanisms of crystal growth.

## Approach

The experiments will utilize specially designed reactors (fig. 5) with three or more compartments separated by valves to keep the reactant solutions and solvent separated until the apparatus reaches low gravity. There will be a mechanism for opening the valves automatically to initiate the diffusion and growth processes. The reactant reservoirs will be large enough to take advantage of the time provided by the LDEF flight. An array of several reactors will be mounted in a 12-in.-deep end center tray located on the Earth-facing end of the LDEF. Several reactors operating simultaneously will allow experimentation with more than one crystal growth system and/or variations of conditions for each. The reactors will be enclosed in a vacuum-tight container and will be surrounded by thermal insulation. The temperature (approximately 35°C) will be regulated and any departures from the desired temperature will be recorded. Power requirements will be provided by $LiSO_2$ batteries.
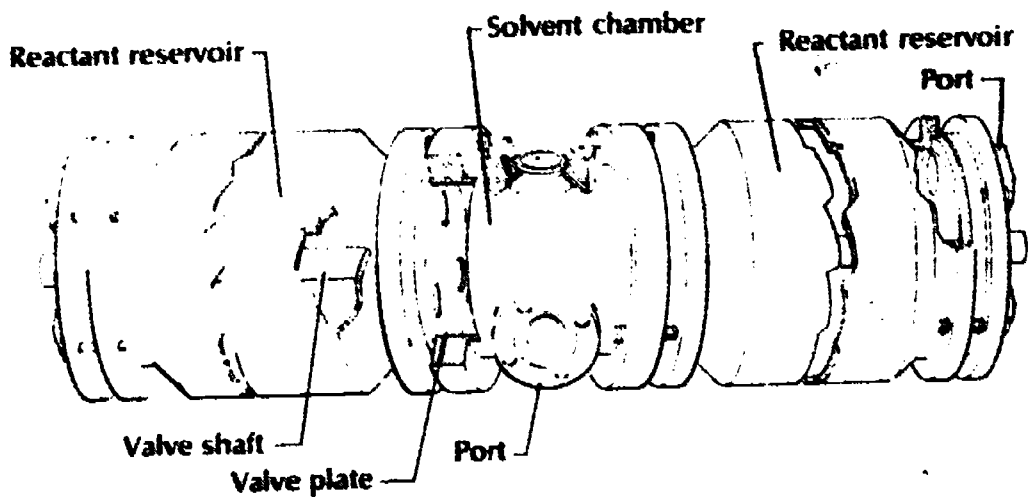


(a) Reactor configuration.

Figure 5.—Crystal growth experiment.
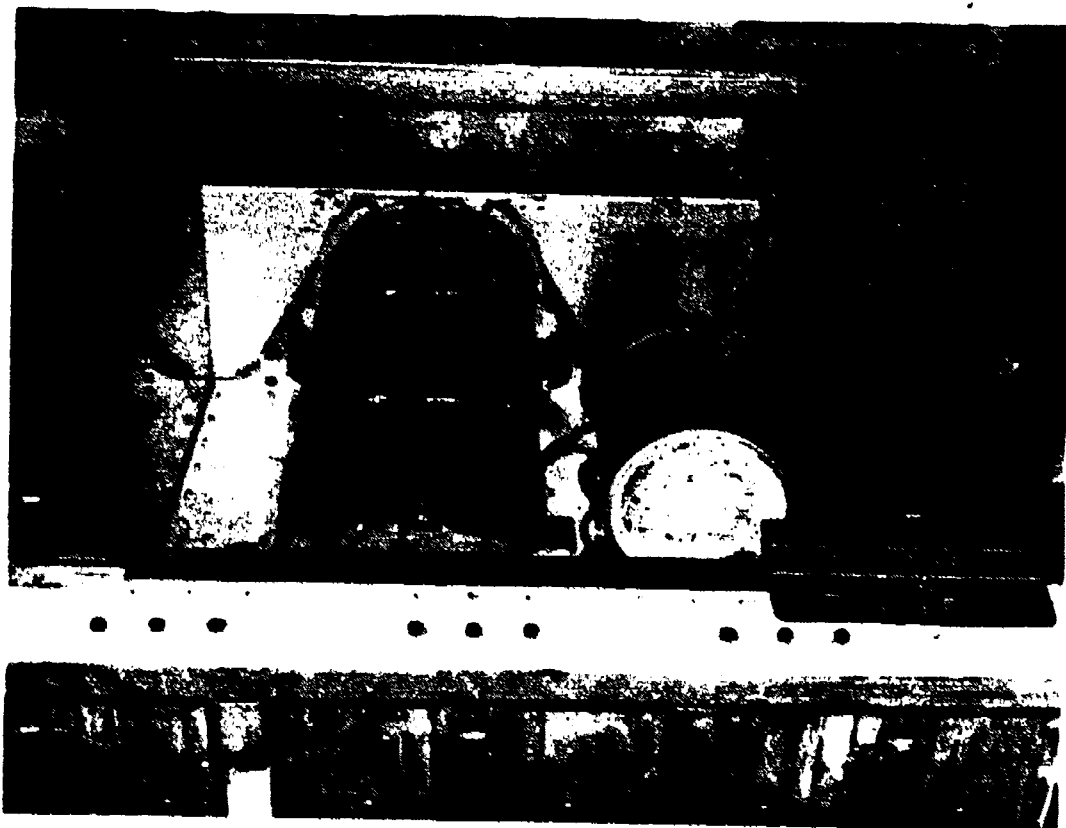
(b) Tray configuration shown without thermal cover.

Figure 5.-- Concluded.

10

17

# Atomic-Oxygen-Stimulated Outgassing
## (A0034)

Robert L. Scott, Jr.
Southern University
Baton Rouge, Louisiana

Roger C. Linton
NASA George C. Marshall Space Flight Center
Huntsville, Alabama

## Background

Many materials (e.g., thermal control surfaces) are known to produce outgassed products and possible particulate contamination when exposed to a space environment. This contamination can produce severe optical damage to the surface. It can cause an increase in surface absorption of incident radiation, thereby altering a thermal control surface, or it can cause off-axis scattering of incident radiation, thereby reducing the imaging characteristics of a specular reflector.

The NASA Marshall Space Flight Center initially became involved in the contamination problem when it investigated the potential contamination problems associated with the Apollo Telescope Mount experiments. Since then, areas of interest which have been investigated are sources, effects, and abatement of contamination; restoration of surfaces; and sizing of micron-size particles using light scatter. Thermal control surfaces, solid-rocket plume impingements, and returned Skylab specimens have been examined. The mechanisms of contaminants and synergistic effects of the space environment are not fully understood, and the results of these investigations do not show contamination damage of the magnitude observed on the Skylab mission.

## Objective

The objective of this experiment is to determine if the impingement of atomic oxygen in near-Earth orbit is a major factor in producing optically damaging outgassed products. The expected results will be to obtain samples which have been exposed to atomic oxygen for long durations. Analysis of these samples will determine if the impingement of atomic oxygen on the thermal control surfaces stimulates a significant amount of outgassed products. This experiment will give a clearer picture of the contamination problem and will assist in assuring that future Shuttle payloads, such as the Space Telescope and High-Energy Astronomy Observatory, will not experience Skylab contamination levels.

11

## Approach

Selected thermal control surfaces will be exposed to the atomic oxygen in the near-Earth orbit. Passive collecting samples will collect any induced outgassing resulting from the oxygen impingement. The optical condition of the passive samples will be measured using a ground-based integrating sphere reflectometer and a directional reflectometer.

Two packages are required, each occupying one-sixth of a 3-in.-deep tray. (See fig. 6.) One package will be positioned on the leading edge and one on the trailing edge of the LDEF. The thermal control surfaces used on Skylab, as well as newly developed surfaces, will be contained in the packages. The atomic oxygen will impinge on the thermal control surfaces contained in the leading-edge container. Passive specular collecting samples will be positioned to collect any condensable outgassed products produced as a result of the oxygen impingement. The thermal control surfaces, as well as the collecting samples, will be exposed to the available ultraviolet radiation so that environment synergistic effects can be observed. Preexposure and postexposure analysis will include total hemispherical and bidirectional reflectance measurements. The range of these reflectance measurements will be 2.5 to 2500 A. Postexposure analysis of the leading-edge samples exposed to the atomic oxygen will be compared with the control samples positioned on the trailing edge and shielded from the atomic oxygen.

Equal number
of quartz windows
and holes in top

Mirrors

Specimen
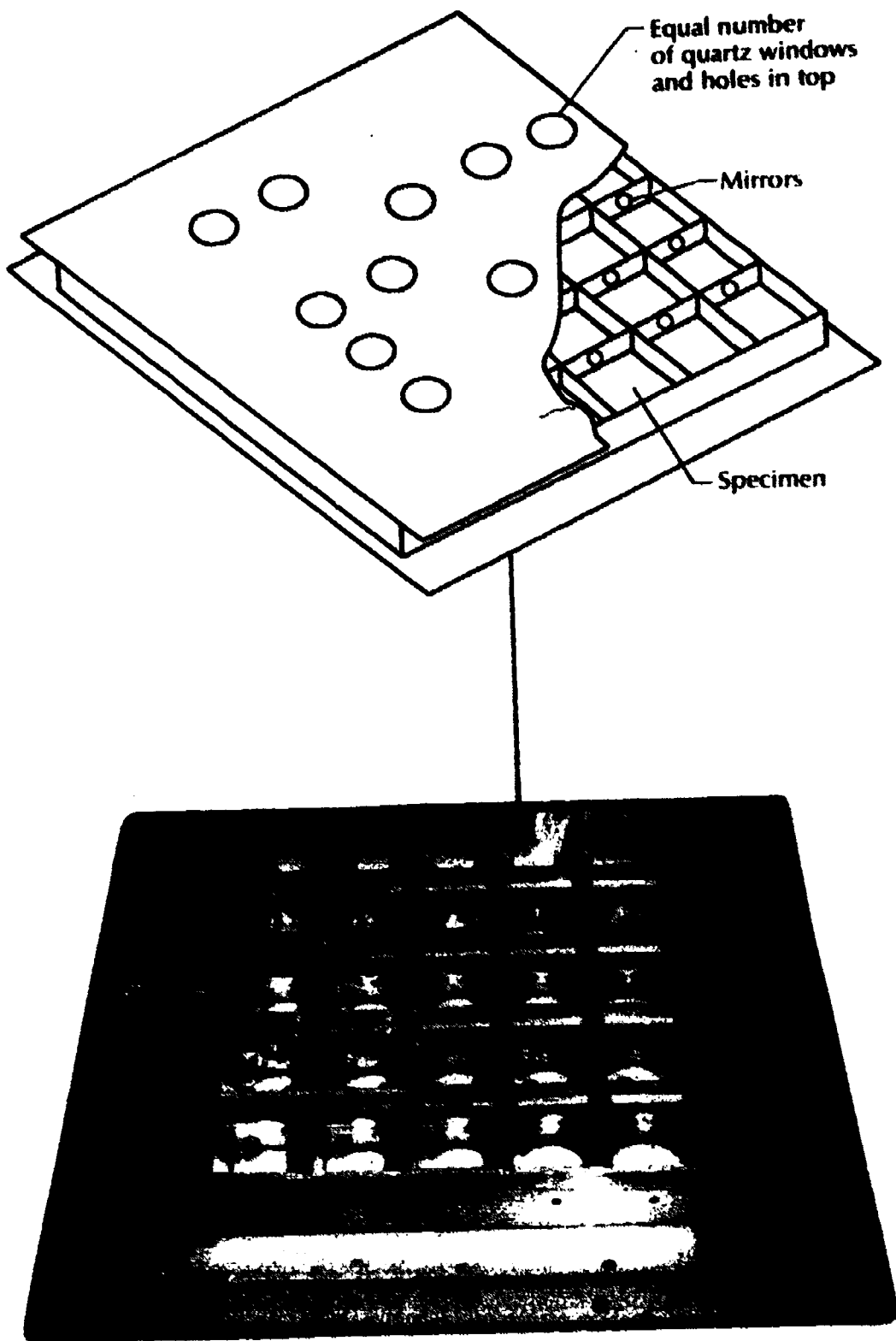
Figure 6.—Atomic-oxygen-stimulated experiment shown with top cover
removed.

# Interaction of Atomic Oxygen With Solid Surfaces at Orbital Altitudes (A0114)

John C. Gregory
The University of Alabama
Huntsville, Alabama

Palmer N. Peters
NASA George C. Marshall Space Flight Center
Huntsville, Alabama

## Background

Atomic oxygen and nitrogen are known to be extremely reactive when impinging on solid surfaces. Chemical changes can occur which alter optical and electrical properties and in some cases even remove layers of material. If the atoms impinge with the kinetic energy of orbital velocity (approximately 5 eV for atomic oxygen), the possibility of physical sputtering exists. There is, however, no experimental evidence for this because laboratory beams of sufficient flux at these energies are extremely difficult to produce.

The mechanisms for these interactions are poorly understood, and at this time it is not possible for a spacecraft designer either to allow for them or to disregard them with impunity. This experiment is designed to expose a wide variety of surfaces to the intense atom flux in orbit in order to determine the gross nature of the effects.

As a platform for this type of experiment, the LDEF is particularly well suited compared with other spacecraft which are usually designed to point or remain fixed in space. The attitude stabilization mode of LDEF results in the same surface always being presented to the ambient atmospheric flux along the velocity factor, while the opposite surface of the vehicle remains in a hard vacuum. Also, since the LDEF is passive, the contamination problems encountered on spacecraft such as Skylab from venting or leaking fluids do not exist.

## Objectives

The objectives of this experiment are to advance the knowledge of atom-surface interactions in the experimentally difficult energy range near 5 eV, to enable surface experiments to be designed for future Shuttle-era programs with greater chance of success, and to provide engineers and scientists in other areas with foreknowledge of the effects of the oxygen atom beam on critical surfaces.

14

## Approach

The basic approach to this experiment, as previously stated, is to expose a wide variety of material surfaces to the atomic flux in orbit. The experiment is passive and depends on preflight and postflight measurements of the test surfaces in the laboratory. The experiment will also include a reflectometer device to measure atomic beam reflection angles and thus momentum accommodations, and a unique passive spacecraft attitude sensor.

### Exposure of Samples

Samples consisting of solid disks or thin film coatings on substrate disks will be mounted in a panel, as shown in figure 7. The face of this panel will be flown on LDEF normal to the incident stream of oxygen atoms. Each disk will have part of its front surface masked so exposure to the atomic-oxygen reaction will be limited to selected areas, the shadowed areas being used as control surfaces in the measurements.

A typical sample is an optically flat quartz disk overcoated with a film of the material of interest. These include Ag, Au, Pt, Nb, Ni, Al, C, Si, Ge, LiF, and a few engineering materials. Some materials for which the expected removal rate is high, such as carbon, will be solid disks rather than thin films.

The experiment consists of two flight units. Each unit occupies one-sixth of a 3-in.-deep peripheral tray with one unit located on the leading edge of LDEF and the other unit on the trailing edge. The samples on the trailing-edge unit will not be subjected to atomic-oxygen impingement and will serve as control samples. A third set of control samples will be kept in the laboratory to aid in postflight analysis. To estimate the effects of contamination encountered during ascent, deployment, and descent of the Shuttle, a few samples will also be contained in an experiment exposure control canister (EECC) located with LDEF experiment S0010, Exposure of Spacecraft Coatings.

Postflight measurement techniques include step-height measurement by interferometry and surface profilometry, optical densitometry, electrical resistivity, and depth profile of chemical composition by Auger electron spectroscopy.

### Reflected Atoms

Angles of reflection of the hyperthermal oxygen atom beam are related to the extent of momentum accommodation, of which little is known at these energies. A strong forward lobe in the distribution of atomic oxygen would be detectable by sensor surfaces arrayed in the reflected beam, rather like the film in a cylindrical X-ray diffraction camera. To examine the momentum accommodation aspect, three cylindrical "reflectometers" will also be included with this experiment. (See fig. 8.) Slits in the panels and cylinders will

**22**
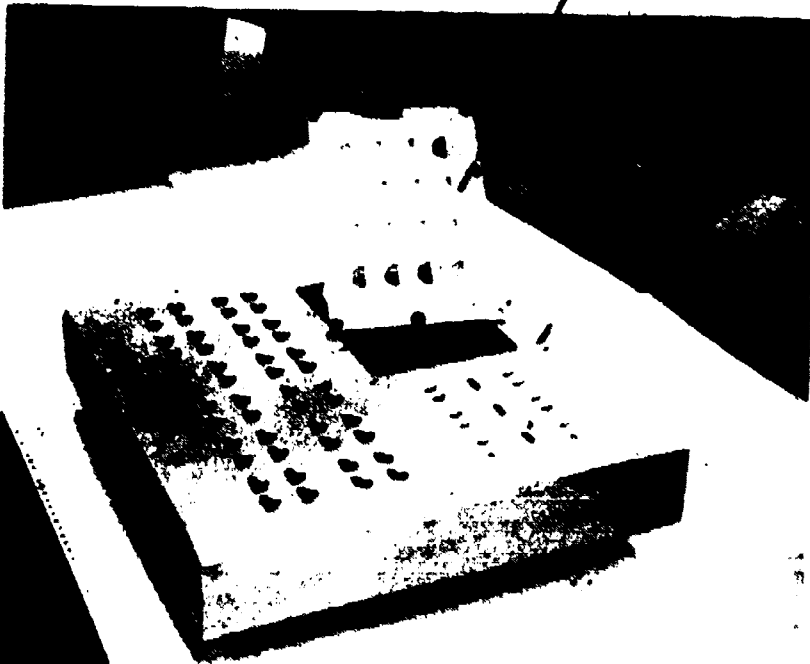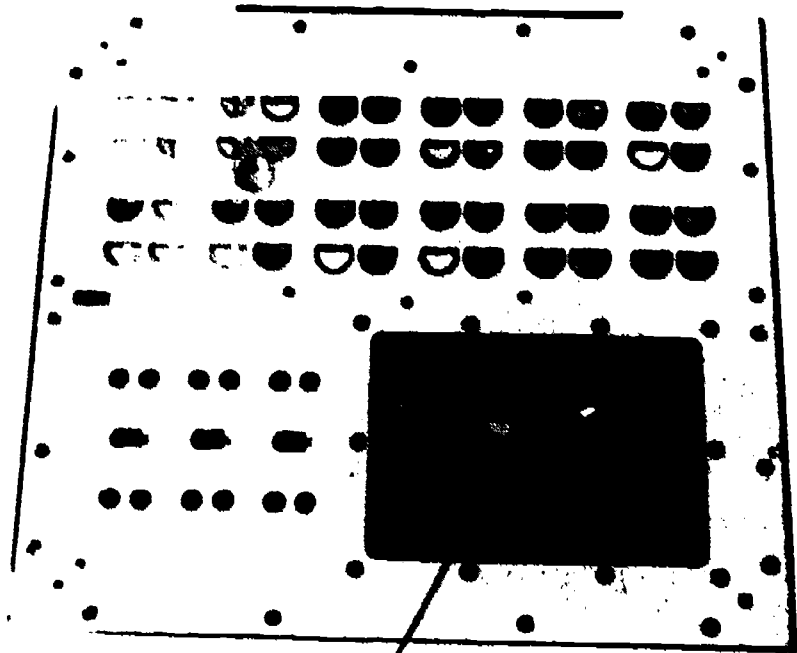
Figure 7.—Photographs of interaction of atomic-oxygen experiment showing the removable small panel which is painted black to provide a hotter surface than the main surface which is painted white.

permit a beam of atomic oxygen to impinge on a given sample at a selected angle of incident. For the first flight of the reflectometers, the objectives are limited to testing the concept of the silver film detectors and distinguishing between specular and cosine law reflectance at the sample surface. Materials chosen include LiF, stainless steel, and aluminum.

## Spacecraft Attitude Sensor

A unique passive spacecraft attitude sensor has been incorporated into each unit of this experiment to serve as a means of determining the orientation of LDEF with respect to its velocity vector. The sensor is designed to measure the angular offset of LDEF from its nominal flight attitude.
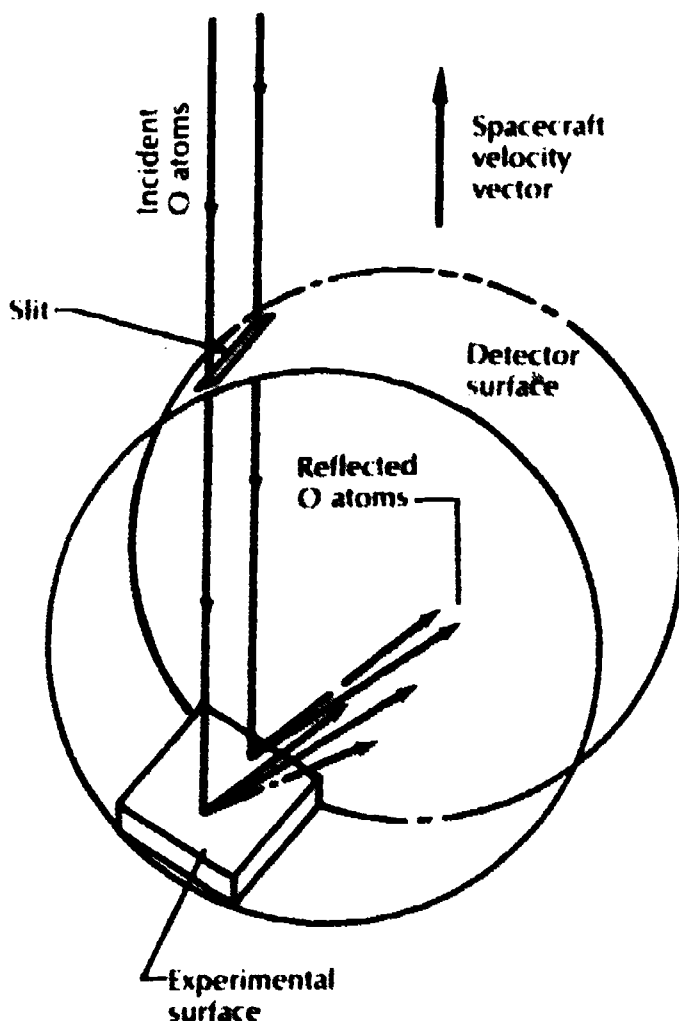
*Figure 8.—Cylindrical reflectometer configuration.*

17

As a subexperiment provided by Dr. Gerald J. Fishman of NASA Marshall Space Flight Center, a number of activation metal samples will be included with the other samples previously mentioned. After exposure to the space environment, these samples will become slightly more radioactive due to ambient proton and neutron irradiation. Upon recovery, the radioactivity will be carefully analyzed by the NASA MSFC Space Sciences Laboratory to provide measurements of the average proton and neutron fluence during the LDEF mission.

# Influence of Extended Exposure in Space on Mechanical Properties of High-Toughness Graphite-Epoxy Composite Material (A0019)

David K. Felbeck
University of Michigan
Ann Arbor, Michigan

## Background

Graphite-epoxy composites are promising candidates for structural use in space vehicles because of their high strength and elastic modulus properties. The problem of low fracture toughness has also been solved by use of recently developed techniques of intermittent interlaminar bonding. Before this material can be adapted for space use, however, confidence must be gained that its mechanical properties are not degraded by exposure to the space environment.

## Objective

The objective of this experiment is to test the effect of extended exposure to a space environment on the mechanical properties of a specially toughened T300/5208 graphite-epoxy composite material. Specimens made by recently developed techniques of intermittent interlaminar bonding will be exposed and afterward tested for fracture toughness, tensile strength, and elastic modulus.

## Approach

The approach of this experiment is to provide a frame on which the specimens can be mounted with their flat sides normal to the LDEF radius, each specimen with an unobstructed exposure of about $2\pi$ sr. The specimens will be mounted so that they neither fracture from high stress nor fail from excessive heating during launch and return. Any damage to the specimens during the orbit period must be considered to be part of the experiment.

Since the experiment is passive, nothing is required except the mechanical and thermal anchoring of the test specimens. There will be six fracture toughness specimens and nine tensile modulus specimens utilizing one-sixth of a 3-in.-deep peripheral tray. (See fig. 9.) An identical set of specimens produced at the same time will be stored in the ground laboratory for final testing at the same time as the orbited specimens. A third set of specimens produced at the same time will be tested a short time after fabrication and

19
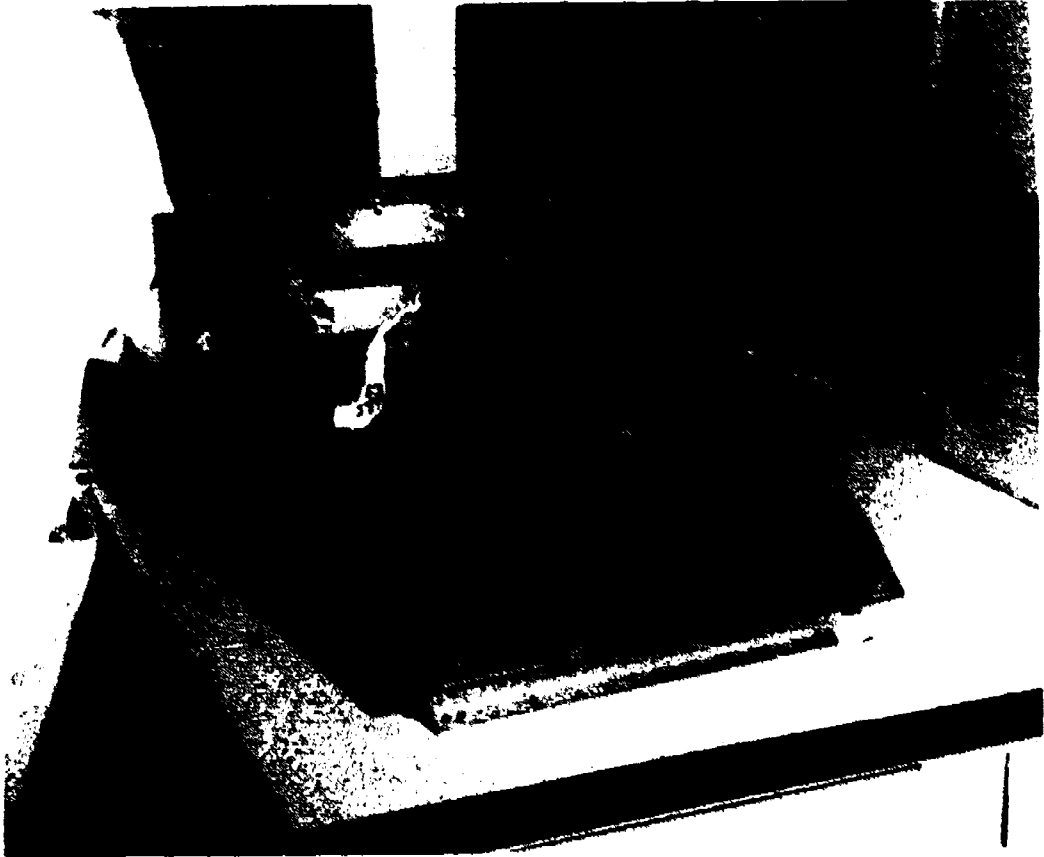
*Figure 9.—High-toughness graphite-epoxy composite material experiment.*

curing. These three sets of specimens will be used to determine the effects of time plus orbit environment, time plus ground environment, and time alone on the mechanical properties of interest.

After the specimens are tested to fracture, those of special interest will be examined by scanning electron microscopy in order to identify any changes in fracture mode or path as a result of exposure to the space environment.

# Effect of Space Environment on Space-Based Radar Phased-Array Antenna (A0133)

Richard J. Delasi, Martin L. Rossi, James B. Whiteside,
Martin Kesselman, Ronald L. Heuer, and Frederick J. Kuehne
Grumman Aerospace Corporation
Bethpage, New York

## Background

Large space structures of low areal density are currently being developed for near-term applications such as space-based radar (SBR). The practical implementation of these structures depends largely on identifying low-cost, low-density, high-strength-to-weight materials that are not degraded by the low Earth orbit (LEO) and geosynchronous Earth orbit (GEO) environments. Because of the necessity for low weight and density, candidate materials, in all likelihood, must be polymeric. However, the nature of the chemical bonds causes these materials to be susceptible to some degree of degradation from either ultraviolet or charged-particle (particularly high-energy electron) components of the space environment. In addition, for materials required to retain stiffness and dimensional stability, thermal excursions become an important factor because of creep at elevated temperatures.

Based on the performance of numerous polymeric materials following accelerated laboratory testing, Kapton polyimide film has been selected as the baseline material for the Grumman SBR concept. To gain the requisite confidence for long-term service durability, it is desirable to subject material specimens as well as a portion of the SBR antenna directly to the combined space environment and compare property degradation to that caused by laboratory simulation.

## Objective

The overall objective of this program is to evaluate the effect of the space environment on polymeric materials currently being considered for the Grumman SBR Phased-Array Antenna. Degradation mechanisms caused by thermal cycling, ultraviolet and charged-particle irradiation, applied load, and high-voltage plasma interaction will be evaluated.

## Approach

The experiment occupies a 6-in.-deep end corner tray located on the space end of LDEF and consists of both passive and active parts. The passive

part addresses the effect of environment and stress on dimensional stability of spliced and continuous Kapton, both plain and reinforced. Flight and ground-based test methodologies to measure the time-dependent deformation of large space structure materials under applied stress have been developed. Deflections on the order of $10^{-3}$ to $10^{-4}$ in./in. will be measured on 10-in.-long specimens. The specimen array shown in figure 10 contains eight 1-in.-wide specimens and sixteen 0.5-in.-wide specimens exposed directly to the space environment and a like number of "shadowed" specimens. The "shadowed" specimens will undergo limited thermal excursions and will be exposed to minimal solar and charged-particle radiation. Each specimen contains a bonded splice located so that both spliced and continuous Kapton regions can be tested after exposure. Four stress levels (30, 150, 300, and 450 psi) were selected based on the anticipated SBR antenna plane average sustained and peak local stresses. The maximum stress was selected to accelerate the extent of creep.

The active part of the experiment addresses the issue of the interaction between high voltage and low-Earth-orbit plasma. A 14- by 28-in. section of the Grumman SBR antenna (two Kapton antenna planes and a perforated aluminum ground plane) has been selected as the test specimen. The electrodes provided by copper dipole elements deposited on the Kapton plane will be held at 1 and 2 kV. A counting circuit and recently available Grumman-designed microprocessor memory using EEPROM's (a nonvolatile, electrically erasable, programmable read-only memory) will be used to record the number of electrical discharges. The experiment timer-sequencer delays the application of high voltage for 16 days and powers up the memory subsystem every 20 minutes for 0.6 second. Special testing circuitry has been included to assure proper circuit operation, and mission time scale speedup capability has been included to permit simulation of the entire flight.
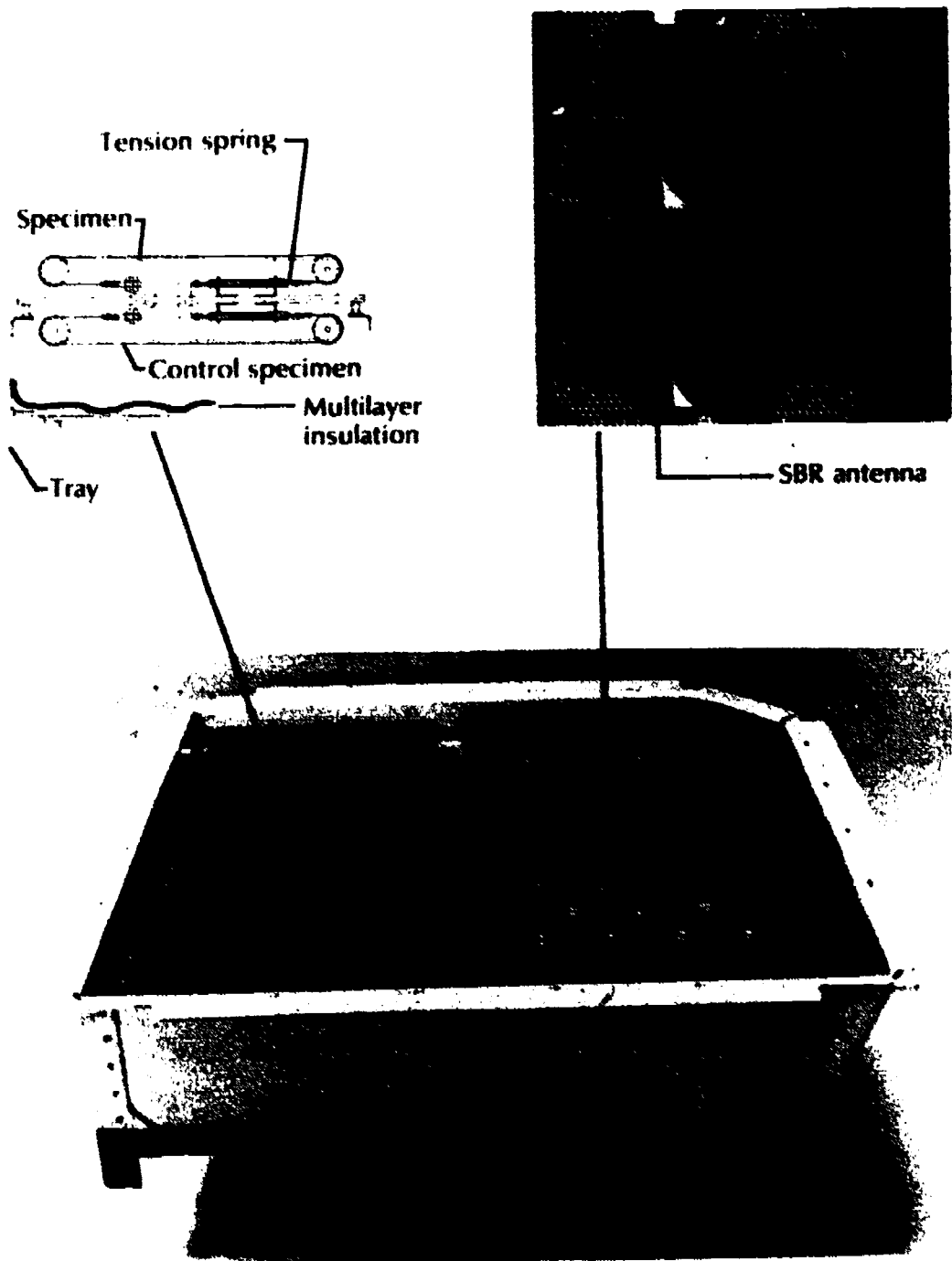
Figure 10.—Space-based radar phased-array antenna experiment.

# Space Exposure of Composite Materials for Large Space Structures
# (A0134)

Wayne S. Slemp
NASA Langley Research Center
Hampton, Virginia

## Background

As space systems become large, more complex, and expensive, they will require much longer lifetimes in space to be economically feasible. Currently these mission lifetimes are projected to be 10 to 20 years for antenna systems and up to 30 years for a solar-powered satellite system.

This requires the structural materials to perform for much longer lifetimes than those required for current spacecraft. It can be assumed that electrical or electronic systems may be replaced or repaired, but the structure should generally be maintenance free for the duration of these missions.

Resin matrix composite materials offer unique advantages over conventional metallic materials for large space system applications due to their superior strength and stiffness-to-weight ratios and their low coefficient of thermal expansion. The major problem in utilizing composites for long-term space structure applications is the absence of data on the effects of space radiation on the mechanical and thermophysical properties of these materials. Although ground laboratory testing programs are in progress, these programs are substantially impaired by lack of information on the effects of space radiation on the properties of these materials. Without a space-flight-generated data base, it is difficult to project the useful life of these materials. The same is true of other classes of materials such as polymeric films.

## Objective

The objective of this experiment is to evaluate the effects of the near-Earth orbital environment on the physical and chemical properties of laminated continuous-filament composites and composite resin films for use in large space structures and advanced spacecraft.

## Approach

The experiment is passive and occupies about one-half of a 6-in.-deep peripheral tray, as shown in figure 11. Specimens of composite materials and polymeric and resin films are arranged above and below the experiment
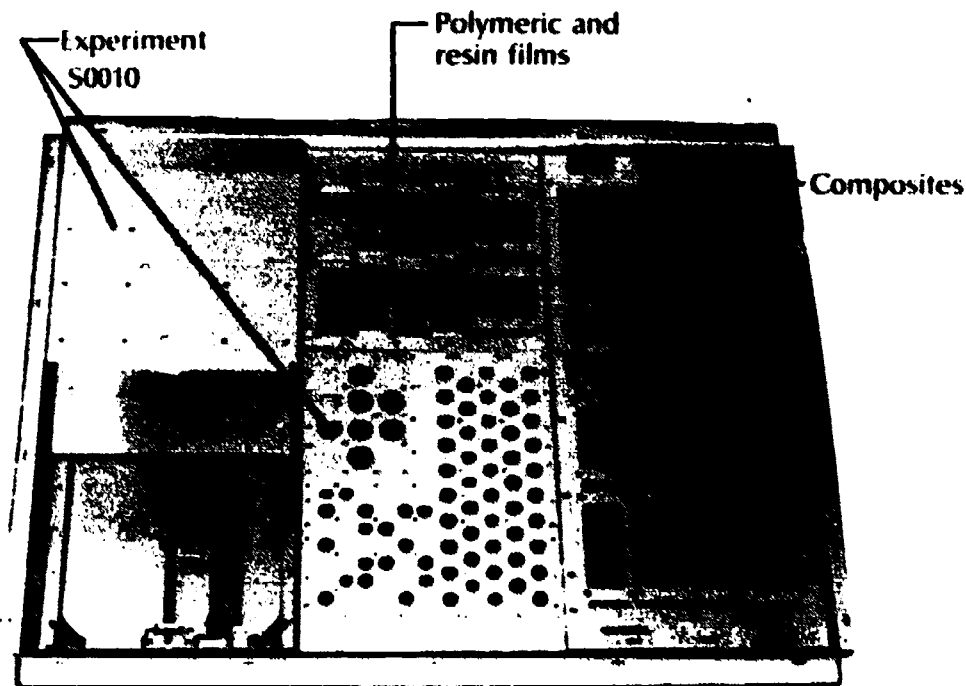
Figure 11.—Space exposure of composite materials experiment shown integrated with Exposure of Spacecraft Coatings experiment (S0010).

mounting plate to enable both exposure and nonexposure to sunlight. This provides a comparison of the effects of ultraviolet plus vacuum plus thermal cycling and those of vacuum plus thermal cycling on these materials. The experiment tray is thermally isolated from the LDEF structure to allow the material specimens to experience a wide range of thermal cycles.

Tensile and compression specimens will be used to evaluate the laminated composite materials. A number of the specimens are precut and ready for testing after space exposure, whereas other specimens will be prepared from larger samples. Both 0.005-in.- and 0.003-in.-ply thicknesses of prepreg (resin-impregnated material) will be used. The tensile specimens will be fabricated with $\pm 45°$ layup. The effects of flight exposure will be evaluated by determining the stress-strain and ultimate tensile strength before and after flight exposure. Table 1 summarizes the specific composite materials to be evaluated. Metal matrix composites are also included to evaluate the changes in coefficient of thermal expansion.

Polymeric and resin films (e.g., Mylar, Kapton, P-1700 polysulfone, and FEP Teflon) will be used to provide additional data on the behavior of polymers in space. Data will be obtained to determine the thermal stability, glass transition temperature, dynamic modulus, and loss modulus using a thermogravimetric analyzer, a thermomechanical analyzer, and a dynamic mechanical analyzer. An IR scan and an elemental analysis will also be performed before and after flight exposure.

25

**Table 1.—A0134 Composite Specimens**

| Resin and/or metal | Reinforcement |
|---|---|
| Epoxy, 5208 | Graphite, T-300 |
| Epoxy, 934 | Graphite, T-300 (0.003 in./ply) |
| | Graphite, T-300 (0.005 in./ply) |
| Polysulfone, P-1700 | Graphite, Celion 3000 (0.003 in./ply) |
| | Graphite, Celion 6000 (0.005 in./ply) |
| Epoxy, 930 | Graphite, GY-70 |
| Mg | Graphite, P-100 |
| Al | Graphite, P-100 |

A series of laboratory tests will be conducted on all materials to simulate LDEF space flight conditions. The laboratory test program will include one set of specimens exposed to UV radiation at one solar constant in $10^{-7}$ torr vacuum for 1000 hours and another set of specimens exposed to vacuum for the duration of LDEF flight exposure. These specimens will provide data to help isolate the effects of ultraviolet light, vacuum, and time on the flight specimens.

33

# Effect of Space Exposure of Some Epoxy Matrix Composites on Their Thermal Expansion and Mechanical Properties (A0138-8)

Robert Elberg
Space Division, Matra S.A.
Le Chesnay, France

## Background

Carbon and Kevlar fiber-reinforced plastic composites are being used increasingly in space structures (e.g., launch vehicles, spacecraft, payload elements such as antennas and optical benches). This extensive interest in composites is due on one hand to their mechanical properties (i.e., high strength and stiffness associated with a low density) and also to the near-zero value, positive or negative, of their coefficient of thermal expansion. This latter characteristic is due to the design of the compo, site (i.e., choice of fibers, fiber arrangement, and resin content).

A particular point that Matra wishes to examine is the effect of space environment on the thermal expansion stability of such products. The thermal expansion stability is a sensitive parameter that assures the desired performance of optical instruments such as telescopes and optical benches. This performance is related to short-term stability, which is assured simultaneously by the thermal control system and the low and stable coefficient of thermal expansion of the structure. Long-term dimensional changes that may occur (for instance, moisture desorption) are often compensated by a refocusing mechanism.

## Objectives

This experiment has three objectives. The first and main objective is to detect a possible variation in the coefficient of thermal expansion of composite samples during a 1-year exposure to the near-Earth orbital environment. A second objective is to detect a possible change in the mechanical integrity of composite products, both simple elements and honeycomb sandwich assemblies. A third objective is to compare the behavior of two epoxy resins commonly used in space structural production.

## Approach

The experimental approach is to passively expose samples of epoxy matrix composite materials to the space environment and to compare preflight

27

and postflight measurements of mechanical properties. The experiment will be located in one of the three FRECOPA (French cooperative payload) boxes in a 12-in.-deep peripheral tray that contains nine other experiments from France. (See figs. 12 and 13.) The FRECOPA box will protect the samples from contamination during the launch and reentry phases of the LDEF mission.

A list of the samples to be tested and their composition is given in table 2. Two identical samples of each type are foreseen and four different configurations of samples are used, as described in figure 14. Two common characteristics of configurations A, B, and C are the length (4 in.) and the existence at each end of the samples of three protrusions. These are the reference points for the measurement of the coefficient of thermal expansion (CTE).

The coefficients of thermal expansion are measured on Earth before and after space exposure. This measurement is based on a laser interferometry method working in a vacuum. The method used consists of forming a fringe pattern generated by two almost-parallel reflecting surfaces fastened to the test sample at the level of the protrusions and illuminated by a stabilized monomode He-Ne laser beam. Length variation due to temperature variation results in a fringe motion, which is measured. CTE measurements are made at ambient temperature with a temperature variation of about 20°C. The accuracy for a sample length of 4 in. is about $\pm 0.1 \times 10^{6}$ per °C.
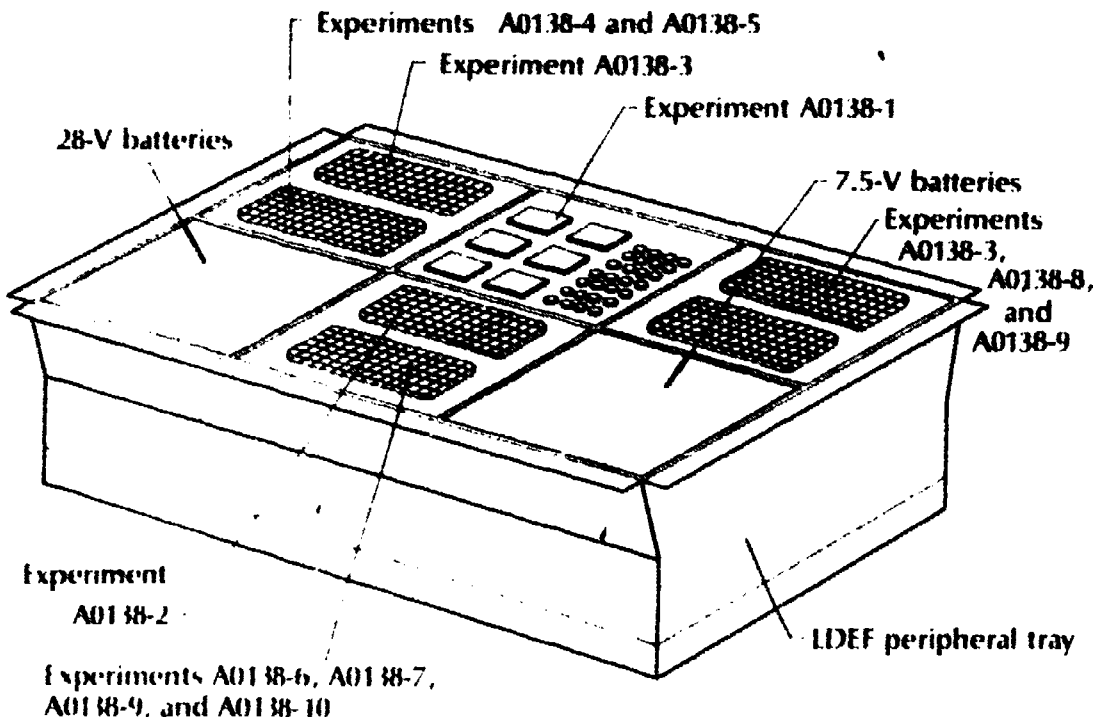


Figure 12.—Layout of French cooperative payload (FRECOPA).
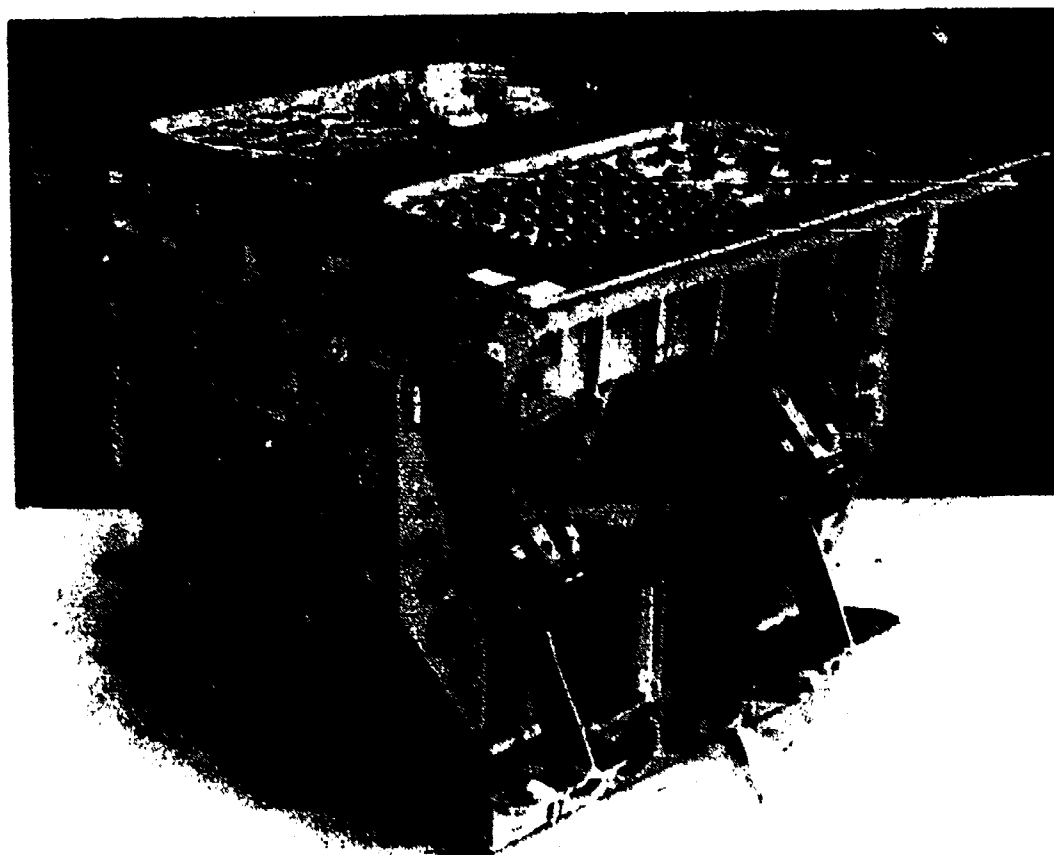
*Figure 13.—Photograph of FRECOPA box (open).*

The test program consists of the following measurements.

Weight measurements of all the samples will be made before launch (samples previously dried and outgassed) and after launch. Any weight variation will be useful information to establish the efficiency of the drying and outgassing process for composite materials.

The coefficient of thermal expansion will be measured on samples 1-1', 2-2', 3-3', 4-4', and 5-5' before and after launch. Any effect on this parameter after a 1-year exposure at ultrahigh vacuum will be detected.

Micrographic inspections will be conducted on cuts made on the various samples at the level of the composite materials and more specifically at the level of the honeycomb—face—sheet assembly on samples 2-2' and 6-6'. These photographs will be compared to similar views of identical materials kept on Earth for reference.

Mechanical tests for interlaminar shear strength, flexural strength, and flatwise tensile strength will be made on elements cut from the samples after return to Earth. These test results will be compared to results from similar samples that were not submitted to the space environment. Although vacuum chamber tests of epoxy matrix composites show good mechanical and thermal

stability, this experiment is expected to increase confidence in the performance of the tested composite specimens, particularly relative to the thermal stability.

Table 2.—List and Composition of Epoxy Matrix Composite Samples

| Reference Number | Sample Type (Shape reference[a]) | Fiber-Resin Material | Additional Material | Fiber Arrangement |
|---|---|---|---|---|
| 1-1' | Circular tube (A) | GY70/934 Unidirectional, $e^b = 0.005$ in. | None | 4 ply (4 0°/±35°/4.0°) |
| 2-2' | Sandwich: aluminum honeycomb, CFRP face sheets (B) | GY70/934 Unidirectional, $e = 0.005$ in. | Aluminum honey-comb, bond film, 312 | (0°/±60°/0°/90°/±42°), |
| 3-3' | Rectangular tube (C) | GY70/934 Unidirectional, $e = 0.005$ in. | None | (0°/±60°/0°/90°/±42°), |
| 4-4' | Rectangular tube (C) | GY70/934 Unidirectional, $e = 0.005$ in. | None | 0° |
| 5-5' | Rectangular tube (C) | GY70/V108 Unidirectional, $e = 0.005$ in. | None | 0° |
| 6-6' | Sandwich: Kevlar honeycomb, Kevlar face sheets (D) | Kevlar/V108, $e = 0.0075$ in. | Kevlar honey-comb | 2 ply (0°/90°) |

[a]Refer to figure 14.
[b]$e$ = fiber diameter.

37

30
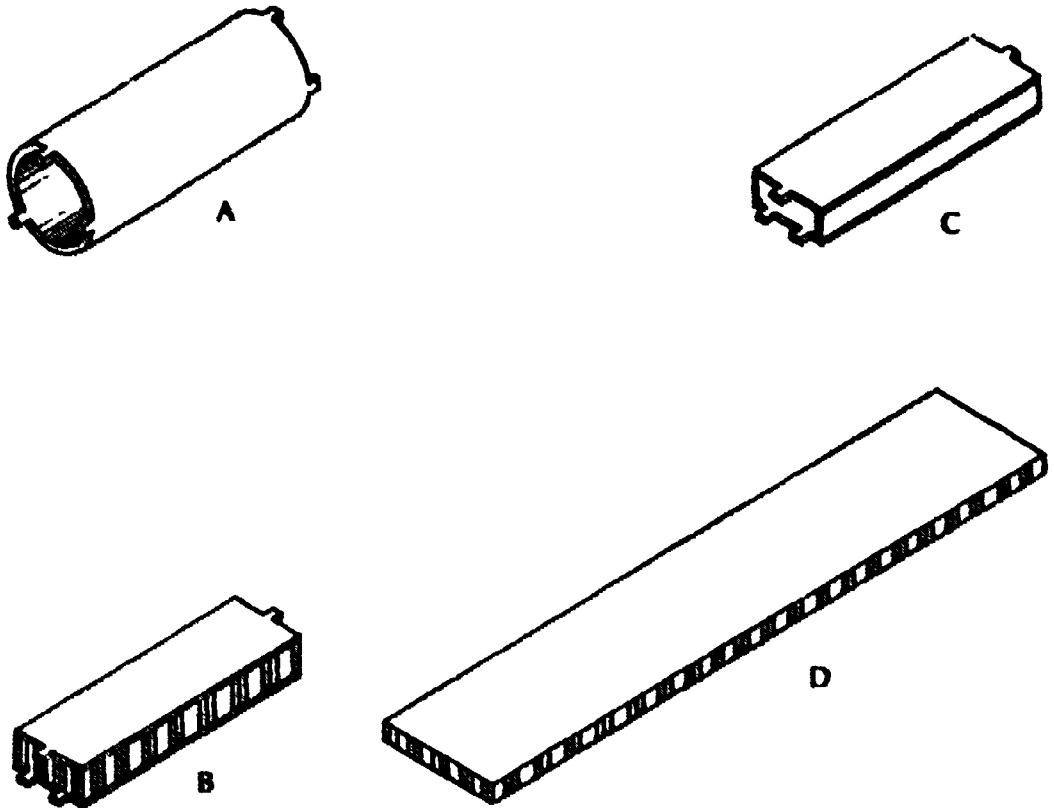
Figure 14.—Experiment A0138-8 sample configurations.

# The Effect of the Space Environment on Composite Materials (A0138-9)

Michel Parcelier
Aerospatiale
Les Mureaux, France

## Background

It is the duty of a manufacturer to verify the characteristics of the products he designs and manufactures. Until now, the space industry has complied with this rule with laboratory simulations and evaluations. The launching of the LDEF by the Space Shuttle will provide an opportunity to observe the actual behavior of materials under exposure to the space environment and will make it possible to correlate with artificial aging tests.

## Objective

The objective is to test different types of materials (laminates, thermal coatings, and adhesives) to determine their actual useful lifetime. These experiments will also make it possible to integrate the histories of the thermal and mechanical characteristics into models of the composite structures.

## Approach

The experiment is passive and is located in one of the FRECOPA boxes in a 12-in.-deep peripheral tray with nine other experiments from France. (See figs. 12 and 13.) The FRECOPA box will provide protection for the samples from contamination during the launch and reentry phases of the LDEF mission. The experiment revolves around four themes of study: thermal coatings, adhesives, dimensional stability, and mechanical characteristics.

The various materials will be arranged in six levels within the FRECOPA box, so only the first level will be subjected to direct solar radiation. (See fig. 15 and table 3.) Each level will consist of plates from which test specimens will be cut after the mission.
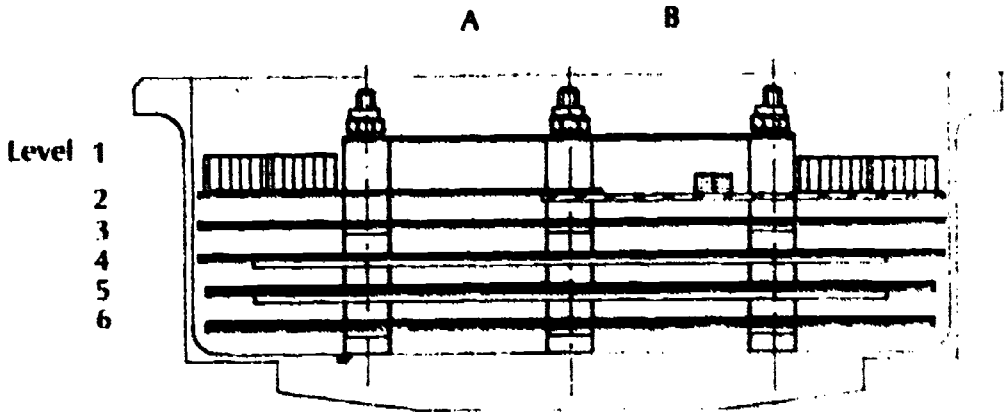
*Figure 15.—Section of FRECOPA box showing arrangement of experiment A0138-9.*

**Table 3.—Composite Materials Test Specimens**

| Level | Test specimens |
|---|---|
| 1A | OSR and SSM on graphite-epoxy composite |
| 1B | OSR and SSM on aluminum support |
| 1A | Sandwich (GY70/code 87 + BSL 312 L) |
| 1B | Sandwich (GY70/BSL 914 + BSL 319 L) |
| 2 | BSL 312 L and BSL 319 L specimens |
| 2A | Redux 408 on graphite-graphite support |
| 2B | Redux 312 L on graphite-aluminum support |
| 3A, 4A | GY70/code 87 |
| 3B, 4B | GY70/BSL 914 |
| 5A, 6A | T300/V 108 |
| 5B | GY70/V 108 |
| 6B | G837/V 108 |

## Thermal Coatings

Optical solar reflectors and second-surface mirrors will be laid on aluminum and carbon supports. The tests will evaluate the level of degradation, the mass of contaminants received, and the alteration of the thermo-optical properties.

## Adhesives

The tests will measure the shear in a joint bonded with 408 (room-temperature curing) and 312 L (high-temperature curing) adhesives. The purpose is to observe the effects of the thermal stresses due to the assembly of

33

materials having different expansion coefficients (carbon and aluminum) and the thermal cycling in the low orbit of the LDEF.

## Dimensional Stability

Tests will be carried out to verify the predicted thermoelastic deformations in sandwich structures that have withstood the space environment. Expansion tests will be made on a sandwich test specimen painted white (located on the upper level) and shaped like a satellite antenna, and also on the constituent parts taken singly. These parts are GY70/87 (0° and 90° orientation) and 312 L. The sandwich will be structured as shown in figure 16. The same experiment will be carried out on a sandwich test specimen cocured with 914 and 319 L.
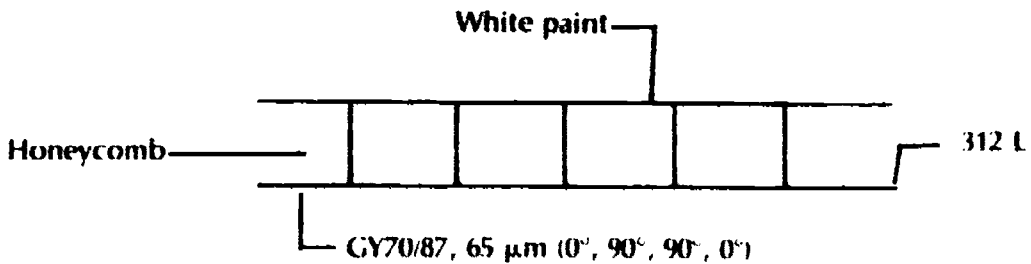


*Figure 16.—Structure of sandwich specimen.*

## Mechanical Characteristics

The degradation of the mechanical properties (tensile, flexural, and interlaminar tests) will be evaluated on the following materials: GY 70/87 (tape), GY70/914 (tape), T300/V108 (tape), and G837/V 108 (fabric).

# Microwelding of Various Metallic Materials Under Ultravacuum (A0138-10)

Jean Pierre Assie
Aerospatiale
Cannes, France

## Background

In the space vacuum environment, the spacecraft mechanisms are liable to sustain damaging effects from microwelds due to molecular diffusion of the spacecraft constituent metals. Such microwelds result in a continuing increase in the friction factors and are even liable to jam the mechanisms altogether.

## Objective

The objective of this experiment is to check the metal surfaces representative of the mechanism constituent metals (treated or untreated, lubricated or unlubricated) for microwelds after an extended stay in the space environment.

## Approach

The experimental approach is to passively expose inert metal specimens to the space vacuum and to conduct end-of-mission verification of the significance of microwelds between various pairs of metal washers. The experiment will be located in one of the FRECOPA boxes in a 12-in.-deep peripheral tray that contains nine other experiments from France. (See figs. 12 and 13.) Table 4 lists the materials to be tested and table 5 and figure 17 show the test sample arrangement and experiment layout.

**Table 4.—Experiment A0138-10 Test Materials**
[Shape: round bars]

| Type of material | Description | Condition | Applicable standard |
|---|---|---|---|
| Aluminum alloy | AZ5GU (7075) | T 7351 | ASN A 3066 |
| | AU4G1 (2024) | T 351 | ASN A 3058 |
| | A5 (1050) | H 24 | NA |
| Copper alloy | CuBe1.9 | TH2 | ASN A 3416 |
| | CuNi3Si (UN 3S) | TF | ASN A 3405 |
| Titanium alloy | TA6V | Annealed | ASN A 3307 |
| | TA6V | Quenched and tempered | ASN A 3306 |
| Stainless steel | EZ6NCT25 | Quenched for 960 MPa | ASN A 3412 |
| | Z100CD17 (440C) | Treated | ASN A 3376 |
| | Z6CNT18/11 (321) | Hyperquenched | ASN A 3140 |
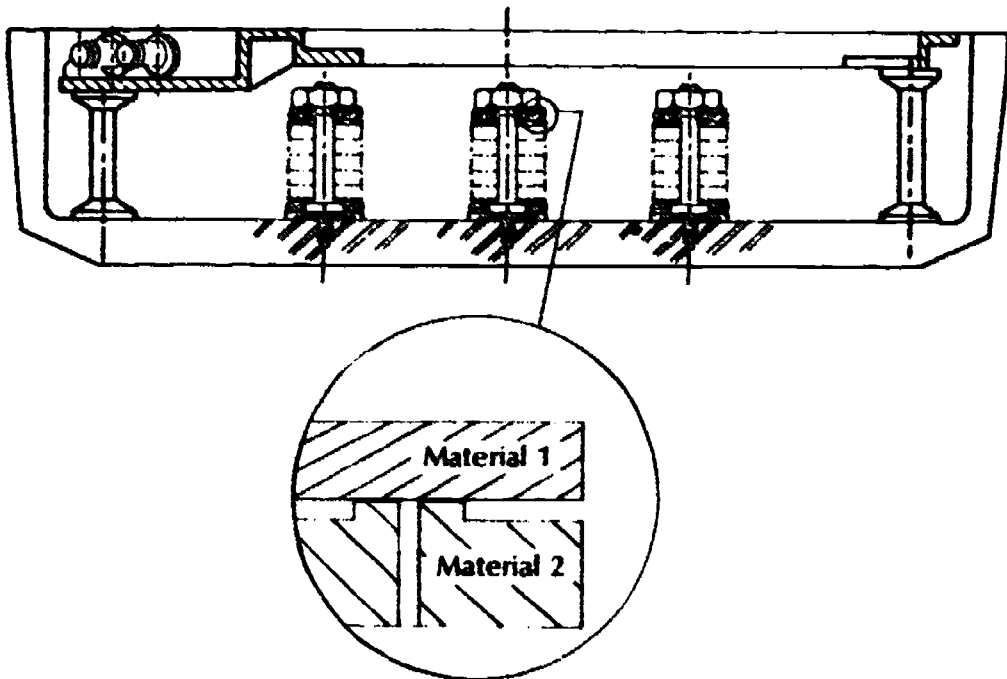


Figure 17.—Layout of the eight washer "spools" within FRECOPA box.

Table 5.—Description and Combination of Constituent Materials of Washers

| 1 | 2 | 3 | 4 |
|---|---|---|---|
| EZ6NCT25 | CuBe1.9 | AZ5GU[a] | AZ5GU |
| EZ6NCT25 | CuBe1.9 | AZ5GU[a] | AZ5GU |
| AZ5GU[a] | AZ5GU | CuBe1.9 | CuNi3Si |
| TA6V annealed[b] | TA6V annealed[b] | CuNi3Si | CuNi3Si |
| AZ5GU[a] | AZ5GU | CuBe1.9 | CuNi3Si |
| TA6V annealed | TA6V annealed | EZ6NCT25 | EZ6NCT25 |
| AZ5GU[a] | AZ5GU | TA6V annealed[b] | TA6V annealed |
| CuBe1.9 | CuBe1.9 | CuBe1.9 | CuBe1.9 |
| AZ5GU[a] | AZ5GU | TA6V annealed[b] | TA6V annealed |
| CuNi3Si | CuNi3Si | CuNi3Si | CuNi3Si |
| AZ5GU[a] | AZ5GU | TA6V tempered[b] | TA6V annealed |
| EZ6NCT25 | EZ6NCT25 | EZ6NCT25 | EZ6NCT25 |

| 5 | 6 | 7 (Analysis of influence of pressure) | | 8 (Analysis of influence of lubrication) |
|---|---|---|---|---|
| TA6V annealed[b] | Z100CD17 | P1 | CuBe1.9 | CuBe1.9/Molykote Z |
| TA6V annealed[b] | Z100CD17 | | CuBe1.9 | CuBe1.9 |
| TA6V annealed | Au on AZ5GU[c] | P2 | CuBe1.9 | CuBe1.9/Molykote Z |
| TA6V annealed | Ag on AZ5GU[c] | | CuBe1.9 | MoS$_2$[d]/AZ5GU[a] |
| Au on AZ5GU[c] | Z6CNT18/11 | P3 | CuBe1.9 | CuBe1.9/Molykote Z |
| Au on AZ5GU[c] | Z6CNT18/11 | | CuBe1.9 | MoS$_2$[d]/TA6V annealed[b] |
| Ag on AZ5GU[c] | A5 | P4 | TA6V annealed | TA6V annealed[b]/MoS$_2$[d] |
| Ag on AZ5GU[c] | A5 | | TA6V annealed | TA6V annealed[b] |
| Cr on AZ5GU | AU4G1 | P5 | TA6V annealed | AU4G1[a]/MoS$_2$[d] |
| Cr on AZ5GU | AU4G1 | | TA6V annealed | TA6V annealed[b] |
| Au on AZ5GU[c] | TA6V quenched | P6 | TA6V annealed | AU4G1[a]/MoS$_2$[d] |
| Ag on AZ5GU[c] | TA6V quenched | | TA6V annealed | AU4G1[a] |

[a]Chromium anodized.
[b]Sulfur anodized.
[c]Au and Ag are reference couples.
[d]Physical vapor deposition.

**44**

# Evaluation of Long-Duration Exposure to the Natural Space Environment on Graphite-Polyimide and Graphite-Epoxy Mechanical Properties (A0175)

J. Howard Powell and Douglas W. Welch
Rockwell International Corporation
Tulsa, Oklahoma

## Background

Graphite-polyimide and graphite-epoxy are two composite materials being used in current spacecraft construction, and both materials are being considered for more extensive use in future lightweight space-oriented structural components. The accumulation of operational data on the effects of long-duration exposure of these two materials to the multiple environmental elements of space is needed to properly evaluate them for both current and future applications. In particular, data are needed on the mechanical properties of these materials.

## Objectives

The primary objective of this experiment is to accumulate the needed operational data associated with the exposure of graphite-polyimide and graphite-epoxy material to the environments of space. Secondary objectives for testing the graphite-polyimide materials are to evaluate laminar microcracking and crack propagation and to eliminate any concerns associated with "unknowns." A specific objective of testing the graphite-epoxy material is to validate the mechanical-property "knock-down" factors that were applied to the design and analysis of the Space Shuttle payload bay doors. The assessment of the degree of matrix cracking and crack propagation phenomena resulting from differential expansion of unlike materials coupled with large thermal excursions, and the deletion of unknowns resulting from simultaneous application of multiple environmental factors relative to the payload bay door composite and adhesive system, are secondary objectives in the graphite-epoxy tests.

## Approach

The experiment will be mounted in two 3-in.-deep peripheral trays. Graphite-polyimide specimens will occupy 1⅓ trays and the graphite-epoxy specimens will occupy two-thirds of a tray, as shown in figure 18.

The experiment approach requires two matched sets of specimens with traceable records that are maintained for materials processing and specimen

Tray A1

| LaRC-160 precured | LaRC-160 precured | T300/934 |
|---|---|---|
| Graphite-epoxy honeycomb sandwich | | |

Tray A7

| F-178/T300 precured | F-178/T300 cocured | PMR-15 precured |
|---|---|---|
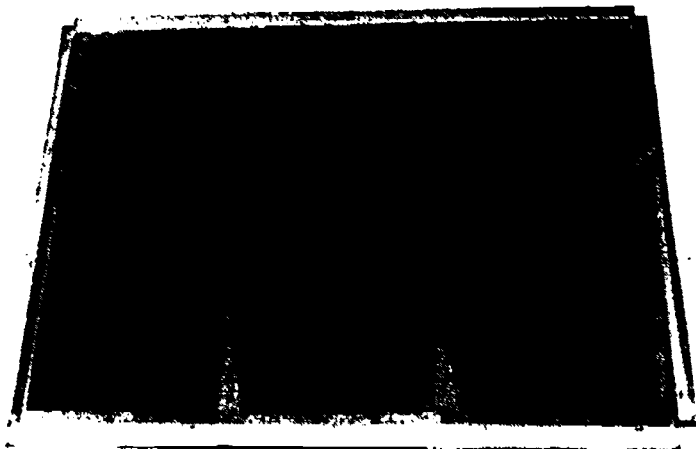
*Figure 18.—Graphite-polyimide and graphite-epoxy experiment.*

39

quality. After fabrication, one set of each test specimen will be sectioned and structurally tested to serve as a data baseline. After the LDEF flight, the other set of specimens will undergo extensive measurements of mechanical properties for comparison with the original data baseline. Figure 19 illustrates the various specimen configurations.



(a) Polyimide test specimens.

(b) Graphite-epoxy sandwich and laminate test specimens.
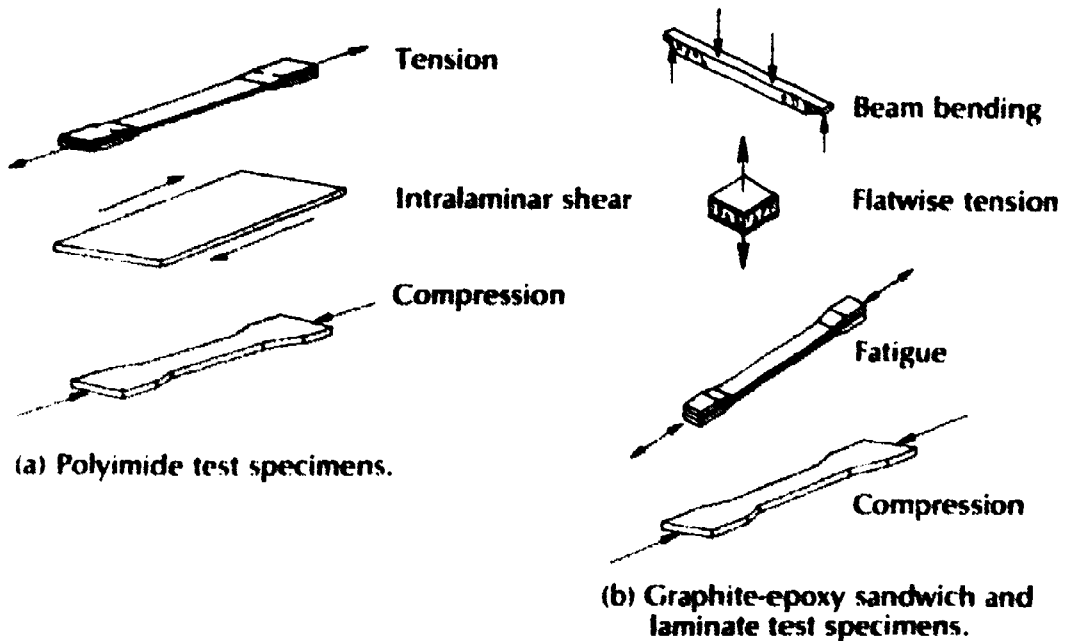
*Figure 19.—Graphite-polyimide and graphite-epoxy test specimens.*

Structural testing of the graphite-polyimide specimens will provide strength and elastic data in tension, compression, and shear. Transverse tension microcracking and crack propagation will be evaluated by photomicroscopy.

Structural testing of the graphite-epoxy specimens will include verification of laminate, core, adhesive, and fatigue properties as applied to the design and analysis of the payload bay door. Microcracking and crack propagation will also be analyzed by photomicroscopy.

47

# The Effect of Space Environment Exposure on the Properties of Polymer Matrix Composite Materials (A0180)

R. C. Tennyson and J. S. Hansen
Institute for Aerospace Studies, University of Toronto
Downsview, Ontario, Canada

## Background

The use of polymer matrix composites in various spacecraft applications is increasing, but the effects of long-term space exposure on the mechanical properties of these materials are not known. Although laboratory simulation using a thermal-vacuum chamber can be employed, the correlation between these results and actual *in situ* behavior has not been established. Consequently, such a correlation should be made in order to provide the design engineer with appropriate correction factors to take into account any degradation of material integrity due to various exposure times in space. Failure to do so will undoubtedly lead to structural failure resulting from material property changes. This can be particularly hazardous when using polymer matrix composites because molecular breakdown (due to radiation), outgassing (due to vacuum), and internal cracking, accompanied by fiber matrix separation and delamination (from thermal cycling), can result.

## Objective

The objective of this experiment is to determine the effect of various lengths of exposure to a space environment on the mechanical properties of selected commercial polymer matrix composite materials. Fiber materials will include graphite, boron, S-glass, and PRD-49. The mechanical properties to be investigated are orthotropic elastic constants, strength parameters (satisfying the tensor polynomial relation), coefficients of thermal expansion, impact resistance, crack propagation, and fracture toughness. In addition, the effect of laminate thickness on property changes will also be investigated.

## Approach

Five groups of test articles made up of laminated cylindrical tubes and flat plates will be manufactured from a given batch of prepreg (resin-impregnated) material. This will be done for each material system selected. One group from each material system will be evaluated under ambient laboratory conditions to determine (1) the orthotropic elastic constants $E_{11}$, $E_2$, $\nu_{12}$, and $G_{12}$, where E is the modulus of elasticity, $\nu$ is Poisson's ratio,

and G is the shear modulus; (2) the tensor polynomial failure parameters $F_i$, $F_{ij}$, and $F_{ijk}$; (3) the impact resistance (residual bending strength as a function of impact energy from a projectile; (4) the crack propagation and fracture toughness (measurement of growth of a given crack size in the specimen as a function of temperature and load cycling); and (5) the coefficients of thermal expansion for various laminate configurations. This evaluation will be repeated with a second group of specimens subjected to thermal-vacuum exposure in a laboratory facility. An evaluation of the effects of ultraviolet and electron beam radiation and atomic oxygen impingement will be included. The evaluation will also be repeated with a third group of specimens subjected to actual space environment onboard the LDEF. Finally, two control batches will be evaluated to assess the effects of storage environment, qualifying tests, and aging on LDEF flight articles.

The experiment will occupy one-half of a 3-in.-deep peripheral tray and is divided into three sections. (See fig. 20.) Each section consists of a layered arrangement of both tubular and flat specimens. The tubular specimens are thin walled (0.02 to 0.06 in.) and approximately 1.75 in. in diameter and 4 in.
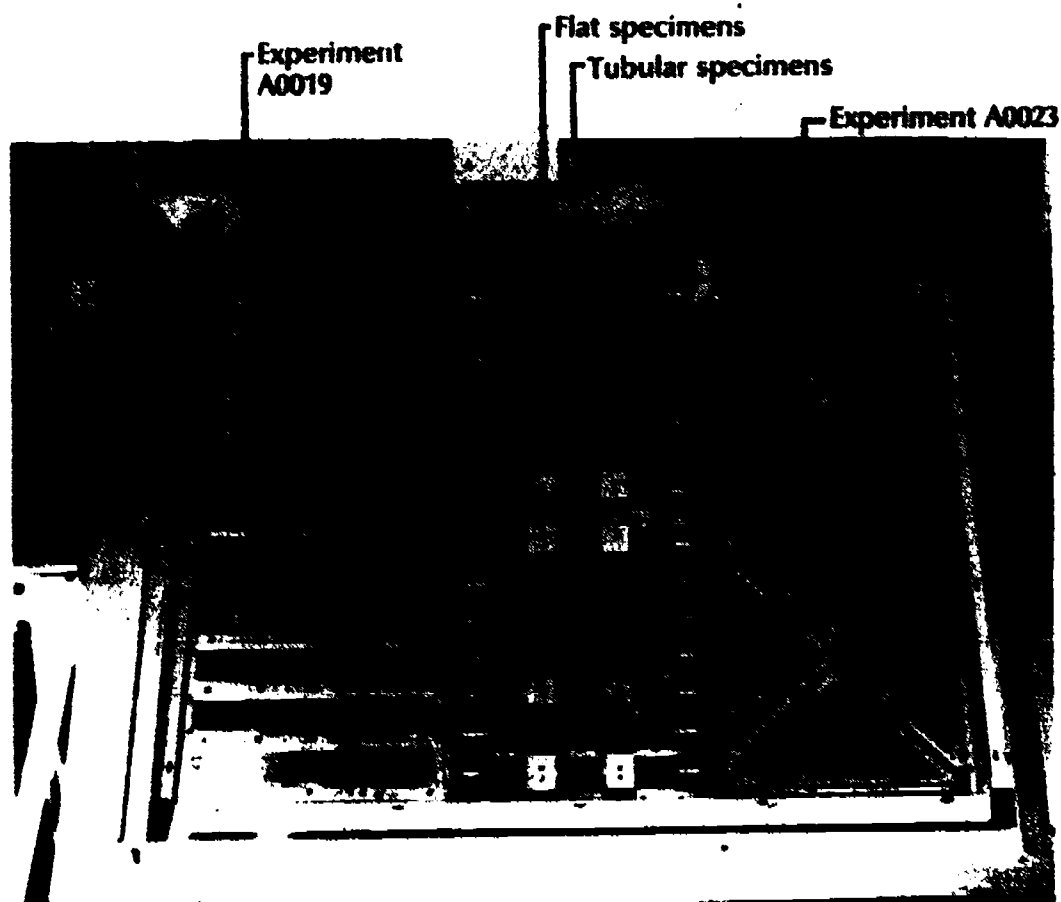


Figure 20.—Polymer matrix composite materials experiment.

42

long. The flat specimens are of similar thickness and measure 2 in. wide and 5 in. long. Aluminum end fittings (which function as test fixtures following space exposure) are bonded to each of the test specimens.

Additionally, thermal and strain gauge outputs on various composite specimens and a stainless steel calibration specimen will be sampled simultaneously approximately every 16 hours during the flight. This information will be transferred to a cassette deck for serial recording within a sealed electronics box beneath one of the experiment sections. (See fig. 21.) Two LiSO$_2$ batteries are required for data recording power and are located beneath the remaining two experiment sections.
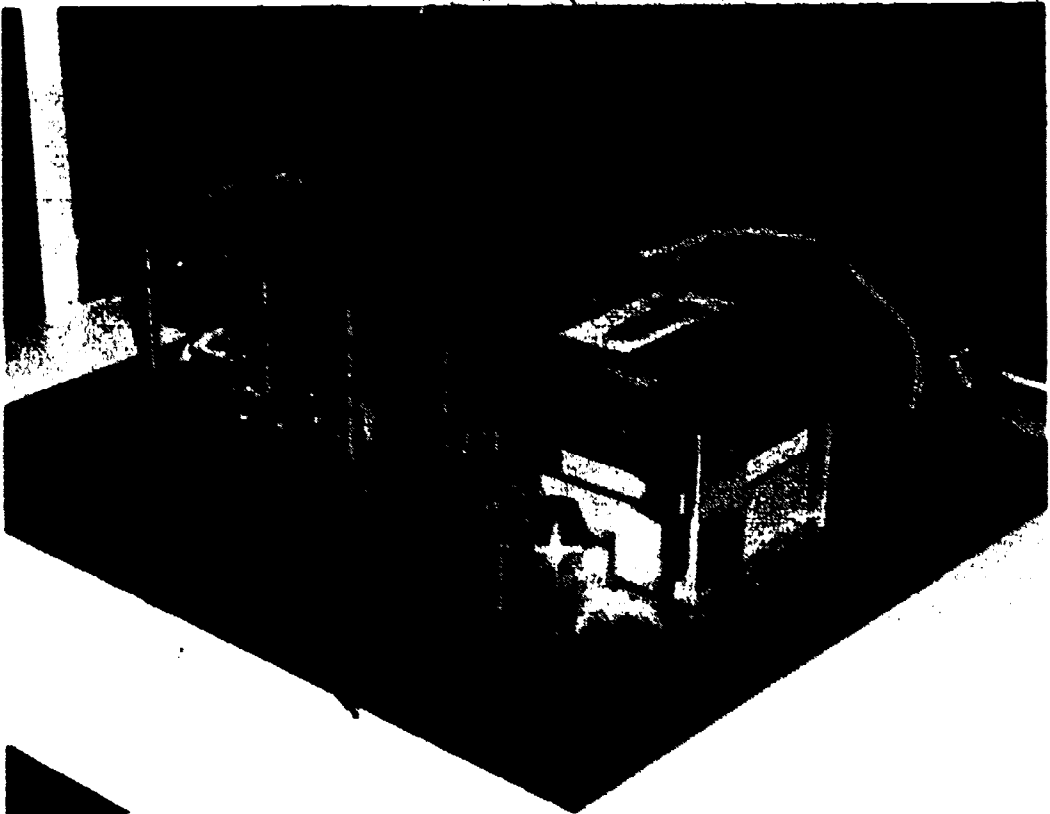


Figure 21.—Data measurement system.

# Space Environment Effects on Spacecraft Materials (M0003)

Paul Schall
The Aerospace Corporation
El Segundo, California

## Background

Data on materials for unmanned NASA and DOD spacecraft have been valuable, but are limited to those items that can be monitored remotely. Causes of failures or performance degradation can often only be inferred from the telemetry data. The Gemini and Apollo missions included some materials experiments. The return of components from the Surveyor III lunar lander was particularly interesting. The NASA Skylab missions contained a thermal control materials experiment; however, the early Skylab problems resulted in contamination that affected results. Although data from unmanned spacecraft will continue to be used to evaluate the performance of materials in space, the LDEF adds a new dimension to space experiments.

The LDEF provides experimenters with an opportunity to recover specimens that have been exposed for long periods in space. The typical approach for the selection of materials for use in spacecraft has involved laboratory testing and limited measurements in space. Although many materials appear to be satisfactory for a variety of applications, there is insufficient knowledge of the physical and optical properties of these materials after long periods in space. Laboratory tests do not simulate the actual space environment; therefore, it is difficult to predict property changes as a function of environment exposure.

In addition to measuring changes in the macroscopic properties of the returned specimens, microstructural properties will also be examined. Thus, it may be possible to increase our understanding of the changes induced by the environment. This increased understanding can then be used to predict the performance of materials based on knowledge of the space environment and the results of laboratory tests.

This experiment will be a cooperative effort and will provide an opportunity for DOD space programs and laboratories to evaluate materials and components after long exposures to the space environment.

## Objectives

The immediate objectives of this experiment are to understand changes in the properties and structure of materials after exposure to the space environment and to compare these changes with predictions based on labo-

ratory experiments. The longer term objectives are to improve the performance and usage of existing materials and to decrease the lead times for application of new materials on DOD space systems.

## Approach

The experiment consists of 19 subexperiments involving a number of DOD laboratories and contractor organizations. (See table 6.) In general, the experimental approach with each of the subexperiments will involve comparison of preflight and postflight analyses. Typical analyses will include the measurement of optical properties (reflectance, transmittance, and refractive index), macrophysical properties, and microstructural properties.

Table 6.—Experiment M0003 Summary

| Sub-experiment number | Scope | Experimenter | Organization |
|---|---|---|---|
| 1 | Radar camouflage materials and electro-optical signature coatings | Gary Grider | AFWAL Avionics Laboratory |
| | | Edward L. Pelton | AFWAL Avionics Laboratory |
| 2 | Laser optics | Alan F. Stewart | Air Force Weapons Laboratory |
| | | Arthur H. Guenther | Air Force Weapons Laboratory |
| 3 | Structural materials | Charles Stein | Air Force Weapons Laboratory |
| 4 | Solar-power components | Joseph F. Wise | AFWAL Aeropropulsion Laboratory |
| | | Kenneth Masloski | AFWAL Aeropropulsion Laboratory |
| 5 | Thermal control materials | William L. Lehn | AFWAL Materials Laboratory |
| | | J. Sierchico | AFWAL Materials Laboratory |
| 6 | Laser communication components | Ismael Otero | Air Force Space Division |
| | | Steven G. Rockholm | McDonnell Douglas Astronautics Co. |
| | | R. M. F. Linford | McDonnell Douglas Astronautics Co. |
| 7 | Laser mirror coating | Terry M. Donovan | Naval Weapons Center |

**Table 6.—Concluded**

| Sub-experiment number | Scope | Experimenter | Organization |
|---|---|---|---|
| – 8 | Composite materials, electronic piece parts, and fiber optics | Morton Kushner | Boeing Aerospace Co. |
| | | Leo P. Buldhaupt | Boeing Aerospace Co. |
| – 9 | Thermal control materials, antenna materials, composite materials, and cold welding | Norman H. Kordsmeier, Jr. | Lockheed Missiles & Space Co. |
| | | Robert Bragg | Lockheed Missiles & Space Co. |
| –10 | Advanced composite materials | David A. Roselius | AFWAL Flight Dynamics Laboratory |
| | | Gary L. Steckel | The Aerospace Corp. |
| –11 | Contamination monitoring | Eugene N. Borson | The Aerospace Corp. |
| –12 | Radiation dosimetry | Eugene N. Borson | The Aerospace Corp. |
| –13 | Laser-hardened materials | T. A. Hughes | McDonnell Douglas Astronautics Co. |
| –14 | Quartz crystal microbalance | Donald A. Wallace | Berkeley Industries |
| –15 | Thermal control materials | Thomas A. Park | The Aerospace Corp. |
| –16 | Advanced composite materials | Camille A. Gaulin | The Aerospace Corp. |
| | | Jim G. Gee | The Aerospace Corp. |
| –17 | Radiation dosimetry | Sam S. Imamoto | The Aerospace Corp. |
| | | J. Bernard Blake | The Aerospace Corp. |
| –18 | Thermal control coatings | Genevieve C. Denault | The Aerospace Corp. |
| –19 | Electronic devices | James Ewan | The Aerospace Corp. |
| | | Douglas H. Phillips | The Aerospace Corp. |

The experiment consists of four peripheral trays, two experiment power and data systems, two experiment exposure control canisters, and $LiSO_2$ batteries to satisfy power requirements. The trays and EECC's will be used to

retain a variety of thermal control coatings, composites, laser optics electronic piece parts, fiber optics, solar cells, and LDEF experiment M0002-1.

A 6-in.-deep tray, a 3-in.-deep tray, a data system, and an experiment exposure control canister will be located near the LDEF leading edge with the trays connected by a wiring harness. A similar configuration will be located near the LDEF trailing edge. Environmental exposure to the two locations will be similar except that the leading-edge location will also be exposed to relatively high fluxes of atmospheric constituents (primarily atomic oxygen). Figure 22 shows photographs of two of the experiment trays.

The experiment is equipped to record temperature, strain, and solar-cell output voltage. These data will be recorded approximately every 107 hours (approximately 78 orbits) for the duration of one orbit. The EPDS will be programmed to record data periodically over a span of up to 15 months. Both EECC units will be programmed to open in three stepped increments to vary the UV exposure times. The first opening will occur approximately 10 days after deployment, to minimize contamination. The second stepped opening will occur at approximately one-third of the expected minimum flight duration. The third stepped opening will occur at approximately two-thirds of the expected minimum flight duration. Prior to LDEF retrieval, the EECC units will close to provide protection from contamination during retrieval operations.
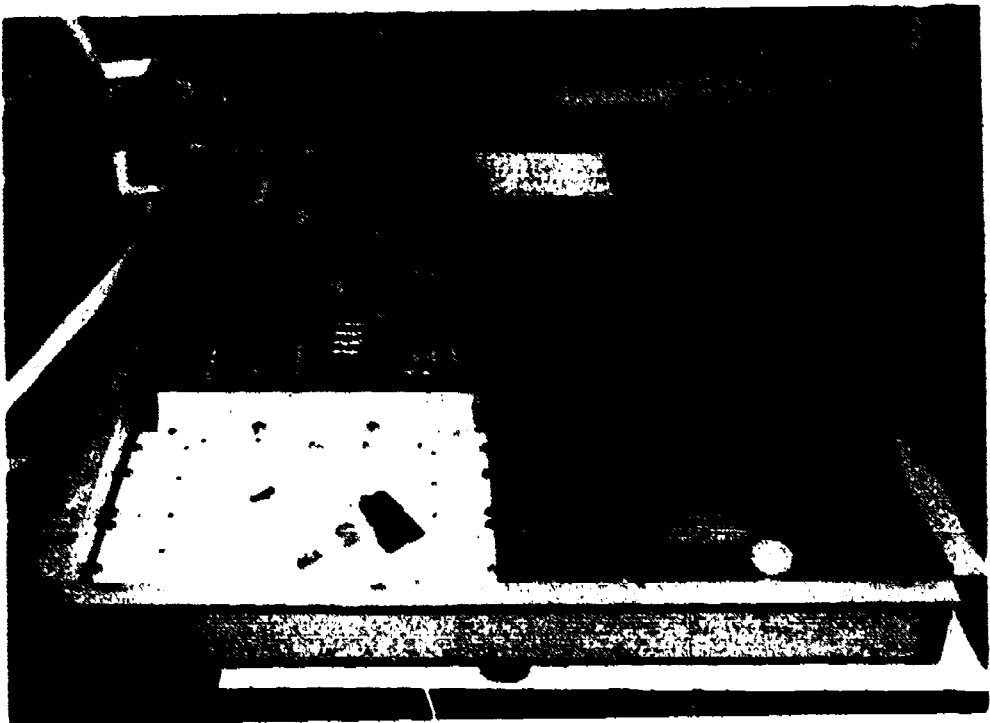


(a) Leading-edge tray, 3 in. deep.

*Figure 22.—Experiment M0003 flight configuration.*

47
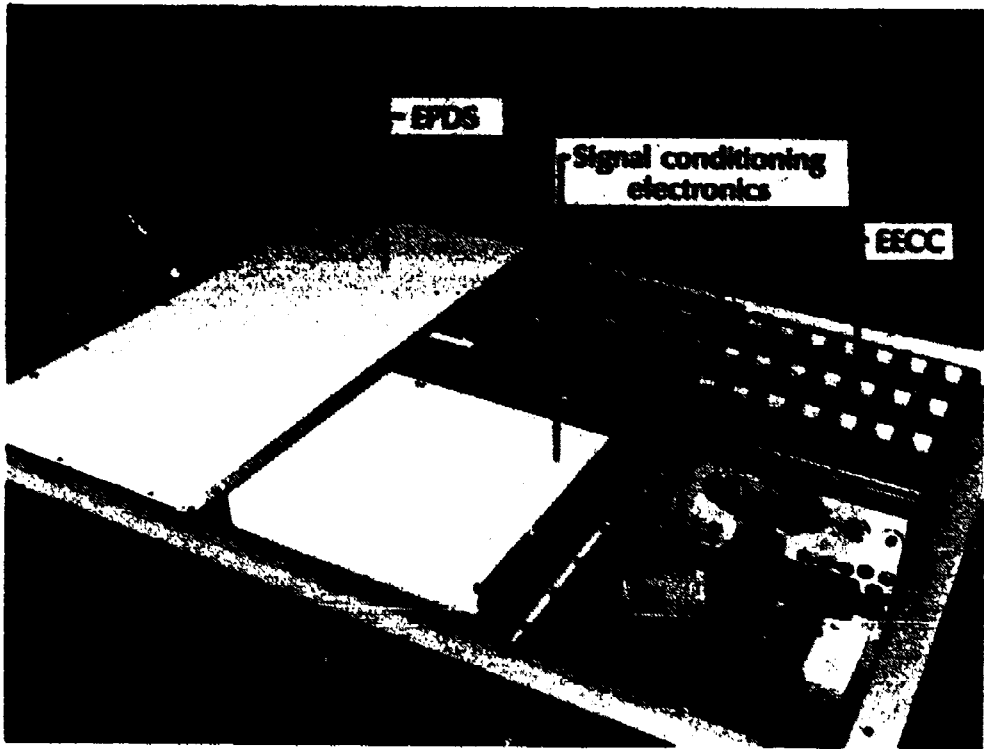
(b) Trailing-edge tray, 6 in. deep.

Figure 22. Concluded.

The fiber optics experiment will investigate the resistance of a fiber optic cable to the effects of the space environment and will involve the illumination of a 1-km fiber by a light-emitting diode (LED) source. A detector will be used to monitor the radiance of the LED and a second detector will monitor the output of the fiber. The difference between the two detectors will represent the loss in the fiber. The fiber will be unsheathed so that radiation effects can be introduced. The LED source, detectors, and fiber will be electrically and optically characterized prior to the test. All composites will be subjected to postflight analysis for comparison to the initial data. Failure analysis will be used as required to identify failure modes and/or mechanisms and indicate potential solutions to identified problems. The detectors will be matched to minimize the difference between the individual detector characteristics.

55

# Balloon Materials Degradation
# (S1006)

David H. Allen
Texas A. & M. University
College Station, Texas

## Background

There exists a need to expose a variety of very thin films to the space radiation environment in order to gain sufficient data to properly support other NASA programs involving the flight of extremely high altitude scientific balloons. In particular, significant scientific benefit will be derived from the development of a long-duration balloon platform capable of carrying payloads on the order of 250 kg to altitudes greater than 40 km for periods in excess of 60 days. The National Scientific Balloon Facility has actively pursued this program for the past 3 years. However, the engineering of these large systems could be significantly accelerated if data regarding degradation and/or alteration of various material properties could be obtained and compared to laboratory simulations of the space environment.

## Objective

The objective of this experiment is to assess the effects of long-term exposure of candidate balloon films, tapes, and lines to the hostile environment above the Earth's atmosphere. Degradation of mechanical and radiometric properties will be observed by a series of tests on exposed materials.

## Approach

The experiment is passive and will test candidate balloon films, tapes, and lines. The experiment will occupy one-third of a 3-in.-deep peripheral tray, as shown in figure 23. The materials to be tested are listed in table 7. Two additional identical sets of material will be prepared. The first set will be tested immediately and the second will be held in a controlled environment until the recovery of the samples placed in orbit. Tests will then be performed on this second set to determine any effects of aging. The specimens that are recovered from the LDEF will also be tested and the effects of long-duration exposure noted. In addition to these specimens, another set of specimens will be exposed to the Texas A. & M. University accelerated exposure facility and the results will be compared with those of specimens exposed *in situ*.

Subsequent to exposure, two types of tests will be performed on each specimen. The films will be subjected to a uniaxial state of stress at room

49
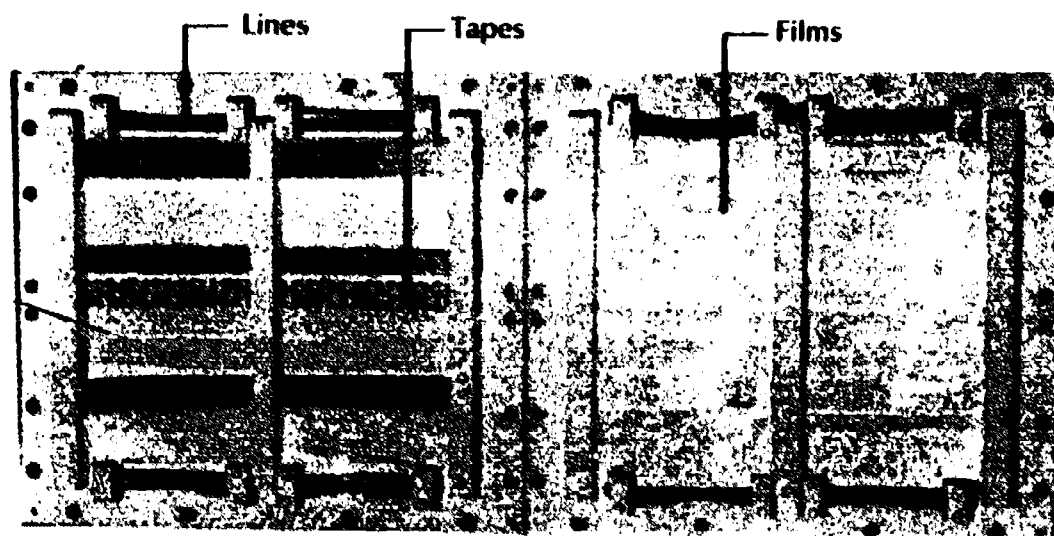
*Figure 23.—Balloon materials degradation experiment.*

**Table 7.—Balloon Materials Specimens**

| Films |
|---|
| 0.5-mil nylon 12 TD[a] |
| .5-mil nylon 12 MD[h] |
| 1.0-mil Stratofilm TD |
| 1.0-mil Stratofilm MD |
| .5-mil Stratofilm TD |
| .5-mil Stratofilm MD |
| 1.0-mil SFX TD |
| 1.0-mil SFX MD |
| .5-mil SFX TD |
| .5-mil SFX MD |
| .35-mil SFX TD |
| .35-mil SFX MD |
| .35-mil aluminized polyester |
| .92-mil Hostaphan 2000 |
| .48-mil to .48-mil polyester with 400-denier Kevlar 29 |
| .92-mil to .92-mil laminated Hostaphan 2000 |

| Tapes |
|---|
| Nylon-reinforced polyester (500 lb) |
| Kevlar-reinforced polyester (1000 lb) |
| Pressure-sensitive adhesive tape (polyethylene substrate with reinforcing polyester backing and silicon adhesive) |

| Lines |
|---|
| Nylon (500 lb) |
| Kevlar (500 lb) |
| Kevlar (1000 lb) |

[a]TD — transverse direction
[h]MD — meridional directional

50

temperature and at $-80°C$ with a constant strain rate of 0.2 percent per minute. The load and deformation will be recorded as a function of time and stress-strain diagrams will be prepared. Five specimens of each film type will be used to insure repeatability. After detailed elastic data have been taken, the film will be loaded to failure.

It is anticipated that significant chemical changes will occur which will affect the effective absorptivity and emissivity properties of the film. Therefore, care will be taken not to clean or otherwise alter the surface of the exposed films.

# Thermal Control Coatings Experiment
## (A0138-6)

A. Paillous
CERT/ONERA-DERTS
Toulouse, France

J-C. Guillaumon
CNES/CST
Toulouse, France

## Background

In order to assess the degradation of thermo-optical properties of coatings used on satellites, a space environment simulation is needed. It is difficult to perform such a task in the laboratory because the simulation involves good vacuum, temperature programming, and irradiation by ultraviolet light and particles. In most cases, caution must be used in interpreting the results because it is impossible to obtain light sources with a spectrum similar to that of the Sun and also because accelerated tests are generally used. A comparison of degradations obtained in the laboratory with degradations obtained in space would be very valuable.

## Objectives

The objectives of this experiment are to verify the validity of space environment simulation performed in the laboratory in order to measure the stability of the thermo-optical properties of thermal control coatings, and to compare the behavior in space of some materials for which the available ultraviolet solar simulation is inadequate (especially in the far ultraviolet).

## Approach

The experimental approach is to passively expose samples of the thermal coatings of interest. These coatings include black paint, aluminum paint, white paint, a solar absorber, an optical surface reflector, second-surface mirrors, metal coatings, and silica fabrics. Preflight and postflight measurements of thermo-optical properties will be compared to determine the effects of space environment exposure.

The experiment will be located with nine other experiments from France in a 12-in.-deep peripheral tray. The thermal coating samples will be housed in one of the three FRECOPA boxes located in the tray. (See fig. 12.) The

52

FRECOPA box (fig. 13) will protect the samples from contamination during the launch and reentry phases of the LDEF mission.

Samples will be independently maintained in sample holders that allow their front face to receive maximum solar illumination when the FRECOPA box is open. (See fig. 24.) Thirty samples will be tested. Twenty-nine samples are ¾ in. by ¾ in. and one sample is 1½ in. by 1½ in. Sample thickness is less than ⅛ in. The maximum temperature during space exposure will ⌐. recorded by passive temperature indicators fixed to the sample mounting plate. Additionally, the ionizing radiation dose will be measured by a passive LiF dosimeter.

The FRECOPA box will be closed in space after exposure and will be kept under vacuum until optical measurements are completed in the laboratory. The entire closed box containing samples under vacuum will be placed in a vacuum chamber, where the optical reflectance spectrum of each sample will be recorded using an integrating sphere. An additional set of samples will be maintained in the laboratory for comparison with samples subjected to space exposure.
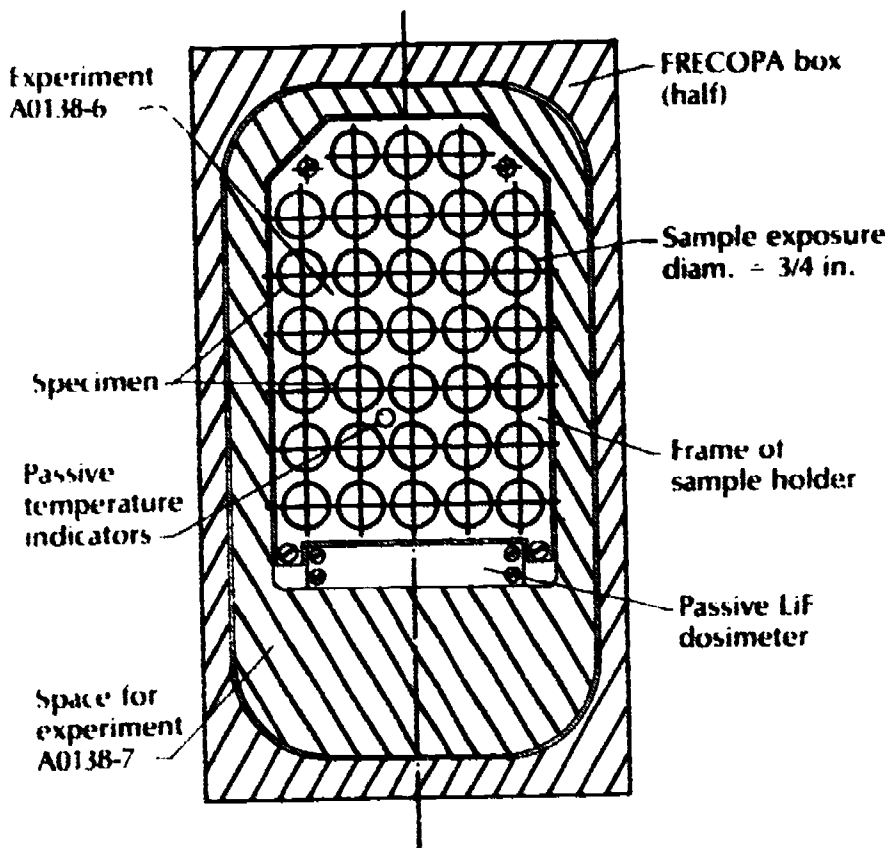


Figure 24.—Layout of thermal control surfaces experiment.

# Exposure of Spacecraft Coatings
# (S0010)

Wayne S. Slemp
NASA Langley Research Center
Hampton, Virginia

## Background

The degradation of thermal control coatings due to space radiation exposure has caused spacecraft to overheat, leading to problems with subsystems and mission lifetimes. To prevent such problems, designers need to be able to accurately predict the performance of thermal control coatings. Several flight experiments have been conducted to obtain the necessary coating performance data. Unfortunately, these data were limited to telemetry information and the experiments were not returned for postflight evaluation. Coating performance was determined from temperature measurements made on sample coatings and increases in sample temperature were interpreted as being caused by space radiation. With these experiments it was not possible to distinguish between damage caused by space radiation and that caused by some other means, such as mechanical stress or contamination. To properly isolate the cause of coating degradation, an experiment is necessary which provides for the return of coating samples after space exposure for ground laboratory evaluation.

## Objectives

The objectives of this experiment are to determine the effects of both the Shuttle-induced environment and the space radiation environment on selected sets of spacecraft thermal control coatings.

## Approach

The experimental approach is to passively expose samples of thermal control coatings to Shuttle-induced and space radiation environments and to return the samples for postflight evaluation and comparison with preflight measurements to determine the effects of the environmental exposure. Two additional sets of samples will remain in the laboratory and will be analyzed for comparison with the flight data. Optical measurements of the samples will include total normal emittance and spectral reflectance.

The experiment will utilize a 6-in.-deep peripheral tray and an experiment exposure control canister (EECC). (See fig. 25.) The EECC will provide protection for some of the samples against exposure to the launch and

54
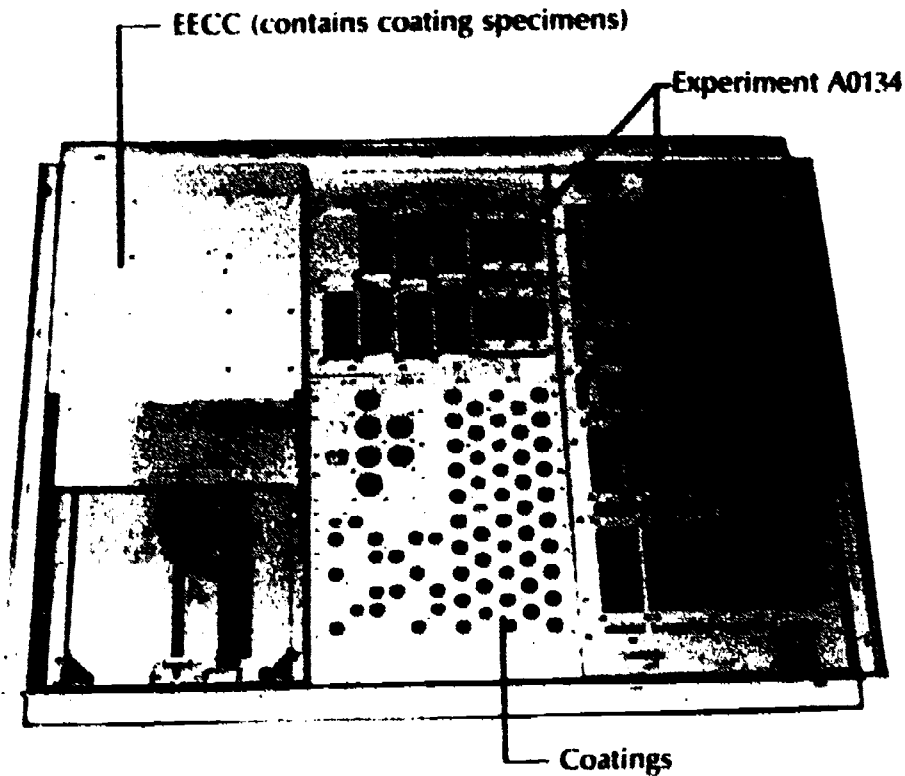
*Figure 25.—Exposure of spacecraft coatings experiment shown integrated with experiment A0134.*

reentry environments. The EECC will be programmed to open about 2 weeks after LDEF deployment and close prior to LDEF retrieval by the Shuttle and reentry.

Some samples will not be housed in the EECC and will be exposed to the Shuttle-induced environment during launch and reentry. Comparison of the data from these samples with data from samples in the EECC exposed to only the space radiation environment will yield information about possible contamination-induced degradation effects.

Table 8 provides a list of the thermal control coatings that will be included in this experiment. Additionally, several materials specimens will be located in the EECC as control specimens for other LDEF experiments (e.g., A0114 and A0187).

**Table 8.—S0010 Thermal Control Coatings**

| Type | Composition | Substrate |
|---|---|---|
| Second-surface mirrors | Quartz-Ag<br>Teflon-Ag<br>Diffuse Teflon-Ag<br>Kapton-Al | Al<br>Al<br>Al<br>Al |
| Black paints | Chemglaze, Z-306<br>IITRI, D-111 | Al<br>Al |
| White paints | Zinc oxide-silicate, Z-93<br>Zinc oxide-silicone, S-13GLO<br>Zinc orthotitinate-silicate, YB-71<br>Chemglaze, A-276 | Al<br>Al<br>Al<br>Al |
| Anodized | Chromic acid, high emissivity<br>Chromic acid, medium emissivity<br>Chromic acid, low emissivity | Al<br>Al<br>Al |
| Sputtered | Ni-Al<br>Ni-SiO$_2$<br>Ni-Al-SiO$_2$<br>Cr-SiO$_2$ | Graphite-epoxy<br>Graphite-epoxy<br>Graphite-epoxy<br>Graphite-epoxy |

63

# Thermal Control Surfaces Experiment
## (S0069)

Donald R. Wilkes and Harry M. King
NASA George C. Marshall Space Flight Center
Huntsville, Alabama

## Background

The optical properties of thermal control surfaces in the solar region of the spectrum are of primary interest to spacecraft thermal designers since these properties govern the solar-heat input to exposed surfaces (such as the thermal radiators) and therefore influence the temperature of the spacecraft. These properties, however, have been shown to be altered considerably under the space environment, which includes solar irradiation, thermal vacuum, micrometeoroid bombardment, and contamination. One such mechanism of solar ultraviolet degradation is caused by photodesorption of oxygen, which is immediately and completely reversible upon exposure to a very small amount of oxygen ($10^{-4}$ to $10^{-6}$ torr partial pressure). This type of bleaching mechanism shows the necessity of *in situ* measurements of the optical properties of environmentally damaged surfaces (i.e., in vacuum before repressurization).

Until now, no optical measurements of thermal control surfaces have been made in space. Temperature measurements of thermally isolated samples have been used to back-calculate solar absorptance and thermal emittance. This type of measurement is not as definitive as required and does not describe the spectral character of the sample surface. Spectral reflectance measurements of the samples are required to differentiate between different damage mechanisms of environmental effects and to separate contamination effects.

Additionally, because of the inability to simulate exactly the conditions of the coating surface temperature and the solar spectrum, there is a major difference between laboratory test data and in-flight experiment data. Although the current generation of laboratory test apparatus is extremely complex and well thought out, it provides only relative data on the degradation of coatings in actual space conditions. The only accepted test for flight qualification of new coatings is to have them evaluated in actual conditions of space flight in the space environment where they will be used.

## Objectives

The objectives of this experiment are to determine the effects of the near-Earth orbital environment and the Shuttle-induced environment on

spacecraft thermal control surfaces. Spectral reflectance measurements will be obtained and used to differentiate between different solid-state damage mechanisms of environmental damage, to separate the effects of contamiration from those of natural-environmental damage, and for comparison and correlation with laboratory test data.

## Approach

The experiment is designed to measure certain physical properties of 25 "active" spacecraft thermal surface samples in an environment that approximates their normal use. The parameters to be measured include the hemispherical reflectance as a function of wavelength (100 wavelength steps from 0.25 to 2.5 μm) and the temperature of these samples as a function of time in a calorimeter configuration. The latter measurements will be made in two different physical configurations that allow calculation of the emittance and the ratio of solar absorption to emittance for each sample. In addition, 24 passive samples will be exposed to approximately the same environment as the active samples.

Figure 26 shows a simplified block diagram of the experiment, figure 27 shows the experiment layout in a 12-in.-deep tray, and figure 28 is a photograph of the flight hardware. The active samples are contained in calorimeter assemblies and are mounted along with the passive samples on the carousel. In addition, three radiometers (solar and Earth albedo, Earth albedo, and earthshine) are also mounted on the carousel. The radiometers are used to measure the radiant energy incident upon the samples, which is required for calculating the ratio of absorption to emittance, and to provide a record of the total exposure of the samples to the solar ultraviolet.

The carousel has two fixed positions, referred to as in IN, or protected, and OUT, or exposed. The OUT position exposes the samples to the environment. The samples are in this position approximately 23½ hours for every Earth day, including the 1½-hour period each day when temperature and radiometer measurements are being recorded to determine the ratio of absorption to emittance. The carousel is rotated 180° from the OUT position to the IN position for the emittance measurements for approximately ½ hour each day. For these measurements, the samples view a massive heat sink (aluminum "emittance" plate) which maintains a relatively constant temperature, and temperature change as a function of time is recorded for each sample.

The IN, or stowed, position also places the samples and radiometers in a protected enclosure for launch and reentry. This position is also maintained for 10 days after launch to allow volatiles to outgas prior to starting experimental operations.

The reflectometer assembly includes an integrating sphere, which is located at the bottom of the carousel assembly. The carousel is rotated by a stepping motor through a geneva drive mechanism to position each of the 25 active samples in the integrating sphere aperture, where sample reflectance can be measured. Each sample will be measured 20 times during the LDEF mission, nominally once per month with measurements slightly more often near the beginning of the mission.
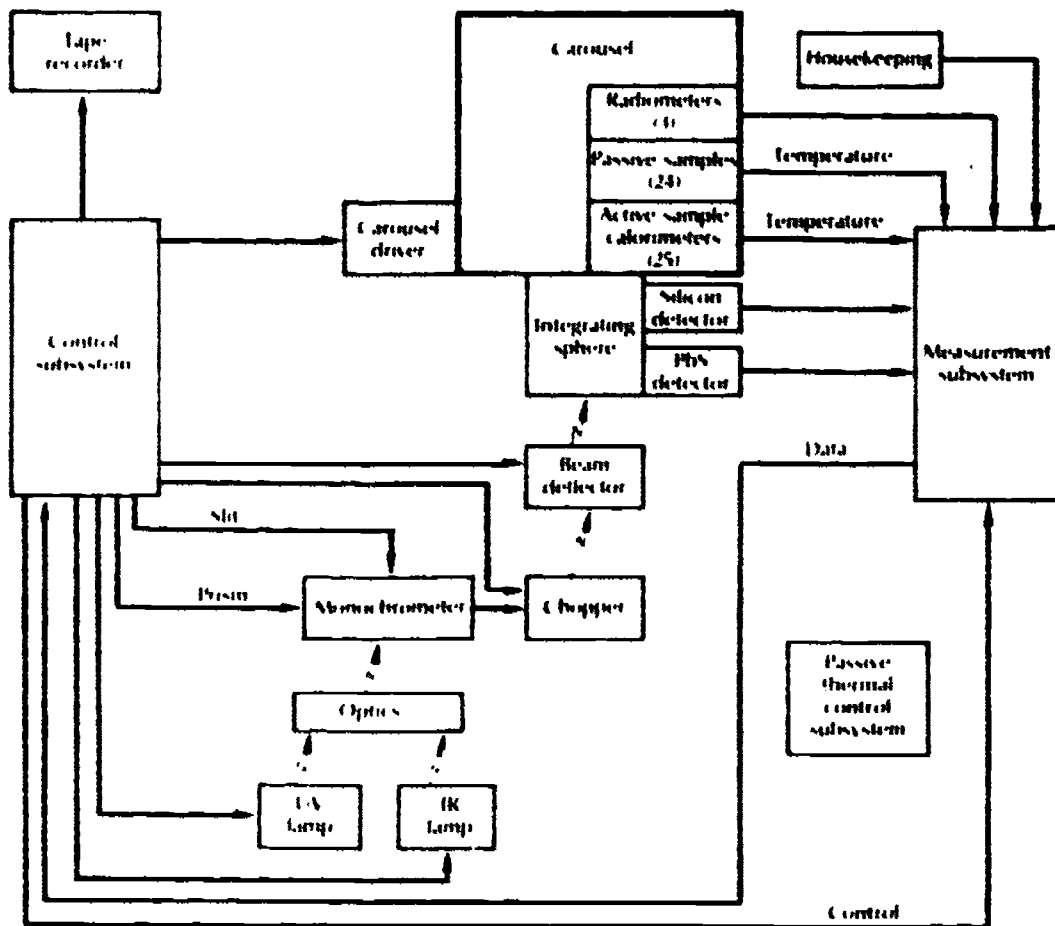


Figure 26.—Simplified block diagram of thermal control surfaces experiment.
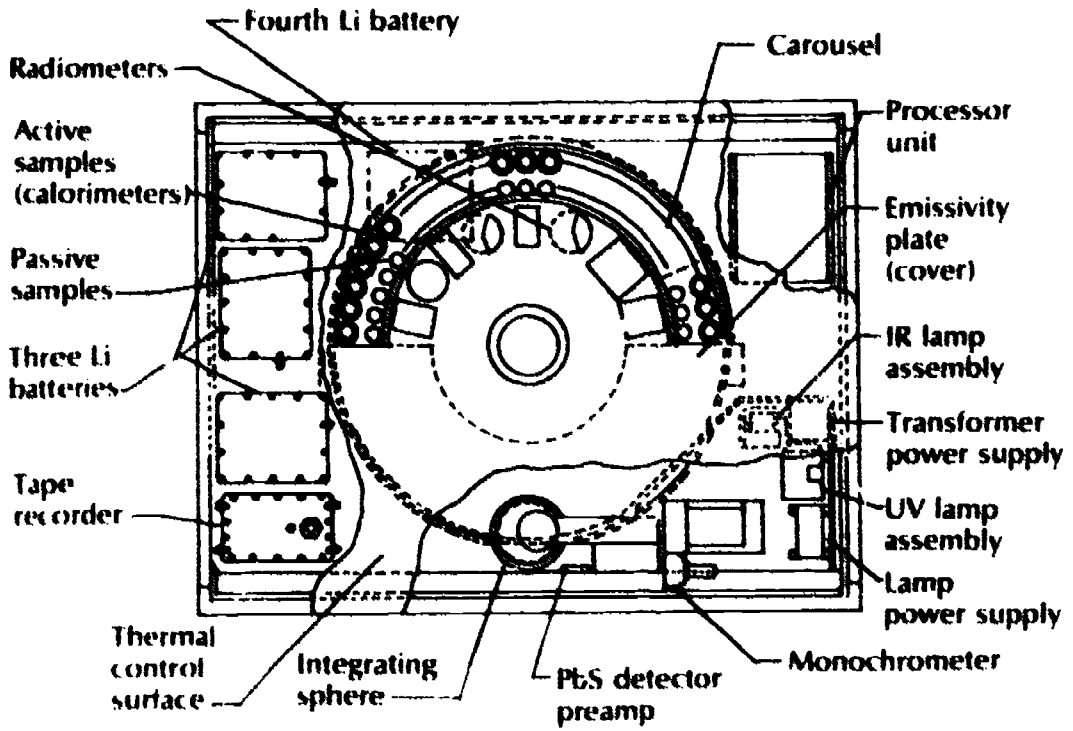
Figure 27.- *Thermal control surfaces experiment layout showing location of components.*
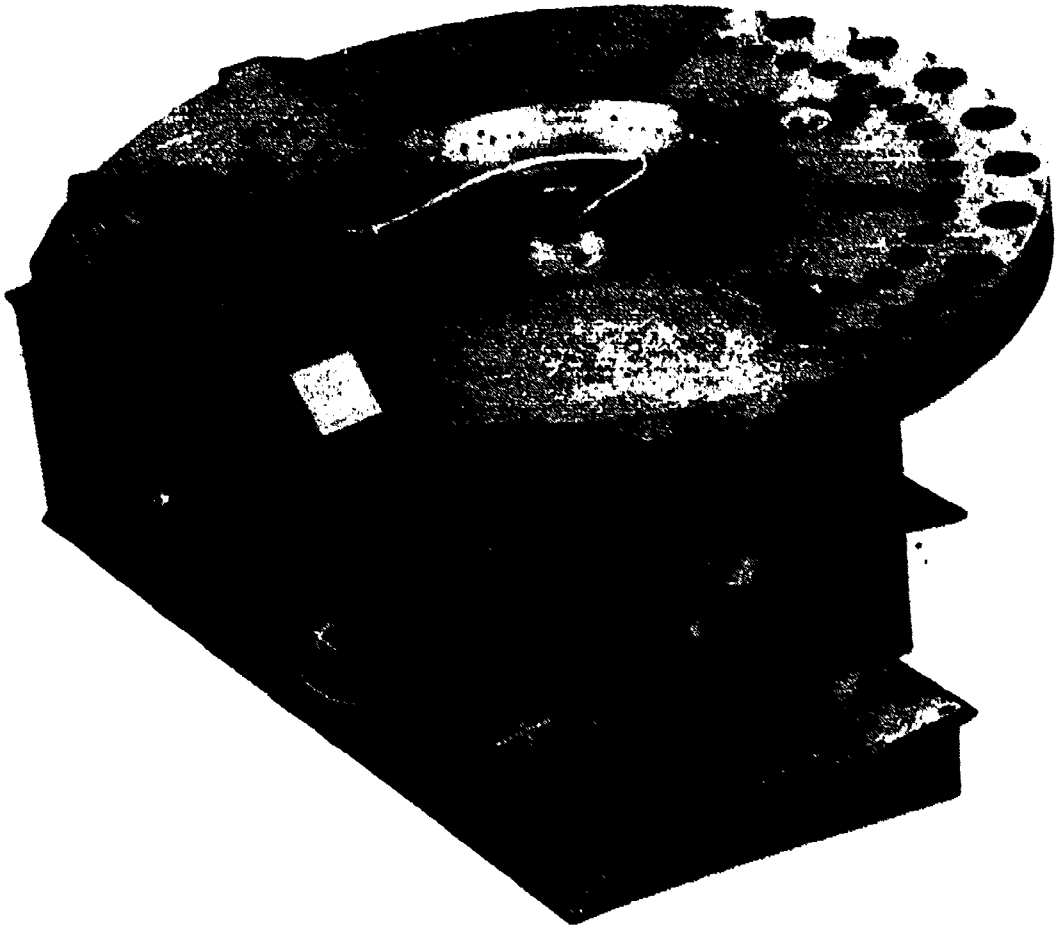
Figure 28.—Photograph of carousel showing samples.

# Ion-Beam-Textured and Coated Surfaces Experiment (S1003)

Michael J. Mirtich, Jr.
NASA Lewis Research Center
Cleveland, Ohio

## Background

Future spacecraft relying on thermal control surfaces or solar thermal power generation will be subjected to the near-Earth Shuttle environment prior to insertion into a geosynchronou. orbit. The combined effects of the near-Earth Shuttle environment may be synergistic and may cause appreciable degradation prior to geosynchronous-orbit operations. *In situ* exposure of various candidate surfaces is required to evaluate material, optical, and/or electrical property durability so that a choice of surface materials can be made with respect to optical and/or electrical performance, durability, and contamination protection requirements.

## Objective

.ne objective of this experiment is to measure the effects of exposure to the Shuttle launch and near-Earth space environments on the optical properties of ion-beam-textured high-absorptance solar thermal control surfaces, the optical and electrical properties of ion-beam-sputtered conductive solar thermal control surfaces, and the weight loss of ion-beam-deposited oxide-polymer films.

The various types of surfaces to be tested include six major categories: (1) ion-beam textured surfaces suitable for space solar-thermal (solar concentrator) application (e.g., materials such as copper, aluminum, Inconel, stainless steel, d silver); (2) painted and/or state-of-the-art solar thermal surfaces (e.g. black chrome); (3) ion-beam-sputtered conductive coatings for thermal and space charge control (e.g., indium-oxide-coated metalized FEP Teflon); (4) ion-beam-sputtered conductive coated solar-sail materials for space charge control and cooling through emittance (e.g., sputtered coatings on Kapton such as indium oxide, aluminum, and chromium); (5) micrometeoroid-sensitive samples whose optical properties change only as a result of micrometeoroid impact; and (6) Kapton coated with oxide-polymer films to minimize oxygen degradation at near-Earth-orbit altitudes.

The objective for the first two categories of samples is to verify that the optical properties of the microscopic cone or ridge-type ion-beam-textured surfaces are more resistant to degradation than conventional solar thermal surfaces. The objective for the third and fourth categories of samples is to evaluate the electrical and optical durability of conductive coatings for thermal control and solar-sail radiative cooling applications. The objective for the

fiflfi-category sample is to identify changes in the optical properties which can be attributed to micrometeoroid impact. The objective for the sixth category is to measure any changes in optical or material properties of oxide-polymer-coated Kapton after exposure to the oxygen atom environment in near-Earth (Shuttle) orbit.

## Approach

The experimental approach is to passively expose the samples to all environments of the entire mission. The optical properties (absorptance and emittance) of each surface will be measured in ground tests both before and after exposure to the environment. This will be done by experimentally measuring the spectral reflectivity between 0.33 and 2.16 µm using a Gier–Dunkle integrating sphere to obtain the solar absorptance. The emittance will be obtained by measuring the spectral reflectance in the infrared between 1.5 to 15.5 µm using a Holraum reflectometer.

Electrical conductive coatings will be resistance documented before and after the LDEF flight. Comparisons will be made between the durability of the painted surfaces and the ion-beam-textured or sputtered surfaces. Additional tests, including weight loss, Auger and SEM measurements and/or chemical analyses may also be performed as the data warrants.

The experiment requires one-sixth of a 3-in.-deep peripheral tray. Figure 29 illustrates the experiment configuration and table 9 lists the samples that will be tested.
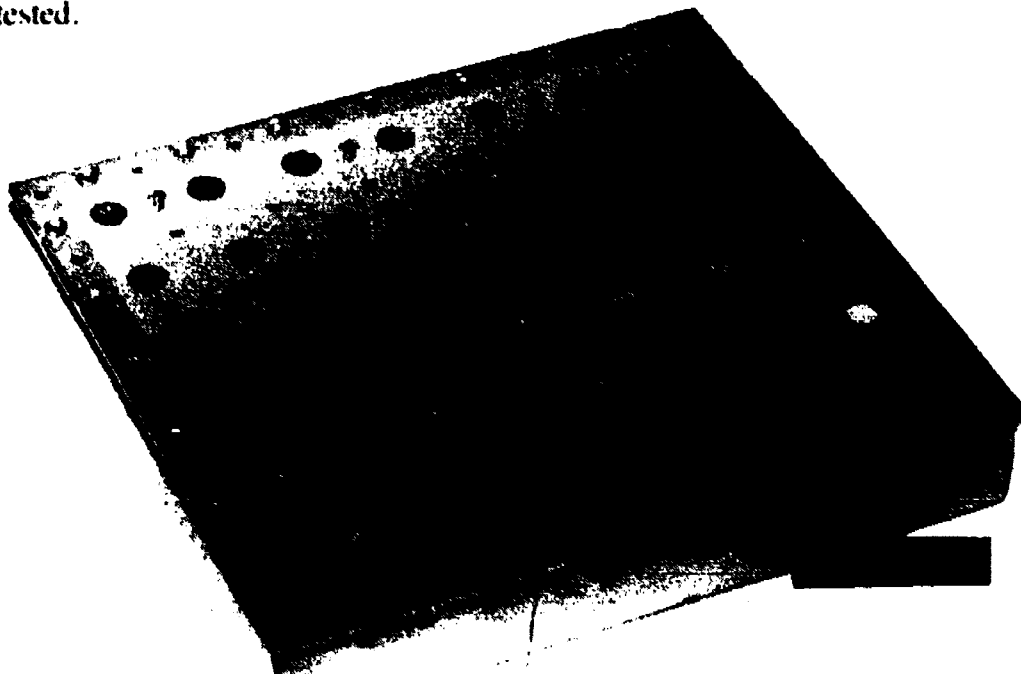


*Figure 29.—Ion-beam-textured and coated surfaces experiment.*

**Table 9.—Ion-Beam-Textured and Coated Surfaces Samples**

| Sample number | External exposed surface | Substrate | Internal unexposed surface |
|---|---|---|---|
| 1 | 0.1-μm Au on textured surface | FEP Teflon | Untreated |
| 2 | 0.1-μm Au on textured surface | FEP Teflon | Untreated |
| 3 | Textured | Si | Polished |
| 4 | Textured | Si | Polished |
| 5 | Textured | Ti (6% Al, 4% V) | Untreated |
| 6 | Uncoated | Kapton | Untreated |
| 7 | 0.065-μm 4% PTFE + 96% SiO₂ | Kapton | Untreated |
| 8 | Textured | 304 stainless steel | Untextured |
| 9 | 0.065-μm SiO₂ | Kapton | Untreated |
| 10 | Textured | Inconel | Untreated |
| 11 | 0.1-μm Al on textured surface | Cu | Untreated |
| 12 | 0.070-μm Al₂O₃ | Kapton | Untreated |
| 13 | Textured | Cu | Untextured |
| 14 | 0.065-μm 4% PTFE + 96% SiO₂ | Kapton | Untreated |
| 15 | Textured | Pyrolytic graphite | Untextured |
| 16 | 0.065-μm SiO₂ | Kapton | Untreated |
| 17 | Textured | Kapton | 0.1-μm Al |
| 18 | Textured | Kapton | 0.1-μm Al |
| 19 | Textured | Kapton | 0.2-μm Ag on textured surface |
| 20 | Textured | Kapton | 0.2-μm Ag on textured surface |
| 21 | In₂O₃ | FEP Teflon | 0.15-μm Ag |
| 22 | In₂O₃ | FEP Teflon | 0.15-μm Ag |
| 23 | Untextured | FEP Teflon | 0.1-μm Ag on textured surface |
| 24 | Untextured | FEP Teflon | 0.1-μm Ag on textured surface |
| 25 | 0.1-μm Al | Kapton | Textured Kapton |
| 26 | .070-μm Al₂O₃ | Kapton | Untreated |
| 27 | Black chrome | Ti (6 % Al, 4% V) | Untreated |
| 28 | Untreated | Grafoil | Untextured |
| 29 | Untreated | Kapton | 0.1-μm Al |

**Table 9.—Ion-Beam-Textured and Coated Surfaces Samples**

| Sample number | External exposed surface | Substrate | Internal unexposed surface |
|---|---|---|---|
| 1 | 0.1-μm Au on textured surface | FEP Teflon | Untreated |
| 2 | 0.1-μm Au on textured surface | FEP Teflon | Untreated |
| 3 | Textured | Si | Polished |
| 4 | Textured | Si | Polished |
| 5 | Textured | Ti (6% Al, 4% V) | Untreated |
| 6 | Uncoated | Kapton | Untreated |
| 7 | 0.065-μm 4% PTFE + 96% $SiO_2$ | Kapton | Untreated |
| 8 | Textured | 304 stainless steel | Untextured |
| 9 | 0.065-μm $SiO_2$ | Kapton | Untreated |
| 10 | Textured | Inconel | Untreated |
| 11 | 0.1-μm Al on textured surface | Cu | Untreated |
| 12 | 0.070-μm $Al_2O_3$ | Kapton | Untreated |
| 13 | Textured | Cu | Untextured |
| 14 | 0.065-μm 4% PTFE + 96% $SiO_2$ | Kapton | Untreated |
| 15 | Textured | Pyrolytic graphite | Untextured |
| 16 | 0.065-μm $SiO_2$ | Kapton | Untreated |
| 17 | Textured | Kapton | 0.1-μm Al |
| 18 | Textured | Kapton | 0.1-μm Al |
| 19 | Textured | Kapton | 0.2-μm Ag on textured surface |
| 20 | Textured | Kapton | 0.2-μm Ag on textured surface |
| 21 | $In_2O_3$ | FEP Teflon | 0.15-μm Ag |
| 22 | $In_2O_3$ | FEP Teflon | 0.15-μm Ag |
| 23 | Untextured | FEP Teflon | 0.1-μm Ag on textured surface |
| 24 | Untextured | FEP Teflon | 0.1-μm Ag on textured surface |
| 25 | 0.1-μm Al | Kapton | Textured Kapton |
| 26 | .070-μm $Al_2O_3$ | Kapton | Untreated |
| 27 | Black chrome | Ti (6 % Al, 4% V) | Untreated |
| 28 | Untreated | Grafoil | Untextured |
| 29 | Untreated | Kapton | 0.1-μm Al |

**Table 9.—Concluded**

| Sample number | External exposed surface | Substrate | Internal Unexposed surface |
|---|---|---|---|
| 30 | Untreated | FEP Teflon | 0.15-μm Ag |
| 31 | Nextel paint | Ti (6% Al, 4% V) | Untreated |
| 32 | S-13G | Al | Untreated |
| 33 | Embossed | FEP Teflon | 0.15-μm Ag |
| 34 | Uncoated | Kapton | Untreated |
| 35 | 2000-A Al | 304 stainless steel | Untreated |
| 36 | 1.0-μm Mo | Fiberglass composite | 0.2-μm Mo |

# Cascade Variable-Conductance Heat Pipe (A0076)

Michael G. Grote and Leslie D. Calhoun II
McDonnell Douglas Astronautics Company
St. Louis, Missouri

## Background

A number of spacecraft applications could benefit from a precise tempera-ture control system which requires zero electrical power. The dry-reservoir variable-conductance heat pipe (VCHP) system will provide this capability, but its performance capabilities have not been adequately demonstrated in flight.

## Objective

The objective of this experiment is to verify the capability of a cascade variable-conductance heat pipe (CVCHP) system to provide precise temperature control of long-life spacecraft without the need for a feedback heater or other power sources for temperature adjustment under conditions of widely varying power input and ambient environment.

## Approach

The approach to conducting the experiment is consistent with the LDEF capabilities (i.e., relatively long duration, zero gravity environment, and mini-mal electrical power and data system capability). Solar energy is the heat source and space the heat sink for thermally loading two series-connected variable-conductance heat pipes. Electronics and power supply equipment requirements are minimal. The experiment power data system (EPDS) in LDEF experiment S1001 (Low-Temperature Heat Pipe Experiment Package (HEPP) for LDEF) will be used for data recording. A 7.5-V lithium battery supplies the power for thermistor-type temperature sensors for monitoring system performance, and a 28-V lithium battery supplies power for valve actuation.

The experiment will occupy a 6-in.-deep peripheral tray located on the leading edge of the LDEF. Two external-surface subpanels will be employed which are thermally coupled to opposite ends of two series-connected variable-conductance heat pipes. One panel will be designed as a heat absorber through application of a high $\alpha/\epsilon$ (absorptivity/emissivity) surface coating, and the second will be a radiator with a low $\alpha/\epsilon$ surface coating. Multilayer insulation and fiberglass structural attachments are used to thermally isolate the experiment from the LDEF tray structure and interior. Each of the heat pipe evaporators will be maintained within preselected temperature ranges by sizing the collector.

radiator, and insulation and by servicing the noncondensible dry gas reservoirs, thus demonstrating passive variable-conductance heat pipe operation.

Figure 30 shows the CVCHP experiment configuration, which uses two gas-loaded, dry-reservoir VCHP's in series. The coarse-control heat pipe temperature is controlled to plus or minus 3°C and is used as a sink for the fine-control heat pipe. The dry gas reservoir temperatures are controlled by locating the reservoirs next to the heat pipe evaporators. The principal concern is drift in the set point temperature due to many heat load and/or environment temperature cycles. The cyclic operation will move vapor into or out of the
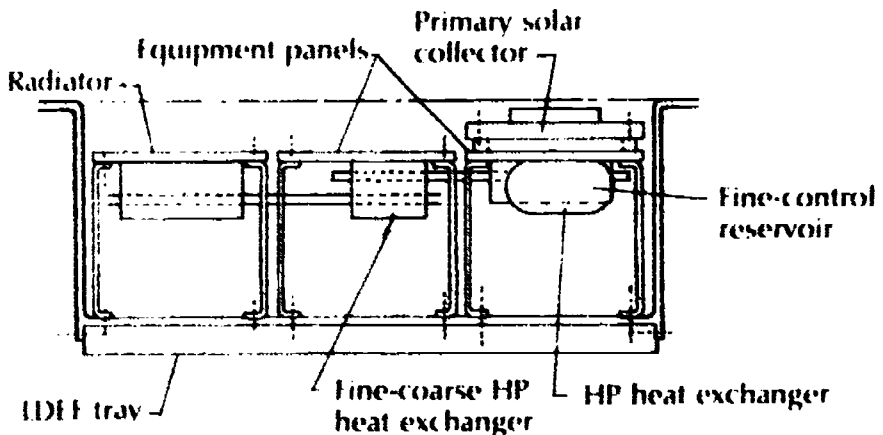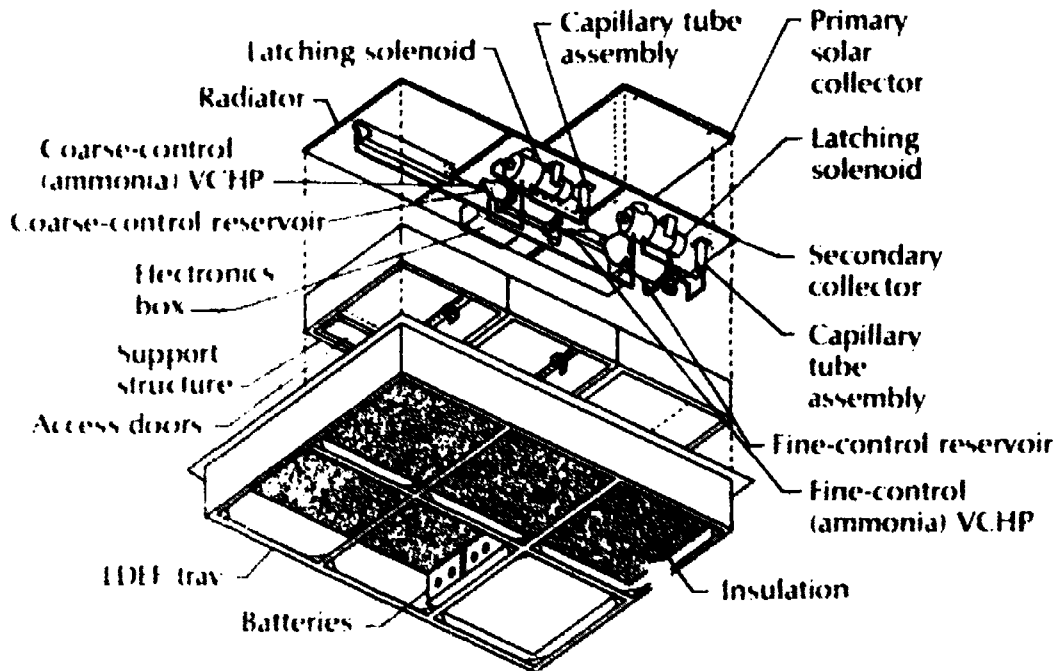


*Figure 30. Cascade variable-conductance heat pipe configuration.*

noncondensible gas reservoir, which changes the set point temperature by introducing a varying working-fluid partial pressure into the gas reservoir. The capillary tube is located between the heat pipe and the reservoir to prevent working fluid from entering the reservoir. The diameter and length of the capillary are selected to satisfy two criteria. First, the capillary must provide sufficient volume to accommodate the entire volume of gas displaced when the vapor front moves from its minimum to its maximum position. Second, the capillary length must be sufficient to prevent diffusion into the reservoir for the mission lifetime.

The heat pipe wick design, shown in figure 31, has a single-pedestal artery with seven tubelets enclosed in a sheath of two layers of 400-mesh screen. The sheath provides the high capillary pumping pressure and the tubelets provide high permeability to reduce the axial pressure drop. The wall wick has a 200-mesh outer layer for low pressure drop and a middle layer of 400 mesh for capillary pumping.

Ammonia is used as the working fluid for both heat pipes. The coarse-control VCHP has a reservoir-to-condensor volume ratio of 20, which will yield



200-mesh outer layer
400-mesh middle layer
0.375-in.-diameter stainless-steel tube
Interleaved 400-mesh continuous wall screen
200 mesh
Middle 400-mesh layer
Seven tubelets of 400-mesh screen 0.032 in. diameter
Two 400-mesh screen layers
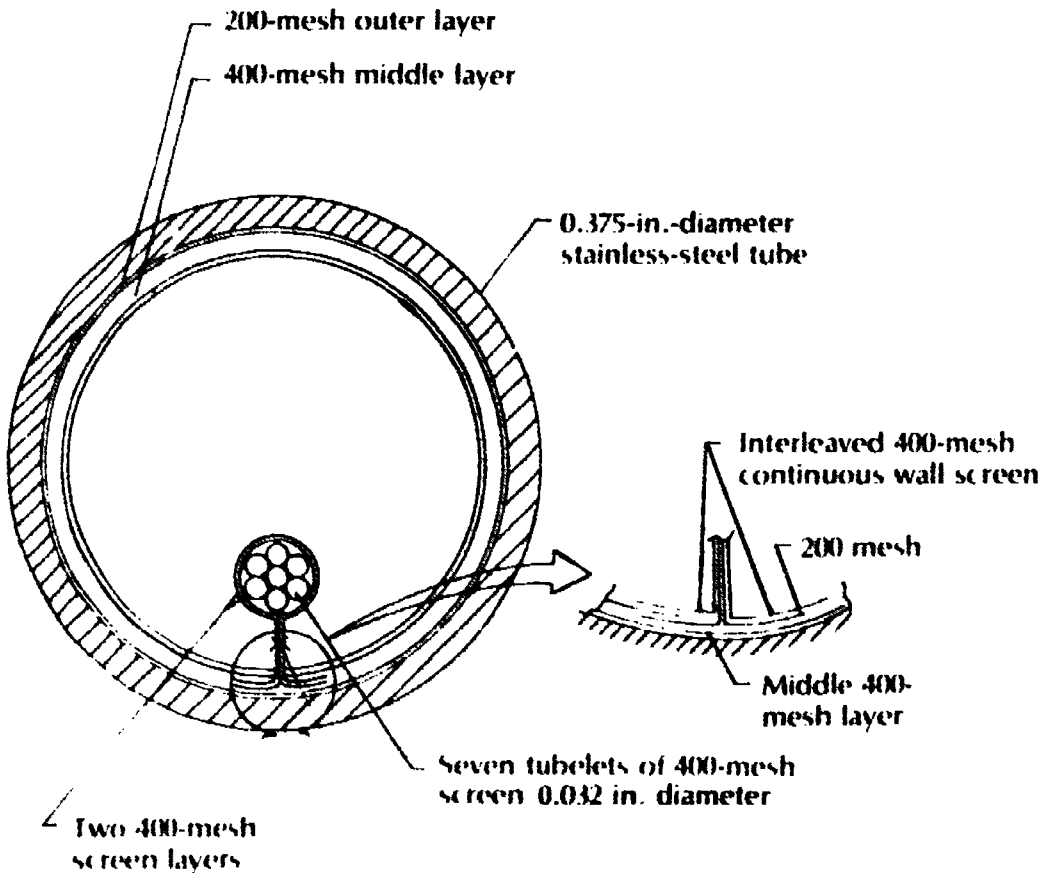
*Figure 31.— Heat pipe wick design.*

a control band of plus or minus 3°C. A larger 90-to-1 volume ratio is used on the fine-control heat pipe to attain a control of plus or minus 0.3°C. The fine-control VCHP has 8.5 m of capillary, and the course-control VCHP has a larger 13.4-m section because of its larger condenser volume.

Experiment operation begins when the battery circuit is initiated at LDEF deployment from the Shuttle. When the temperature of the fine-coarse heat exchanger falls below − 7°C, a valve opens to permit initiation of the coarse-control VCHP and allow the heat pipes to prime prior to beginning VCHP operation. This temperature-controlled initiation ensures that heat pipe temperatures are below their operating set point so that vapor is not forced into the reservoirs. Twenty-five hours later, another valve opens to initiate the fine-control VCHP operation. This delayed opening permits data to be taken on a stabilized coarse-control VCHP before fine-control VCHP operation. Data will be collected at least twice daily during the LDEF mission and will be stored on magnetic tape for subsequent retrieval and playback.

# Low-Temperature Heat Pipe Experiment Package (HEPP) for LDEF (S1001)

Roy McIntosh, Jr., and Stanford Ollendorf
NASA Goddard Space Flight Center
Greenbelt, Maryland

Craig R. McCreight
NASA Ames Research Center
Moffett Field, California

## Background

Experience gained in the development of heat pipes has demonstrated the necessity of obtaining performance data in the space environment. This is due to the fact that the pumping in a heat pipe is derived from relatively weak capillary forces. As a result, particularly in the case of the axially grooved geometry, reliable 1-g performance measurements are often very difficult to obtain. Also, many of the candidate low-temperature and cryogenic fluids have relatively low surface tensions and wicking heights, which compound the problem of 1-g tests.

## Objectives

The principal objectives of the experiment are to determine zero-g start-up performance for conventional and diode low-temperature heat pipes, to evaluate heat pipe performance in zero-g for an extended period of time, to determine zero-g transport capability of each heat pipe, and to determine diode operation, including forward conductance, turndown ratio, and transient behavior.

## Approach

The heat pipe experiment package (HEPP) is designed to test the performance of low-temperature ($<190$ K) heat pipes on the Long Duration Exposure Facility (LDEF). Two heat pipes, a fixed-conductance transporter heat pipe and a thermal-diode heat pipe, are coupled with a radiant cooler system.

Both pipes are charged with ethane. Also integrated with the radiator is a phase change material (PCM) canister which provides temperature stability during transport tests. N-heptane, which has a melting/freezing point of 182 K, is used as the PCM. The high heat capacity (28 W-hr of latent heat) provided by the canister permits high-power heat pipe testing (e.g., 40 W for 40 minutes) at constant temperature. Multilayer insulation blankets are employed, and a shield-

70

77

ing configuration was developed to minimize parasitic inputs from the Earth and maximize radiation to deep space.

HEPP is a completely self-contained and thermally isolated package designed to fit in a 12-in.-deep peripheral tray, as shown in figure 32. The necessary electrical equipment, including electronics for signal conditioning sequencing and command functions, will also be contained within the experiment tray. A standard LDEF experiment power and data system (EPDS) will be used for data collection and recording. Power for the experiment will be provided by a dedicated solar-panel Ni-Cd battery system in another 12-in.-deep tray (fig. 33). This tray will be located on the space-facing end of the LDEF to take maximum advantage of Sun input for experiment operation.

After completion of the LDEF mission, the recorded data will be unpacked and converted to engineering units. The existing thermal model will be used to analyze and correlate the flight data. The flight data will be used to establish boundary conditions; the thermal program will then determine individual heat pipe heat flows and conductances, diode shutdown energy, and PCM performance. Data tabulations and plots will be generated and compared with preflight predictions and thermal-vacuum test results. Performance results derived from the analysis will be reported following preflight and postflight tests.

Additionally, as a result of Kapton erosion seen on Shuttle flights, control samples have been added to some of the trays as an atomic-oxygen coatings investigation to determine ways of protecting Kapton (polyimide) film from atomic-oxygen degradation. Several specimens (a Kapton control, Kapton with coatings of $In_2O_3$, urethane-acrylic, and silicones) will be taped to Kapton film (14 in. square) using Kapton-back.. pressure-sensitive tape. This sheet will then be taped to the HEPP tray Kapton blanket. A duplicate set of specimens will be similarly taped to the CVCHP blanket. In the case of the power tray, a lesser number of specimens will be taped directly to the metal lip of the tray.

Multilayer insulation —

Transporter heat pipe
(coupled with PCM
and radiator)—

Diode heat pipe —

PCM canister
(rear of radiator)—

Shields

Shield radiators

— Main radiator
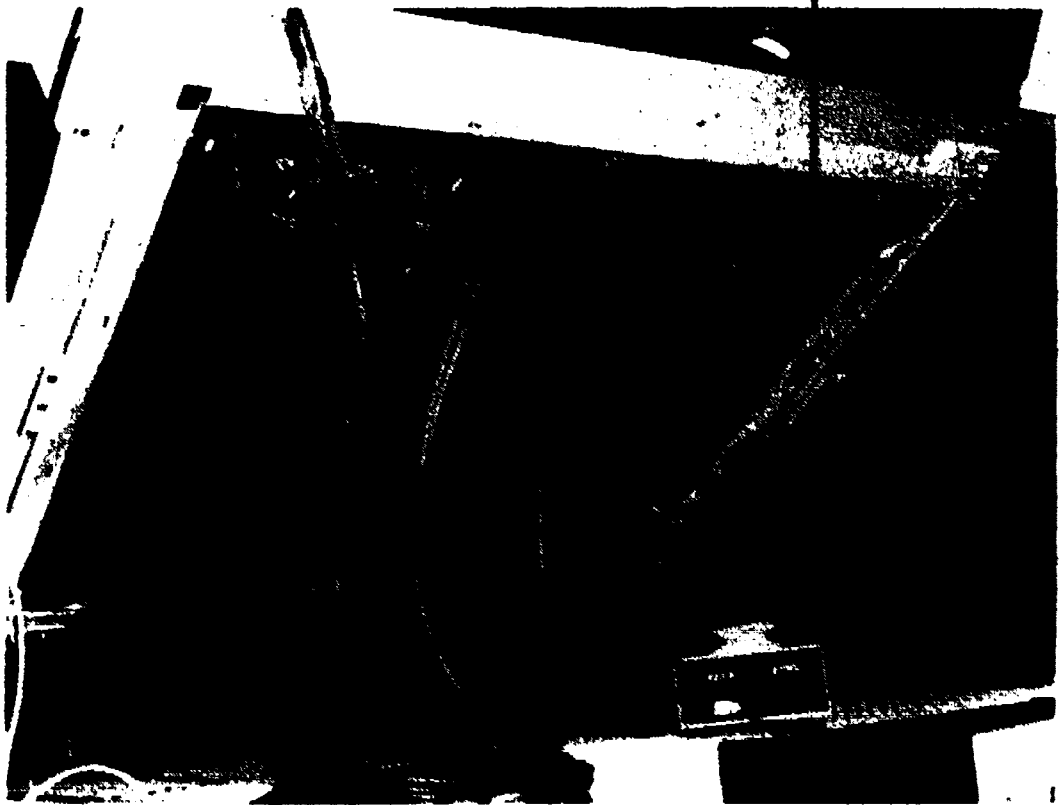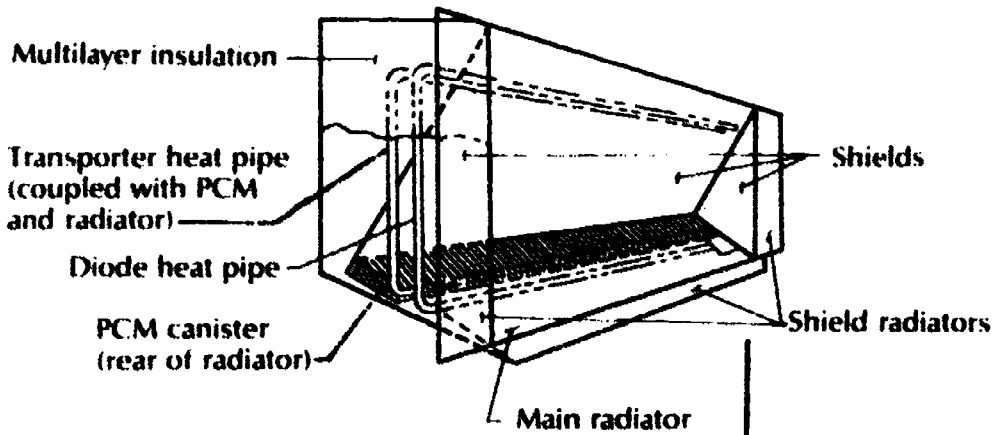
*Figure 32.—Low-temperature heat pipe experiment shown during LDEF compatibility test.*

**79**

Base plate

Paint (thermal control)

Solar panels (four)

Power electronics

Battery

Thermal blanket

Honeycomb structure

I-beams

Insulators

Corner tray
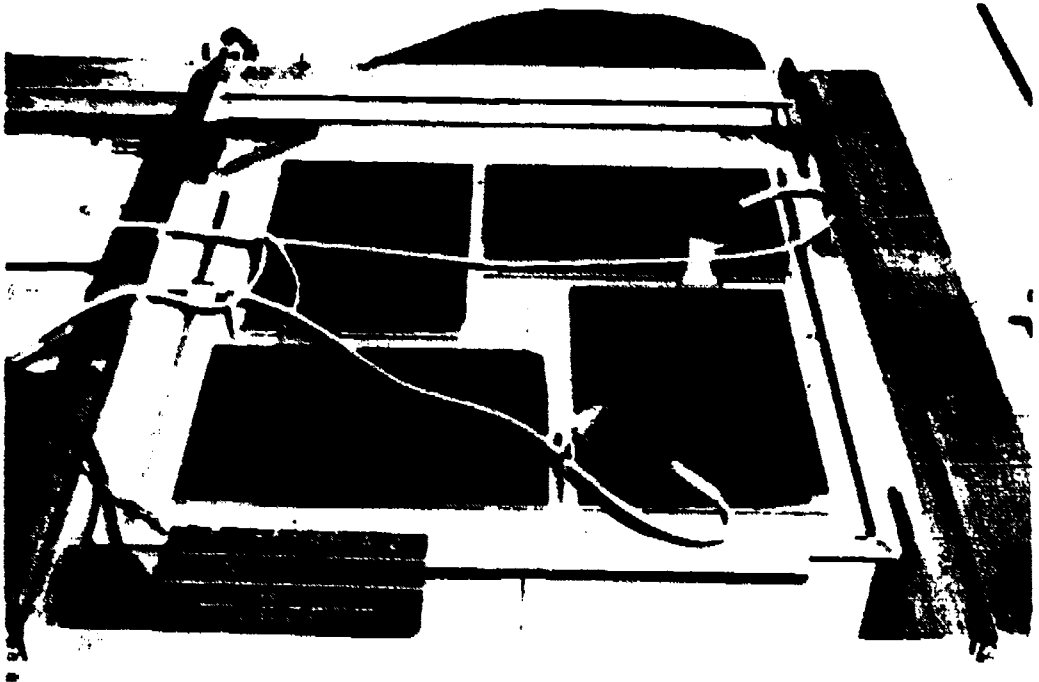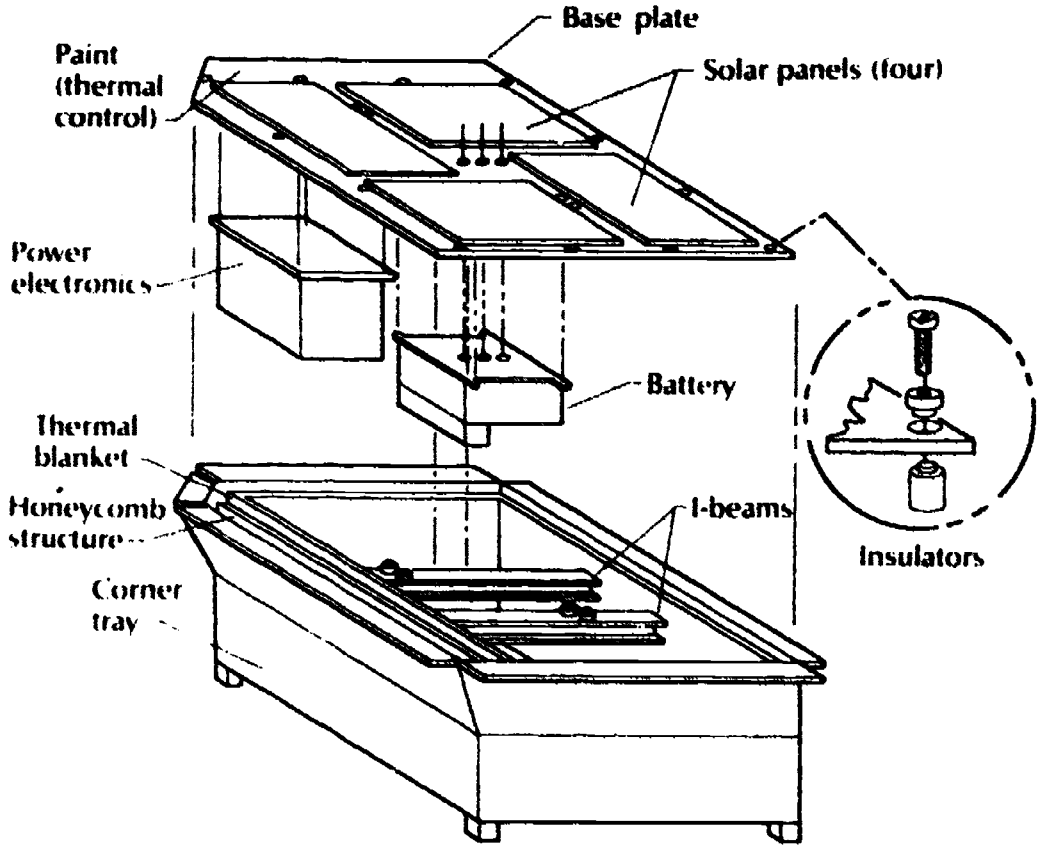
Figure 33.—Solar-panel Ni-Cd battery system.

73

# Transverse Flat-Plate Heat Pipe Experiment (S1005)

James W. Owen
NASA George C. Marshall Space Flight Center
Huntsville, Alabama

Fred Edelstein
Grumman Aerospace Corporation
Bethpage, New York

## Background

For a number of years, NASA Marshall Space Flight Center has actively pursued the practical application of heat pipe technology to actual thermal control hardware. A number of heat pipe concepts have been developed into breadboard hardware and extensively tested under thermal vacuum conditions to verify performance. For example, programs have been successfully completed which demonstrated a deployable heat pipe radiator, transverse heat pipes, an isothermal heat pipe plate, and a total heat pipe thermal control system. In addition to these hardware programs, thermal investigations of future vehicles, such as the space station, strongly indicate the advantages of heat pipe thermal control systems. With this overwhelming support favoring heat pipe thermal control systems, future payloads currently in the early design phase still revert to flight-proven thermal control techniques. This experiment offers a unique opportunity to provide flight demonstration of currently available heat pipe thermal control technology to remove the stigma from its general acceptance for space applications.

A transverse heat pipe is a variable-conductance heat pipe (VCHP) which can handle relatively large thermal loads. It was developed to circumvent the gas bubble artery blockage problem associated with conventional artery wick designs which limited their capacity to small loads in the VCHP mode. In the basic design of a transverse heat pipe, liquid flows in a direction transverse or perpendicular to the vapor flow. Temperature control is achieved by using conventional noncondensible-gas techniques.

The concept of this investigation is to utilize current basic heat pipe technology to design and fabricate a heat pipe thermal control module experiment, demonstrate the hardware capability and performance in the Shuttle flight environment, and verify the ground versus flight data correlation. It is anticipated that the self-regulated transverse flat-plate heat pipe will maintain the temperature control areas of the experiment within the tolerance specified with varying heat inputs independent of LDEF orientation.

74

## Objective

The objective of this experiment is to evaluate the zero-g performance of a number of transverse flat-plate heat pipe modules. Performance will include the transport capability of the pipes, the temperature drop, and the ability to maintain temperature over varying duty cycles and environments. Additionally, performance degradation, if any, will be monitored over the length of the LDEF mission. This information is necessary if heat pipes are to be considered for system designs where they offer benefits not available with other thermal control techniques.

## Approach

As shown in figure 34, three transverse flat-plate heat pipe modules will be installed in a 12-in.-deep peripheral tray. Heat will be supplied to the evaporator side of the module by a battery power supply that will simulate various watt density equipment heat dissipators. This heat will be radiated to space from the outboard-facing radiator surface of the modules. Pretimed heater duty cycles will provide load inputs at discrete mission times. Thermocouple data recording the performance of the heat pipes will be stored on magnetic tape for analysis after retrieval of the experiment. The entire experiment will be self contained with respect to power supply, data storage, and on-orbit cycling. An experiment power and data system (EPDS) will be used for the data recording and $LiSO_2$ batteries will provide EPDS power.

Heat will be supplied to the modules through foil heaters bonded directly to the interior surface of the modules. The batteries and other components are not utilized to supply heat to the modules because it was desired to be able to accurately control the module environments and vary the heat loads to allow a more detailed verification of the experiment capability. Heater power will be provided by 28-V lithium monofluorographite batteries.

The experiment timeline is shown in figure 35. Three identical experiment "on" times are planned during the mission. Each "on" time will last approximately 13 hours (8.6 orbits) and will have heat input to the modules as shown in figure 36. Each "on" period will be subdivided into two 4.3-orbit heater input periods to verify proper operation of each module. The initial "on" will occur approximately 1 month after launch, the second "on" 67.5 days later, and the third 67.5 days after that. The three identical "on" periods at different times of the mission should allow identification of any performance changes during orbital lifetim .
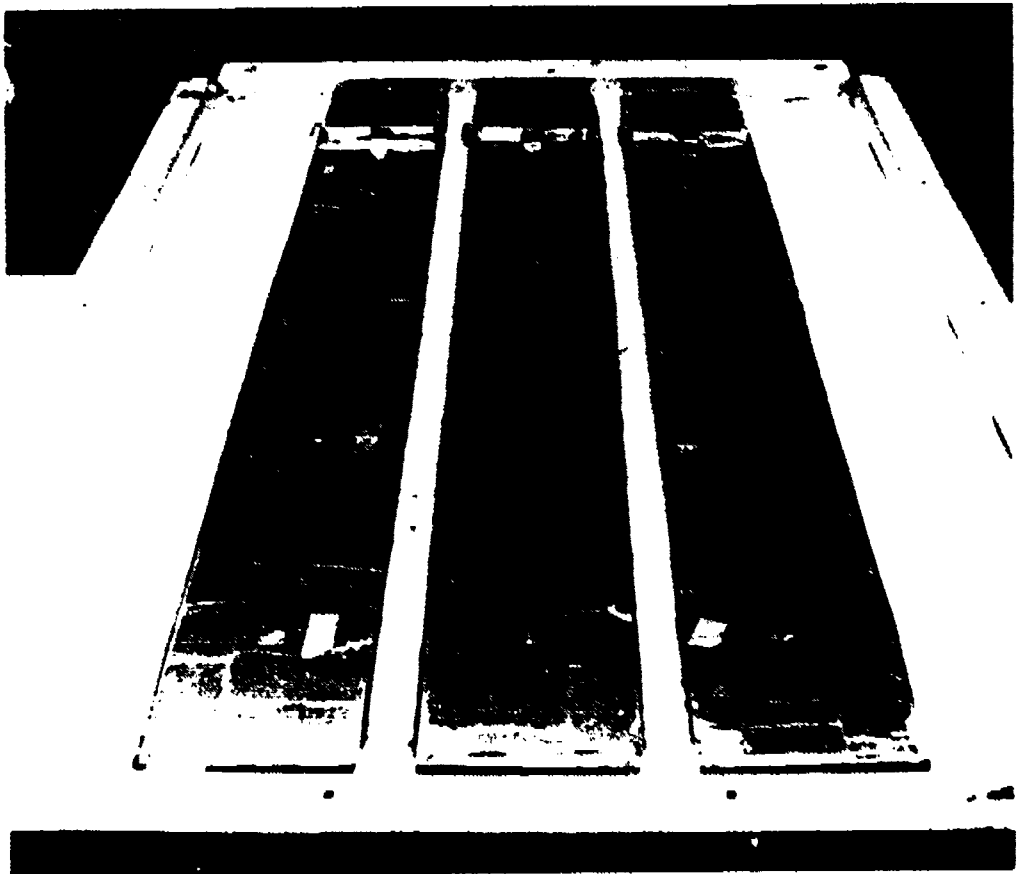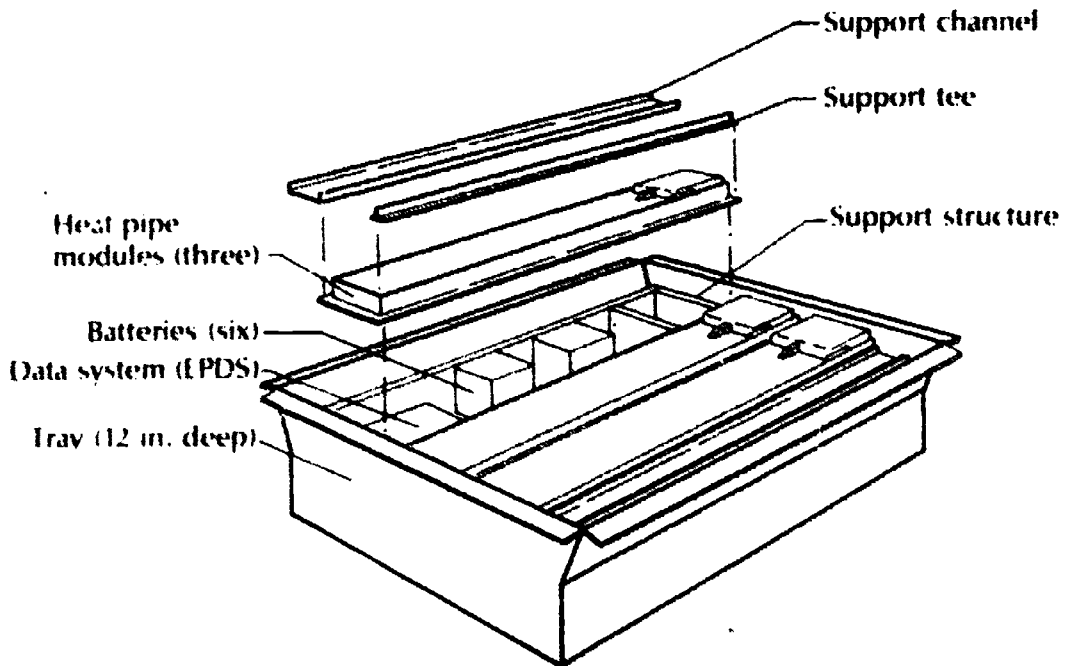
Figure 34.—Transverse flat-plate heat pipe experiment.

83
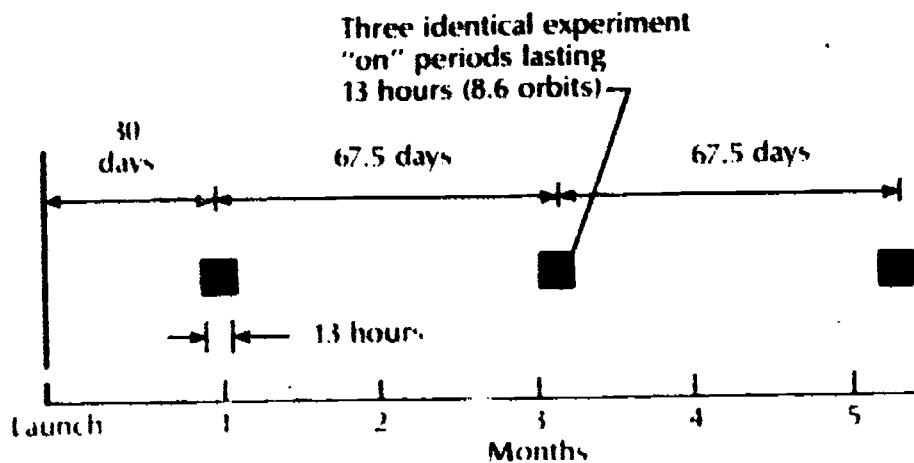
Figure 15. – Experiment timeline.
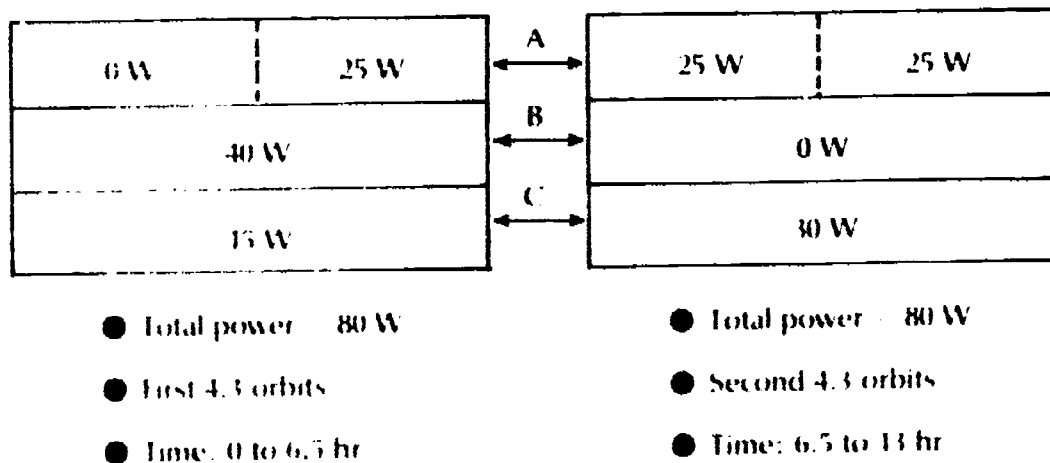


Figure 16. – Heating sequence

84

# LDEF Thermal Measurements System
## (P0003)

Robert F. Greene, Jr.
NASA Langley Research Center
Hampton, Virginia

## Background

Many of the passive experiments flying on LDEF will be significantly enhanced if data are available postflight to indicate the temperature-time histories of test materials and other specimens exposed in the experiments. The baseline LDEF approach was to provide postflight calculated temperature histories of experiment boundaries and solar flux data for the mission, which can in turn be used by each investigator to calculate the temperature-time histories for critical experiment components. Without in-flight temperature measurements, a substantial uncertainty ($\pm 40°F$) will exist in the calculated temperatures. The data measured by the thermal measurement system (THERM) will significantly improve postflight knowledge of temperatures experienced by LDEF experiments. The THERM data will also be valuable in validating the LDEF thermal design concept and in providing better design data for experimenters on future LDEF missions.

## Objectives

The objectives of this experiment are to determine the history of the interior average temperatures of the LDEF for the total orbital mission and to measure the temperatures of selected components and thermal boundary conditions.

## Approach

The THERM system consists of six copper-constantan thermocouples (T/C's), two thermistor reference measurements, an electronic system, one 7.5-V battery, and an interface harness with the HEPP experiment. Data are recorded on dedicated channels of a shared EPDS tape recorder in the low-temperature heat pipe experiment package (HEPP) (S1001).

The THERM hardware locations are shown on LDEF in figure 37. Measurement 1 provides the temperature of the center structure and a backup measurement of the average temperature. Measurement 3 is on the top of the dome surrounding the viscous magnetic damper. Measurement 4 is on a radiometer suspended in the middle of the center ring and is designed to track the average interior temperature of LDEF. Measurement 5 is on a side longeron structure that is expected to see the maximum structural tempera-
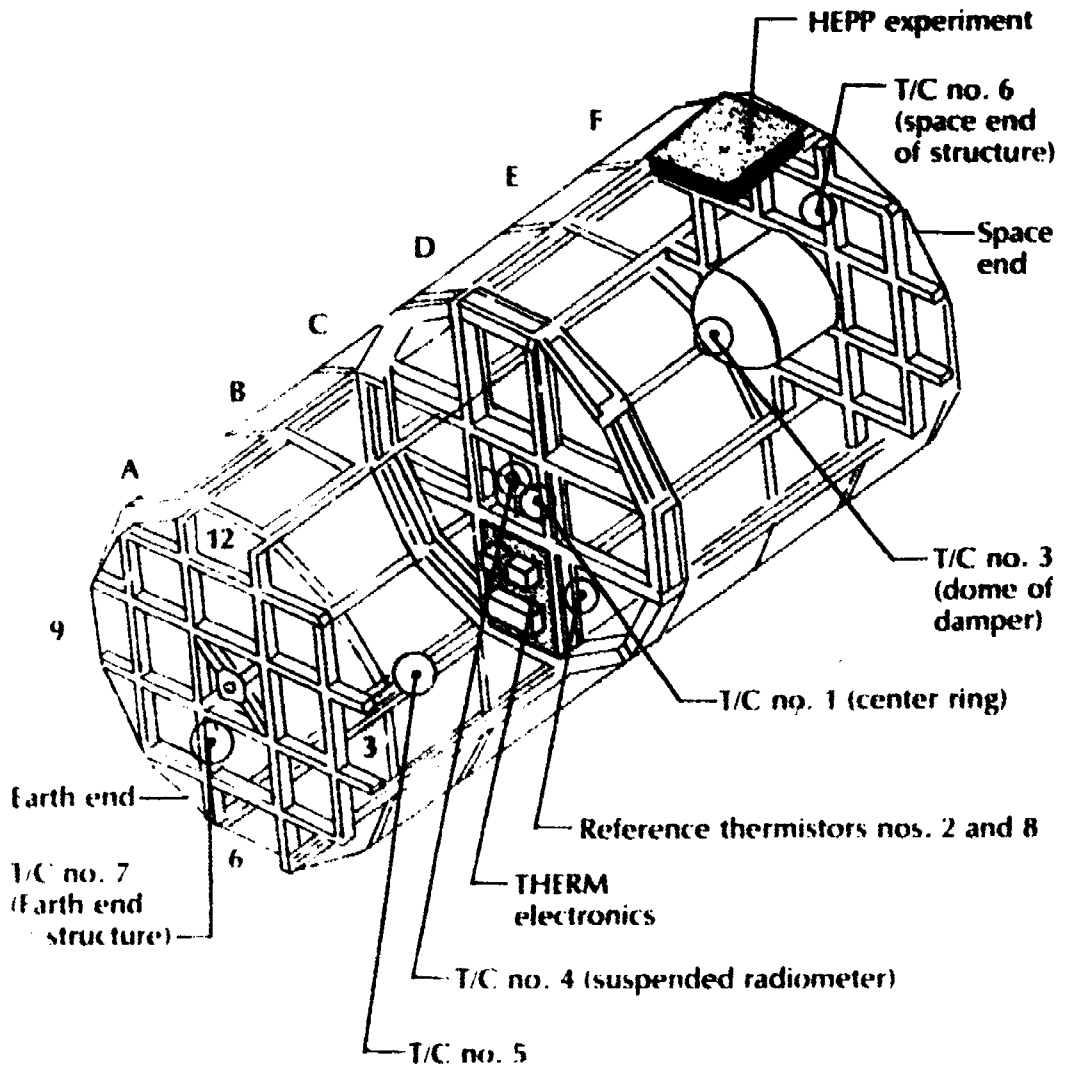
*Figure 37.- Location of THERM hardware on LDEF.*

ture. This measurement can also be used for rough attitude determination of the LDEF. Measurement 6 is on the space end of the structure and provides a representative boundary condition for the experiments mounted on the space end. Measurement 7 gives similar data for the Earth-facing end. Measurements 2 and 8 are thermistors that measure the reference junction temperature in the THERM electronics.

Operationally, THERM will be activated when it receives its own initiate or "set" signal from LDEF just prior to LDEF deployment into orbit. Routine scans of data will be taken about 12 times daily; however, on occasions during the mission the HEPP logic will trigger the EPDS to record data in the high-frequency data recording mode for periods up to 15 days. During the high-frequency mode, data scans will be taken every 5 minutes to

provide temperature profiles throughout typical orbits. The THERM data will therefore provide both long-term and transient temperatures. Total system accuracy is within plus or minus 10°F for all measurements over a range from −30°F to 170°F.

The THERM data, other experiment temperature data, and LDEF attitude information will be reduced and analyzed postflight to provide each experimenter with an improved time history of the experiment boundary conditions encountered during the LDEF mission.

80

*Power and Propulsion*

# Space Plasma High-Voltage Drainage Experiment (A0054)

William W. L. Taylor and Gene K. Komatsu
TRW Space and Technology Group
Redondo Beach, California

## Background

Thin dielectric films are frequently employed as the coating materials for solar arrays and in thermal control applications. These films are subject to electric stress as a result of either voluntary or involuntary actions. For solar-array applications, the presence of array voltages causes electric stress across the dielectric film and to the space plasma, with resultant current drainage from the plasma to the array cells. As array voltages are raised, electric stress and current drainage levels also rise and may impact array operation and efficiency. For both thermal control coating materials and array coating materials on spacecraft immersed in energetic particle environments in space, involuntary charge buildup occurs and results in both transient and steady-state current drainage that may impact spacecraft operation.

## Objectives

The objectives of this experiment are to place large numbers of dielectric samples under electric stress in space; to determine their in-space current drainage behavior; to recover, inspect, and further test these samples in laboratory facilities; and finally to specify allowable electric stress levels for these materials as applied to solar-array and thermal control coatings for prolonged exposure in space. These findings, in turn, will pace the design of encapsulated, lightweight, high-voltage solar arrays as well as the development of coating materials for spacecraft operation in energetic charged-particle environments such as that experienced at geosynchronous altitudes during magnetic substorms.

## Approach

The drainage current behavior of thin dielectric (insulating) films in space is determined by placing the forward (exposed) face of the film in contact with the space plasma while applying a bias voltage to a conducting layer on the rear (nonexposed) face. Current flow from the rear-face conduction film through the dielectric to the charged-particle environment of space occurs as a result of the bias potential. The completion of the current loop occurs when charged particles are collected from the space plasma by the

frame of the LDEF and are then delivered to the ground return of the bias voltage supply. Figure 38 illustrates the experimental arrangement. The bias potential is developed by a self-contained battery and power processor unit. Each dielectric sample has an associated battery and power processing unit, except for the "spectator" samples, which are not electrically stressed in flight and hence allow a determination of the effects of merely being present on the LDEF. Figure 39(a) illustrates the dielectric sample construction. The actual experiment will occupy two 3-in. deep peripheral trays. One tray will be located near the LDEF leading edge and the other will be near the trailing edge. This configuration will allow the determination of charged-particle drainage as a function of plasma density. Figure 39(b) shows a top view of one tray, minus the test samples.

The dielectric sample power processor is equipped with two cou-lometers. The first of these is in series with the bias voltage lead and determines the integral of the drainage current during the flight. The second coulometer, which has a high-value in-series resistor, is placed between the
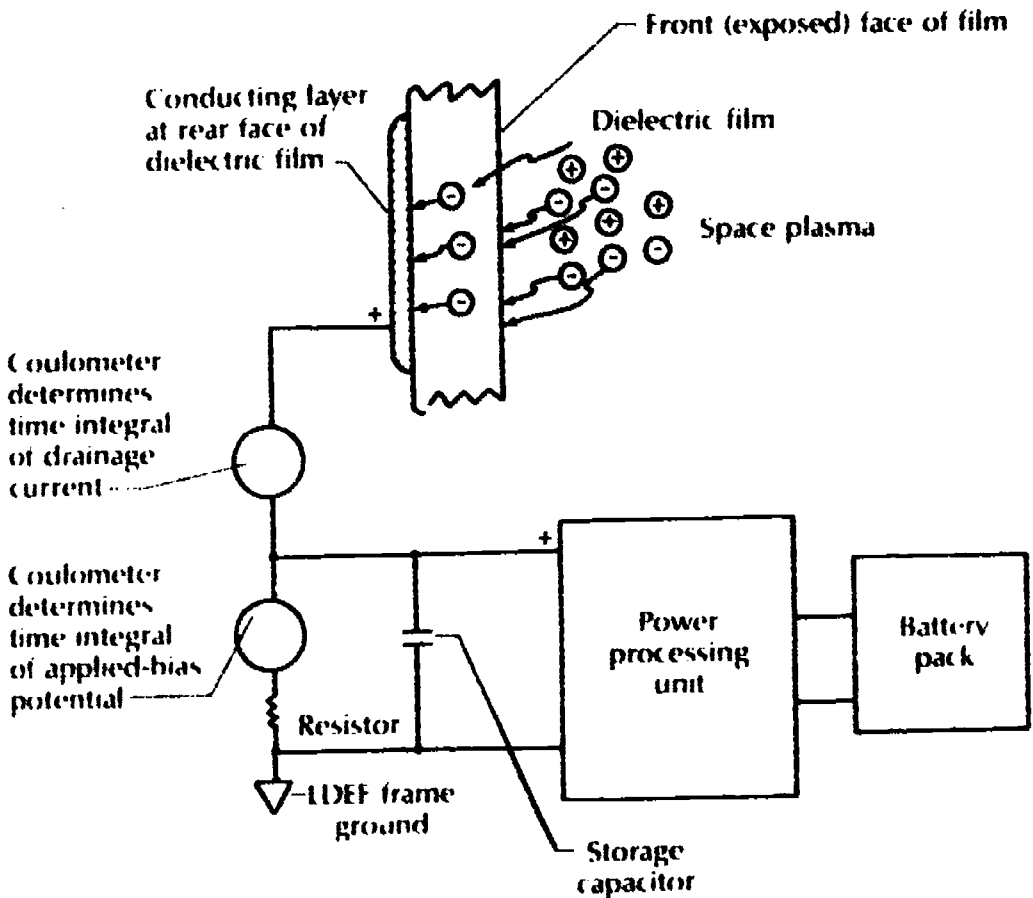


Figure 38. High-voltage drainage experiment concept.

83

Connector details

LDEF exterior
surface

Electronics package

Kapton
VDA film
Conducting epoxy
Aluminum sheet
Epoxy
Kevlar

Sample details
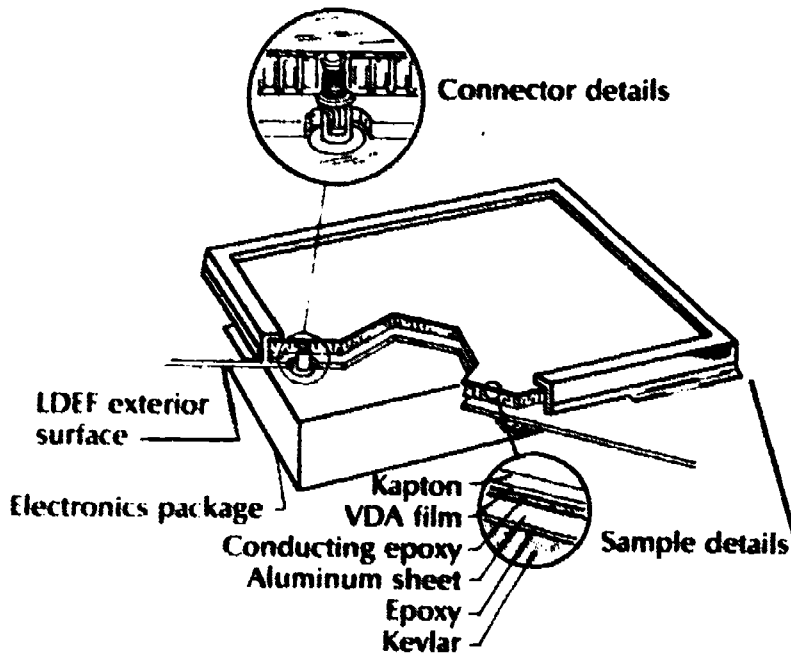
(a) Dielectric sample construction.
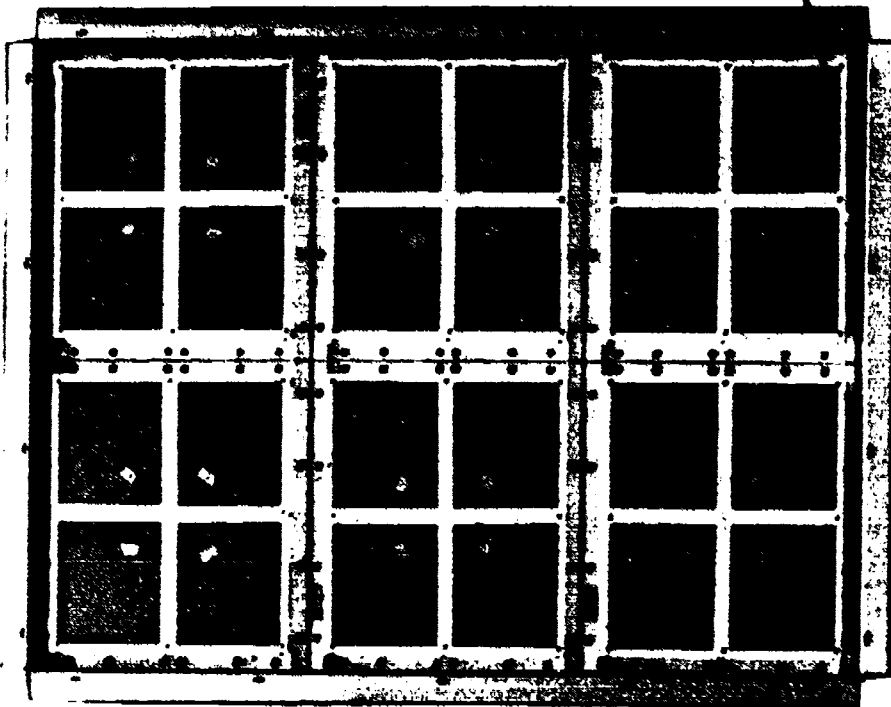
(b) Top view of tray.

Figure 39. *Space plasma high-voltage drainage experiment.*

84

bias potential and LDEF ground to determine the time-integrated applied-bias voltage. An average front-to-back resistance of the dielectric sample is determined from the measured time integrals of drainage current and bias potential, and the bulk resistivity of the dielectric material under applied stress and in the space environment is determined from known surface area and film thickness. If this bulk resistivity remains greater than certain minimal limits for a given bias potential, then use of the material for high-voltage solar arrays would be permitted for this series of specified environmental and electrical conditions. Deterioration of dielectric properties under continued stress would rule out use in the high-voltage arrays and would present significant long-term equilibration data for spacecraft coating materials subjected involuntarily to charge and voltage buildup because of energetic charged-particle deposition.

85

# Solar-Array-Materials Passive LDEF Experiment (A0171)

Ann F. Whitaker, Charles F. Smith, Jr., and Leighton E. Young
NASA George C. Marshall Space Flight Center
Huntsville, Alabama

Henry W. Brandhorst, Jr., and A. F. Forestieri
NASA Lewis Research Center
Cleveland, Ohio

Edward M. Gaddy and James A. Bass
NASA Goddard Space Flight Center
Greenbelt, Maryland

Paul M. Stella
Jet Propulsion Laboratory
Pasadena, California

## Background

The long-duration functional lifetime requirements on lightweight high-performance solar arrays demand careful selection of array materials. The space environment, however, is a hostile environment to many materials, and some of the problems are well documented. A thermal-vacuum environment can affect materials by accelerating the outgassing of volatile species. The condensation of these outgassed products on array cover slips will lead to reduced solar-cell electrical output, a situation that is especially critical at high astronomical units (AU's). Outgassing can reduce mechanical strength in materials, which will affect the integrity of the array substrate, hinges, and deployment mechanisms and create electrical problems through insulation breakdown. A further effect of outgassing is the degradation of thermal control and reflector surfaces. Some extended performance arrays that have been studied but never flown utilize deployable concentrators whose reflectance is especially important at large AU's. Protons, electrons, atomic oxygen, and UV irradiation contribute to surface damage in these array materials. Thin-film materials can become embrittled and thermal control surfaces can become discolored by this irradiation. Severe mission environments, coupled with the lack of knowledge of space environment materials degradation rates, require the generation of irradiation and outgassing engineering data for use in the design phase of flight solar arrays.

## Objective

The objective of this experiment is to evaluate the synergistic effects of the space environment on various solar-array materials, including solar cells, cover slips with various antireflectance (AR) coatings, adhesives, encapsulants, reflector materials, substrate strength materials, mast and harness materials, structural composites, and thermal control treatments.

## Approach

The experiment is passive and consists of an arrangement of material specimens mounted in a 3-in.-deep peripheral tray. A photograph of the tray, which has been subdivided among the various experiment organizations, is shown in figure 40. The effects of the space environment on the specimens will be determined by comparison of preflight and postflight measurements of mechanical, electrical, and optical properties.
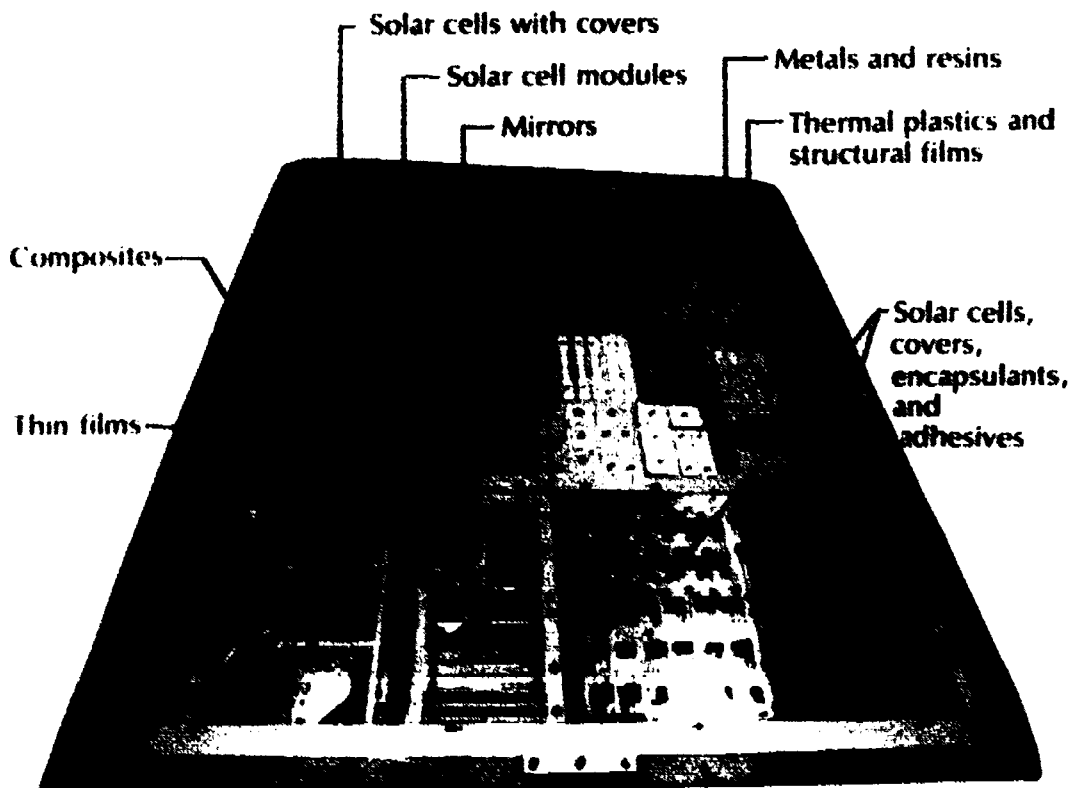


Figure 40.—Solar-array materials experiment.

87

# Advanced Photovoltaic Experiment
# (S0014)

Henry W. Brandhorst, Jr., and A. F. Forestieri
NASA Lewis Research Center
Cleveland, Ohio

## Background

The advanced photovoltaic experiment consists of a group of three photovoltaics-related experiments for investigating a portion of the solar spectrum and the effect of the space environment on photovoltaics. The information will be used to provide correlation between space and ground testing and also to provide for more accurate performance measurement in the laboratory.

## Objectives

Specific objectives of these experiments are to provide information on the performance and endurance of advanced and conventional solar cells, to improve reference standards for photovoltaic measurements, and to measure the energy distribution in the extraterrestrial solar spectrum.

## Approach

The experiment will occupy a 12-in.-deep peripheral tray and will use an experiment power and data system (EPDS) for data recording and $LiSO_2$ batteries to satisfy power requirements. Figure 41 shows a photograph of the experiment.

The experimental approach for the three experiments is detailed below.

Space Exposure of Solar Cells

Space exposure of advanced and conventional cells will provide information on the performance and endurance of such cells in the space environment. Correlation between space environment and ground simulation test results will also be verified by this experiment.

Data to be obtained will include temperatures and short-circuit current of the samples. Six-point current-voltage (I-V) characteristics will be obtained for selected samples. These data will be recorded once a day during the flight. Orbit data will be correlated with preflight and postflight measurements of the samples.
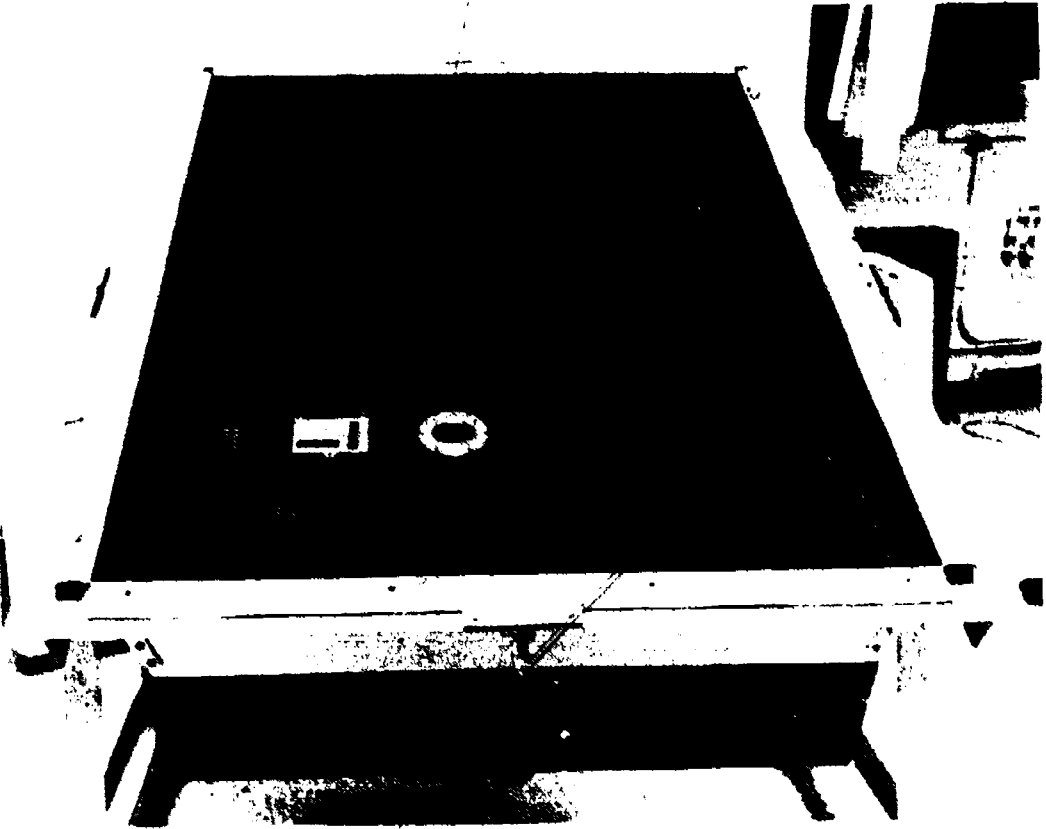
*Figure 41.—Advanced photovoltaic experiment.*

### Reference Solar-Cell Calibration

Various reference cells, including some previously measured on balloon, aircraft, or rocket flights, will be measured before flight and throughout the flight to determine their outputs (short-circuit current). Upon return, those cells with known output in space will serve as laboratory standards for accurate determination of space output from other cells and arrays. The flight of previously calibrated cells will permit verification of the accuracy of the various calibration techniques.

### Solar Spectrum Energy Distribution

A series of optical bandpass filters coupled to solar-cell detectors will be used to determine the energy in 16 spectral regions between 0.3 and 1.1 μm. In addition, the total energy in the spectrum above and below 0.5 μm will be measured using a dichroic 45° mirror. The characteristics of the filters will be measured both preflight and postflight. The energy within the appropriate bandpass will be determined from the short-circuit current of the detector solar cell measured in space. These measurements will be used to assess the accuracy of laboratory instruments such as the filter wheel solar simulator.

89

Finally, the total energy in the solar spectrum will be determined with an absolute radiometer detector.

The following participants have supplied samples for these experiments: Air Force Wright Aeronautical Laboratory; Applied Solar Energy Corporation; Comsat Laboratory; European Space Agency; Hughes Research Laboratory; Jet Propulsion Laboratory; Lockheed Missiles and Space Company, Inc.; NASA Langley Research Center; NASA Lewis Research Center; NASA Marshall Sp:  "light Center; Rockwell International Corporation; Solarex Corporatio     ectrolab Inc.; Spire Corporation; and Varian Associates.

Experiment operatic : will be automatically timed by the EPDS clock, which begins with an init. .e command at LDEF deployment. Data will be recorded once each day when a maximum Sun angle less than $20^\circ$ is reached. (This will be determined by a two-axis Sun angle sensor, which detects the maximum cosine angle for the data period.) A scan of data will consist of timing, Sun sensor output, temperatures, six-point current-voltage data of 16 solar cells, and short-circuit currents of 120 cells. Approximately 1 month prior to planned retrieval of the LDEF, the experiment will be terminated.

# Investigation of Critical Surface Degradation Effects on Coatings and Solar Cells Developed in Germany (S1002)

Ludwig Preuss
Space Division, Messerschmitt–Bölkow–Blohm
Munich, Federal Republic of Germany

## Background

Various coatings developed in the FRG (i.e., second-surface mirrors with interference filters with and without conductive layers, conductive layers on solar-cell covers, and selective absorber coatings) have been qualified by accelerated tests under simulated space environment conditions. Experiments with coatings and solar cells have shown, however, that the thermo-optical behavior can differ considerably when performed on the ground and in space because of the great difficulty in simulating the space environment realistically.

## Objectives

The objective of this experiment is to qualify these coatings under realistic space environment conditions. In addition, the experiment will provide design criteria, techniques, and test methods to insure control of the combined space and spacecraft environment effects, such as contamination, electrical conductance, and optical degradation, on the coatings.

## Approach

Figures 42 and 43 show the experiment arrangement and electronics block diagram, and table 10 lists the samples to be investigated. Test samples will be installed in an experiment exposure control canister (EECC) and on a cover sheet near the upper surface of the 6-in.-deep peripheral tray. The samples in the canister will be exposed only to the space and spacecraft environment because the canister will be opened after LDEF deployment and closed prior to LDEF retrieval. The other samples will be exposed to the complete mission environment. Data to be measured include the temperature of the samples, the electrical resistance of the conductive layers of the samples, the short circuit current of the solar-cell modules, and the deposition of contaminants on the samples (using quartz crystal microbalances (QCM's)).

The data will be measured according to a defined time program and will be amplified, digitized, and stored on a data recorder. After the return of the

98

91
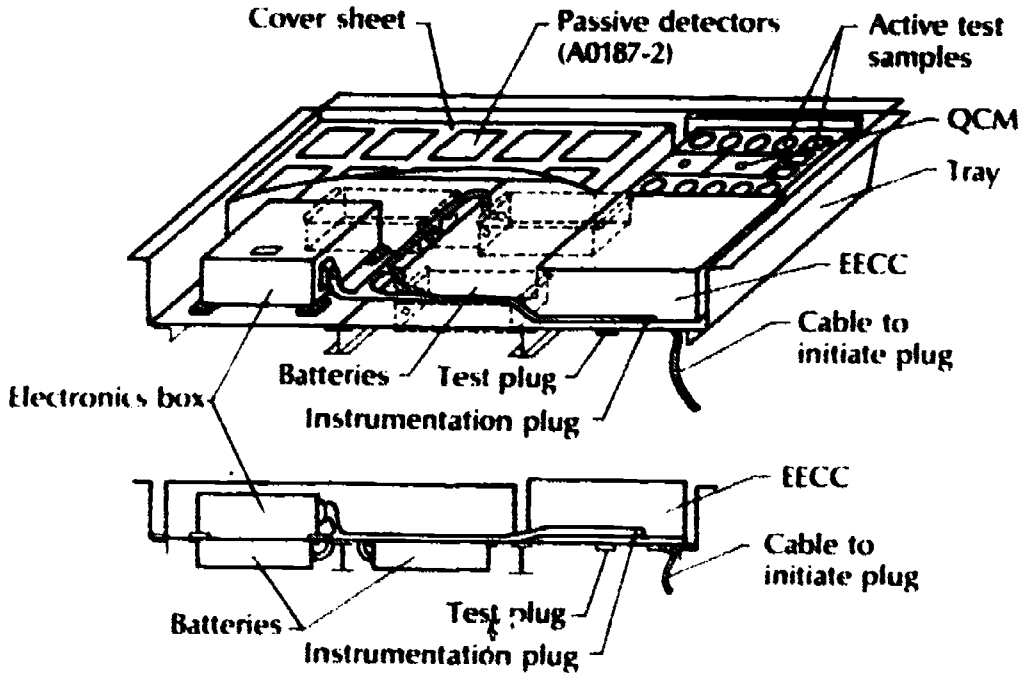
Figure 42. - Experiment arrangement.
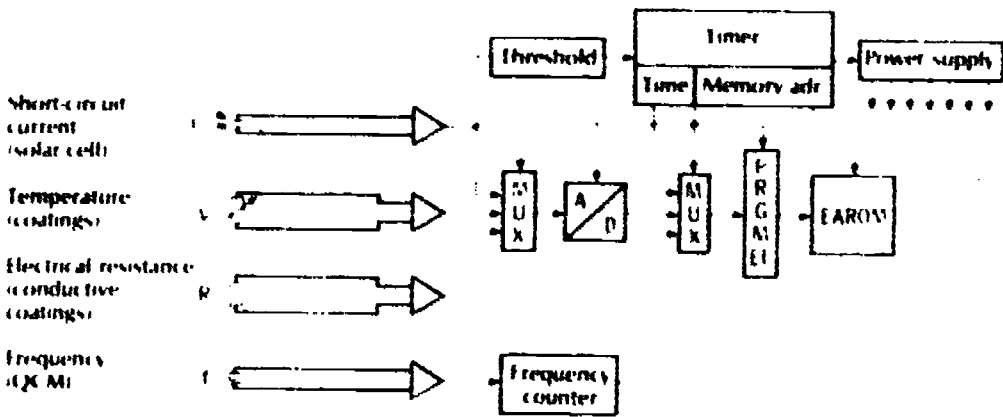


Figure 43.--Electronics block diagram.

experiment, the stored data will be evaluated along with the data for attitude and related solar aspect angles to determine relations between space conditions and surface effects on the test samples. In addition, contamination will be investigated by means of infrared spectroscopy, and the electrical characteristics of the solar cells will be determined.

99

**Table 10.—Test Samples To Be Investigated**

| Components to be investigated |
| --- |
| Second-surface mirror with<br>  Ag reflector and Inconel protection layer on rear<br>  Interference filter on front face<br>Second-surface mirror with<br>  Ag reflector and Inconel protection layer on rear<br>  Interference filter on front face<br>  Doped $In_2O_3$ layer on interference filter<br>Chromium black selective absorbers<br>Solar-cell modules with doped $In_2O_3$ layer on cover glass |
| Reference components |
| Second-surface mirror with Ag reflector and Inconel protection layer on rear<br>Optical solar reflector with Ag reflector and Inconel protection layer on rear<br>Solar-cell module |

93

# Space Aging of Solid Rocket Materials
## (P0005)

Leon L. Jones and R. B. Smalley, Jr.
Morton–Thiokol, Inc.
Brigham City, Utah

## Background

Solid-rocket motors continue to be used extensively in space applications, and future missions have been identified in which the solid motor may be stored in space for an extended time before firing. This indicates a need to gather direct information on the effects of extended storage of rocket materials in the combined vacuum and thermal conditions of space. Tests have been performed in high vacuum to determine outgassing characteristics, but only limited testing has been done on the effects of vacuum on the mechanical and ballistic properties of the materials themselves. Most vacuum aging has been plagued by mechanical problems and subsequent back contamination of the material samples.

## Objective

The objective of this experiment is to determine the effects of long-term orbital exposure on the materials used in solid-rocket space motors. Specifically, structural materials and propellants from the STAR/PAM-D series motors and the PAM DII/IPSM-II motors will be tested, as well as advanced composite case and nozzle materials planned for future use.

## Approach

The experiment approach is to expose samples of solid-rocket propellant, liner, insulation, case, and nozzle specimens to the space environment and to compare preflight and postflight measurements of various mechanical, chemical, and ballistic properties to determine the effects of long-term orbital exposure. A parallel program will be conducted on ground storage san , thus the data will be applicable on a generic basis as well as to the sp     , materials being tested.

Figure 44 shows a view of the IPSM-II space motor with some of the sample materials identified. Table 11 lists the STAR materials and the tests to be performed. These materials will be packaged within a 5- by 6.5- by 11.5-in. aluminum container and attached to an interior plate on the LDEF center ring. The container will be flushed with dry nitrogen and sealed before installation on the LDEF. An air-pressure-activated valve has been designed

Case (Kevlar-epoxy)

Insulation (EPDM rubber)

Case-insulation interface

Skirt (glass-epoxy)

Shear ply (case,
NBR rubber, skirt)

Nozzle throat
(three-dimensional carbon)

Extendable exit cone
(two-dimensional carbon)

Propellant

Igniter housing

Igniter-propellant
interface

Propellant-liner-
insulation interface
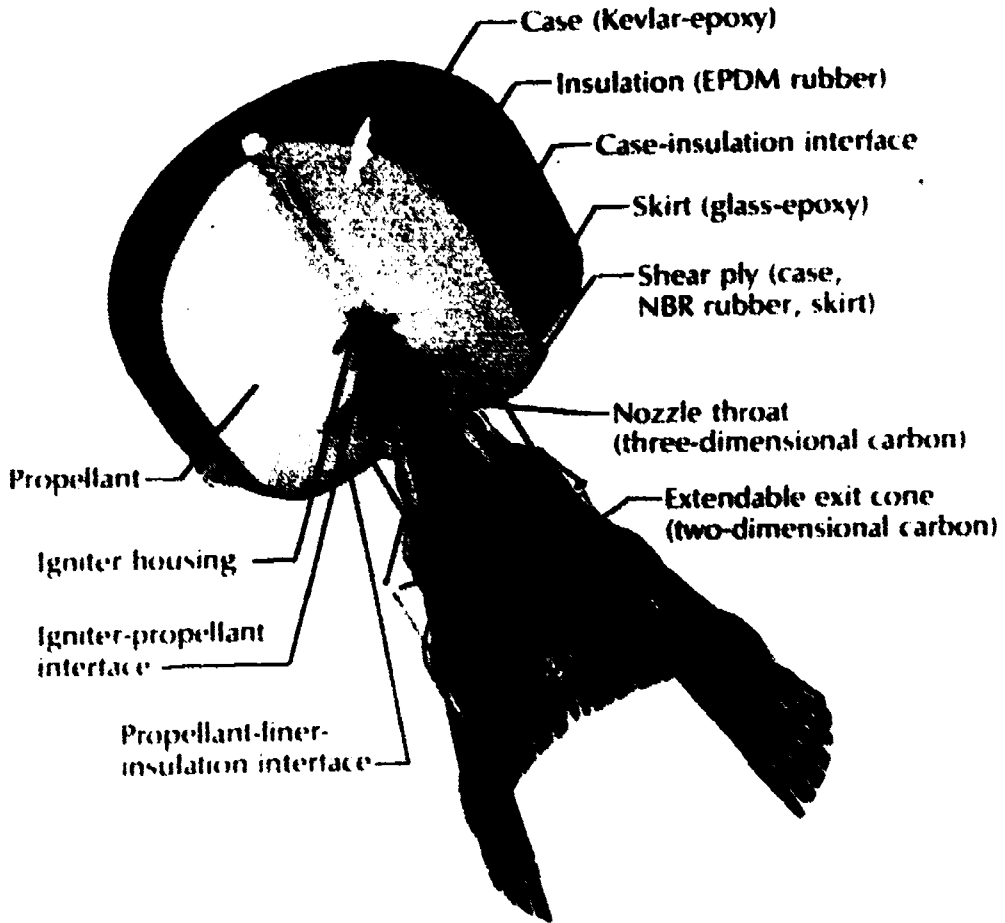
Figure 44.   Sketch of IPSM-II motor showing examples of aging samples.

to vent the box when it is subjected to pressure below 0.2 atm, leaving the box open to the vacuum. On reentering, the valve will close at 0.5 atm external pressure.

**Table 11.—Solid-Rocket Materials** [a]

| Mechanical properties: tensile, relaxation, dynamic | |
|---|---|
| Propellant materials:<br>  IPSM-II PAM-DII<br>  STAR PAM-D | Nozzle materials:<br>  Carbon-carbon<br>  Silica-phenolic<br>  Carbon-phenolic |
| Insulation:<br>  EPDM rubber<br>  NBR rubber | Case materials:<br>  Kevlar-epoxy<br>  Graphite-epoxy<br>  Glass-epoxy |
| **Interface strength: tensile, peel, constant load** | |
| Titanium-insulation<br>Kevlar-insulation<br>Graphite-insulation<br>Kevlar-NBR-glass | Glass-insulation<br>Three propellants-insulation<br>Igniter housing-propellant |
| **Ballistic properties: burning rate** | |
| IPSM-II PAM-DII propellant and igniter assembly<br>STAR PAM-D propellant and igniter<br>Boron-potassium nitrate pellets | |

[a] All of the samples will be subjected to determination of weight loss with attendant chemical analyses

**103**

*Science*

97

# Interstellar-Gas Experiment
## (A0038)

Don L. Lind
NASA Lyndon B. Johnson Space Center
Houston, Texas

Johannes Geiss and Fritz Bühler
University of Bern
Bern, Switzerland

## Background

In the past, the observed regularities in the abundance of elements and their isotopes, upon which the theory of nucleosynthesis rests, have been obtained primarily from solar system abundances, in particular meteoritic, solar, terrestrial, and solar-wind data. However, this sample represents only a tiny fraction of the material of the universe. Thus, even a small sample of extra-solar-system isotopes will give significant insight into the various element-building processes that have occurred in the original nucleosynthesis and those which have been going on in our galaxy. Isotopic analysis of the noble-gas component of the interstellar gas will provide a significant new data source and will complement other promising techniques, such as millimeter-wave, cosmic-ray, and nuclear-gamma-ray astronomy.

## Objectives

The primary objective of this experiment is to collect interstellar gas atoms in metal foils at several locations around the Earth's orbit. These particles arrive in the vicinity of the Earth as the neutral interstellar wind penetrates the heliosphere and enters the region of the inner planets. The flow pattern of the interstellar wind is controlled mainly by the gravitational attraction of the Sun, and its density is reduced through ionization by solar photons and by charge exchange with the solar-wind particles. The flux of the interstellar atoms that survive the upstream journey in the solar wind is increased due to gravitational focusing as they pass beyond the Sun. The angular distribution of these particles is also significantly modified in the gravitational focusing process. Thus the density and angular distribution of the interstellar gas flux vary considerably at different points in the Earth's orbit. In addition to these variations, the velocity of these particles as they impact the spacecraft changes over a wide range as the orbital motion of the Earth moves seasonally first upstream, then cross stream, and finally down-stream in the interstellar wind. These seasonal variations constitute the

signature by which the interstellar particles can be identified. By collecting these particles at several locations in the Earth's orbit, it will be possible not only to achieve an *in situ* detection of the interstellar gas for the first time. but also to study the dynamics of the interstellar wind as it flows through the heliosphere and interacts with the solar photon flux and the solar wind. In addition, because the dynamics of the interstellar wind depend on its density and velocity before entering the heliosphere, it will be possible to investigate these characteristics of the interstellar medium outside the region of the solar system.

Thus, the objectives of this experiment are to collect and isotopically analyze interstellar gas atoms around the orbit of the Earth for the purpose of obtaining new data relevant to understanding nucleosynthesis, and to study the dynamics of the interstellar wind inside the heliosphere and the isotopic composition of the interstellar medium outside the heliosphere.

## Approach

The experiment hardware will act as a set of simple "cameras" with high purity copper-beryllium collecting foils serving as the "film." (See fig. 45.) The experiment housing will mount and thermally control the foils, establish the viewing angles and viewing direction, provide baffling to reject ambient neutral particles, provide a voltage grid to reject ionospheric charged particles, sequence collecting foils, control exposure times, and protect the foils from contamination during the deployment and retrieval of the LDEF. After being returned to Earth, the entrapped atoms can be analyzed by mass spectroscopy to determine the relative abundance of the different isotopes of helium and neon. An attempt will also be made to detect argon. At present, the noble gases are the only species for which this method is sufficiently sensitive.

The experiment will use four trays, two 12-in.-deep peripheral trays and two 12-in.-deep end center trays, on the space-facing end of the LDEF. One of the peripheral trays will contain only one camera and the rest of the trays will contain two cameras. Power requirements will be supplied by LiSO₂ batteries.

**Viewing angle:**
**35.5° to 41°**
**from foil centers**

**High-voltage ion**
**suppression grid**

**Electron**
**suppression grid**

**Neutral**
**particle**
**baffles**

**First collecting foil**
**(exposed and stowed)**

**High-voltage**
**ion suppression**
**grid**

**Second**
**collecting**
**foil**

**Protective**
**cover**
**(open)**

**Third**
**collecting**
**foil**

**Fourth**
**collecting**
**foil**

**Fifth (bottom) foil mounted to**
**base plate (not shown)**
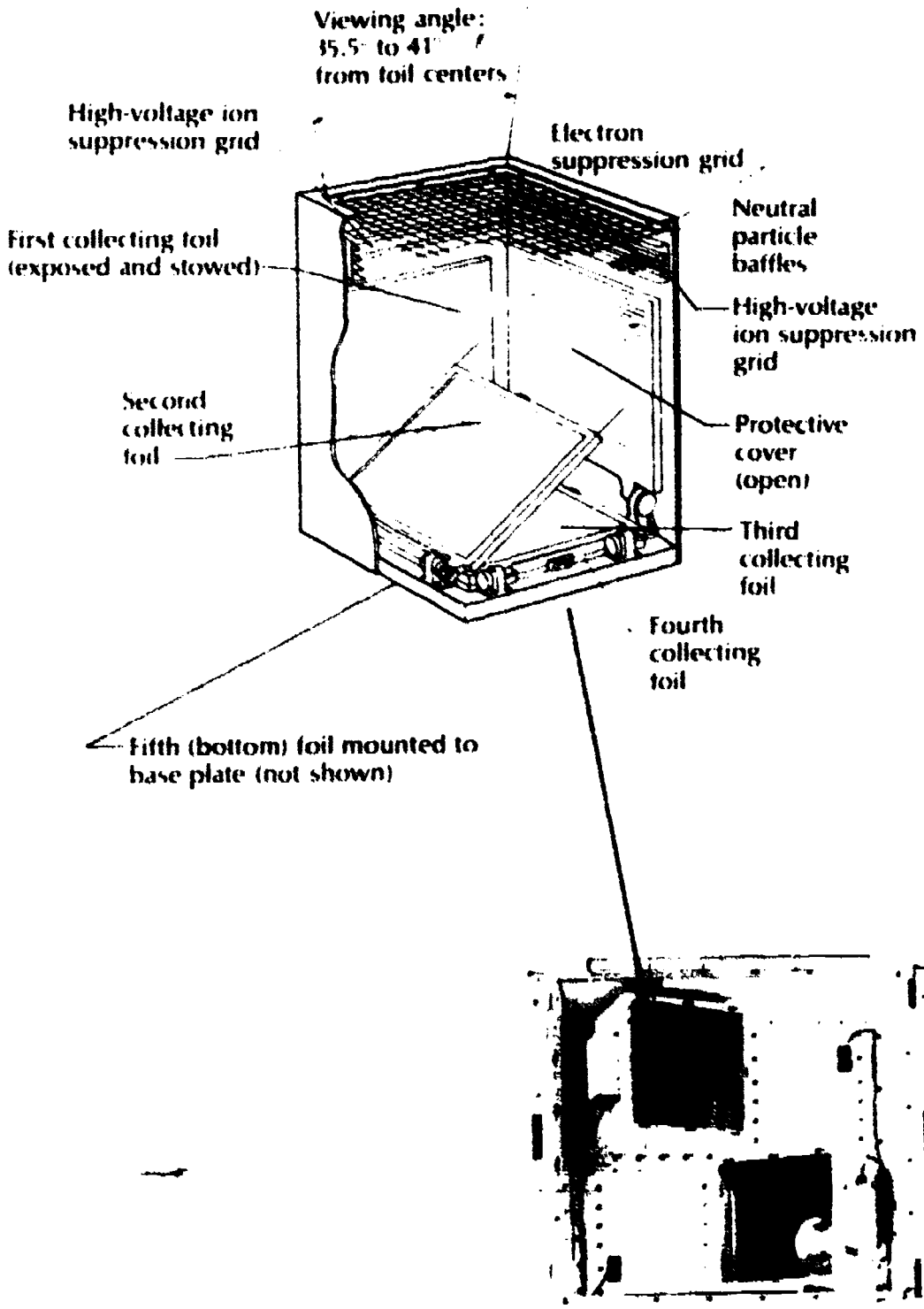
*Figure 45.   Interstellar-gas experiment.*

# A High-Resolution Study of Ultra-heavy Cosmic-Ray Nuclei (A0178)

Denis O'Sullivan, Alex Thompson, and Cormac O'Ceallaigh
Dublin Institute for Advanced Studies
Dublin, Ireland

Vicente Domingo and Klaus-Peter Wenzel
European Space Agency, ESTEC
Noordwijk, The Netherlands

## Background

The measurement of the charge spectrum of ultraheavy cosmic ray nuclei is of vital importance in many areas of astrophysics. Such measurements are relevant to the study of the origin and age of cosmic rays, acceleration and propagation mechanisms, the nucleosynthesis of the heavy elements in our galaxy, and the search for superheavy nuclei ($Z \sim 110$), and may even lead to improved nuclear mass formulas and beta decay rate formulas for the heaviest nuclides. The central theme of this experiment is the utilization of the LDEF's large area time factor to obtain a large and uniform sample of ultraheavy cosmic-ray nuclei in the region $Z \sim 30$.

## Objectives

The main objective of the experiment is a detailed study of the charge spectra of ultraheavy cosmic-ray nuclei from zinc ($Z = 30$) to uranium ($Z = 92$) and beyond using solid-state track detectors. Special emphasis will be placed on the relative abundances in the region $Z \sim 65$, which is thought to be dominated by r process nucleosynthesis. Subsidiary objectives include the study of the cosmic-ray transiron spectrum and a search for the postulated long-lived superheavy (SH) nuclei ($Z \sim 110$), such as $_{110}SH^{294}$, in the contemporary cosmic radiation. The motivation behind the search for super heavy nuclei is based on predicted half-lives that are short compared to the age of the Earth but long compared to the age of cosmic rays. The detection of such nuclei would have far-reaching consequences for nuclear structure theory.

The sample of ultraheavy nuclei obtained in this experiment will provide unique opportunities for many tests concerning element nucleosynthesis, cosmic-ray acceleration, and cosmic-ray propagation. For example, if the r-process domination for $Z \sim 65$ is confirmed, a reliable source spectrum will provide details of the nuclear environment, such as temperature and time

101

scale. This information will be of great importance to both astrophysics and nuclear physics.

The relative abundances of cosmic-ray nuclei in the region $Z > 82$ will lead to a determination of the age of cosmic rays directly from the decay of a primary component, in contrast to estimates based on, for example, Be[10] or Cl[36]. The LDEF exposure may provide a sufficiently large sample of actinides to achieve this objective.

Injection of cosmic-ray particles into the acceleration process may depend upon atomic properties of the elements, such as the first ionization potential. This experiment will help to establish the existence of such mechanisms through their modulation of the ultraheavy charge spectrum.

The cosmic-ray charge spectrum in the region $30 \leq Z \leq 65$, based on the statistics available to date, appears to be generally consistent with solar-system material. The situation is still uncertain, but it is hoped that a radical improvement will be achieved with the LDEF exposure. For example, it is very important to establish the roles played by the helium-burning slow-neutron-capture process in massive stars and the explosive carbon-burning process during supernova explosions.

Since the LDEF orbit inclination is expected to be low (28°), the geomagnetic cutoff will prevent direct measurement of the ultraheavy energy spectrum. However, it is hoped that the slope of the energy spectrum can be determined from an analysis of the abundance distributions about the major axis of the LDEF (east-west effect).

To summarize, cosmic rays constitute a unique sample of material from distant parts of our galaxy which still bears the imprint of the source region. The ultraheavy cosmic-ray composition will provide a great deal of information about the evolution of matter in the universe. This question is closely related to understanding the origins of the elements in the solar system.

## Approach

The experimental approach centers on the use of solid-state track detectors to identify charged cosmic-ray particles. The basic detector component is a thin sheet of polymer plastic (typically 250 µm thick). The determination of charge and velocity depends on the mechanism by which cosmic-ray nuclei that penetrate the plastic sheets produce radiation damage along the particle trajectories. After exposure and recovery, the detector sheets will be chemically processed to reveal the tracks produced by the passage of heavily ionizing particles. The effective amplification of a particle's radiation damage trail results from preferential chemical etching along its trajectory. The rate of etching is a unique function of the particle's ionization.

102

The flux of ultraheavy cosmic-ray nuclei is extremely small (on the order of 1 m$^{-2}$ day$^{-1}$). Consequently, the basic experimental approach entails a large area-time factor exposure coupled with stability in a general radiation environment and the ability to discriminate against the overwhelming background of lower charge components. The main polymer plastic used for the track detectors in this experiment will be Lexan polycarbonate*, which has a registration threshold given by $Z/\beta \sim 56$. It is this threshold property that enables the Lexan to isolate individual ultraheavy nuclei in a very high flux environment of lower charge nuclei.

A new polymer track detector, based on CR-39, is being developed for inclusion in the LDEF experiment. Its predominant characteristic is a very low threshold ($Z/\beta \sim 10$) and it potentially has very high resolving power. By using CR-39 to complement the Lexan, it will be possible to study relativistic nuclei in the lower charge regions, down to iron and below.

The nuclear track detectors, with lead foil energy degraders, will be assembled in stacks that will be mounted in aluminum cylinders designed to fit into 12-in.-deep peripheral trays. Three cylinders, each containing four stacks, will be placed parallel to the x-axis of each tray. (See fig. 46.) The cylinders are approximately 46 in. long and approximately 10 in. in diameter, and have a wall thickness of approximately 0.5 g/cm$^2$. The stacks will have a thickness of approximately 4 g/cm$^2$ and will be mounted parallel to the tray base and placed symmetrically about the main axis of each cylinder using an Eccofoam matrix.

The trays will be thermally decoupled from the LDEF frame and will carry thermal covers flush with their outer rims. Sixteen trays will be employed. Figure 47 shows a photograph of one of the trays.
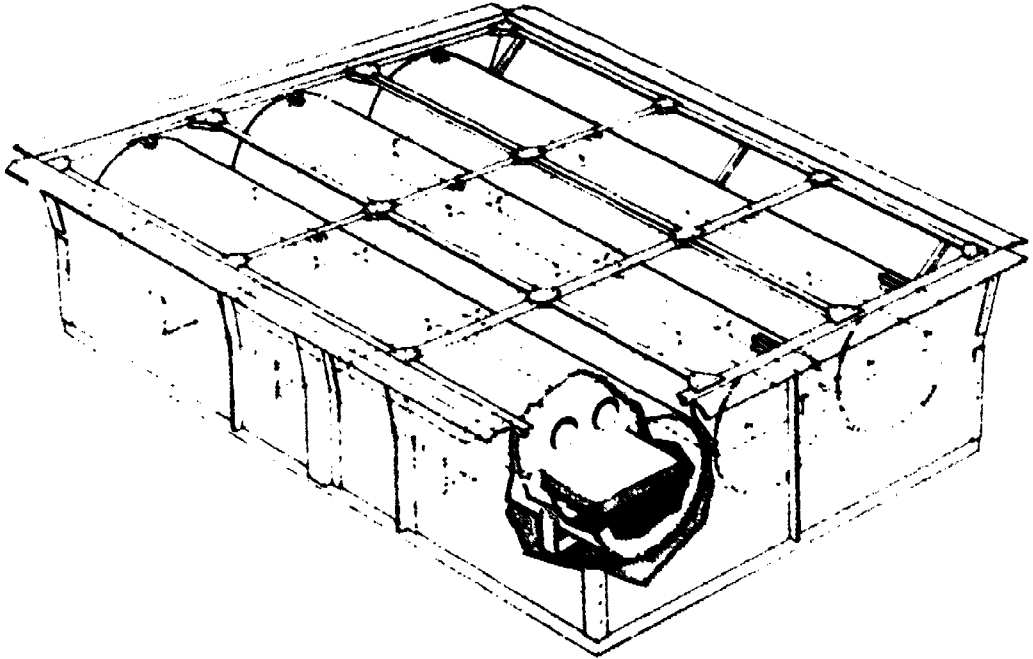
Figure 46. – Cosmic-ray experiment configuration showing location of detector stacks. The light top frame supports the thermal tray cover.



Figure 47 – Photograph of cosmic-ray experiment tray.

104

**111**

# Heavy Ions in Space
## (M0001)

James H. Adams, Jr., Rein Silberberg, and C. H. Tsao
Laboratory for Cosmic Ray Physics, Naval Research Laboratory
Washington, D.C.

## Background

Since 1972, an anomalous flux of N, O, and Ne relative to carbon has been observed in the energy region from 3 to 100 MeV/u. Between 30 and 100 MeV u, the abundance and energy spectrum of this flux are poorly known, and above 100 MeV/u they are completely unknown. A low-inclination orbit would be particularly suitable for studying this component because the geomagnetic field screens out the fully stripped cosmic-ray nuclei below 2250 MeV u. Therefore, the present experiment permits a study of the newly observed nuclei in the unexplored region above 100 MeV/u, which were "covered up" by cosmic-ray nuclei in previous experiments. The source of this component is unknown but is believed to be of extrasolar origin because of the lack of a gradient away from the Sun, anticorrelation with the sunspot cycle, anticorrelation with solar (1 MeV) proton flux, and a C/O ratio that is not typical of the solar abundances. It has been proposed that if the origin of this component is extrasolar, the most likely source is neutral interstellar gas that is first singly ionized by the solar wind and/or solar ultraviolet radiation and then accelerated by the interplanetary solar plasma. Any knowledge of the mechanism by which this component interacts with the solar wind gives important insight into these processes and the nature of the solar plasma. A question to be explored is whether the solar plasma beyond the Earth's orbit can accelerate particles to energies greater than or equivalent to 100 MeV/u. If, on the other hand, the component is of solar origin, it would be most important to understand the production and acceleration mechanisms that are responsible.

The heavy nuclei provide a sensitive probe to test the origin of radiation belt particles. Two processes contribute to the radiation belt particles: neutron decay, and injection and local acceleration of solar-wind particles. Heavy nuclei provide a pure sample of the second type. Hence, they permit us to determine to which energies solar-wind particles can be accelerated in the Earth's field and the magneto tail, and to what extent this contributes to the radiation belt. The previous experiment on Skylab concerning heavy radiation belt nuclei did not permit a clear separation from the anomalous component. The higher geomagnetic cutoff of a low-inclination orbit would provide a clear separation of these components.

The importance of ultraheavy (UH) nuclei measurements lies in the fact

105

that these nuclei can be synthesized only in special astrophysical settings. Thus, the charge spectrum in the UH region reveals the character of the sources more directly than is possible from the charge spectrum of the lighter nuclei. In addition, the UH nuclei provide sensitive indicators of the amount of interstellar propagation and the time of travel of the galactic radiation. The problem in studying UH nuclei has been their extremely low flux. This is aggravated by their short interaction lengths, which lead to rapid absorption in even a few grams per square centimeter of atmosphere. They are best observed above the atmosphere with detectors of prodigious collecting power.

Existing data on heavy ions in space have mostly come from relatively small, electronic detectors exposed in satellites and short-duration rocket flights. This experiment will use a relatively new, independent technique (sensitive plastics) on a recoverable, long-duration exposure. This represents the first opportunity for an experiment of such large collecting power.

## Objectives

This experiment will investigate three components of heavy nuclei in space: (1) a recently observed anomalous component of low-energy nuclei of N, O, and Ne; (2) the heavy nuclei in the Van Allen radiation belts; and (3) the UH nuclei ($Z > 30$) of the galactic radiation.

The study of the anomalous flux of N, O, and Ne nuclei in the unexplored energy region above 100 MeV/u is expected to provide new insights into the source of this component. Its observation in this experiment will confirm that these ions are singly charged.

Knowledge of the energy spectra of the heavy nuclei observed in the Van Allen belts is expected to enhance the understanding of the origin of the belts (e.g., injection and local acceleration processes). The observation of these heavy ions could show, for the first time, that low-energy particles of extraterrestrial origin can diffuse to the innermost parts of the magnetosphere. Measurements of the UH component are expected to contribute information concerning its source, interstellar propagation, and the galactic storage time.

## Approach

The data will be obtained in a stack of passive particle track detectors (special etchable plastic materials) to be exposed above the Earth's atmosphere for 6 to 12 months in a low-inclination orbit, then recovered and subsequently processed under controlled laboratory conditions. Measurements will be made of the composition and energy spectra of the low-energy nuclei of N, O, and Ne and the heavy nuclei in the Van Allen radiation belts and of the charge spectrum of the UH nuclei of the galactic radiation. Each

**113**

detector stack has a active area of 12 in. by 14 in. Eight detector stacks are required for a collecting power of 776 $m^2$-sr-days for a 1-year exposure. Each stack consists of two parts, one for low-energy ions and one for cosmic rays. The portion devoted to cosmic rays is in a sealed container, and the smaller portion devoted to low-energy ions is placed (in a vacuum) on top of the sealed container (fig. 48).

Radiation damage is induced in most solids along the path of a charged particle and is a function of the primary ionization rate. For plastic materials, after appropriate processing (etching), the path, or "track", is visually observable (under a microscope) as an etched cone. The different plastics have their own threshold for track recording. These are related to the charge of the penetrating particle; that is, for each charge (i.e., each atomic nucleus), one can plot the primary ionization rate as a function of velocity. Thus, for example, oxygen nuclei will not register in a Lexan detector until they have slowed down to $\beta$ 0.12, after which the remainder of the track will be etchable. The detector must then be designed to bring oxygen nuclei to rest with a minimum probability of nuclear interaction. UH nuclei will leave etchable tracks over a much larger fraction of their range.

The thickness of the detector is approximately 10 $g/cm^3$. This is necessary to bring to rest oxygen nuclei up to approximately 240 MeV/u. The stacks consist of sheets of track-detecting plastic. Lexan will be used for the low-energy stacks, and the cosmic-ray stacks will consist primarily of CR-39. The detector stacks are completely passive; even temperature and pressure are



Tray

Detector module



Honeycomb lid

Sealed container

Top stack (for low-energy ions)

Main stack (for cosmic rays)
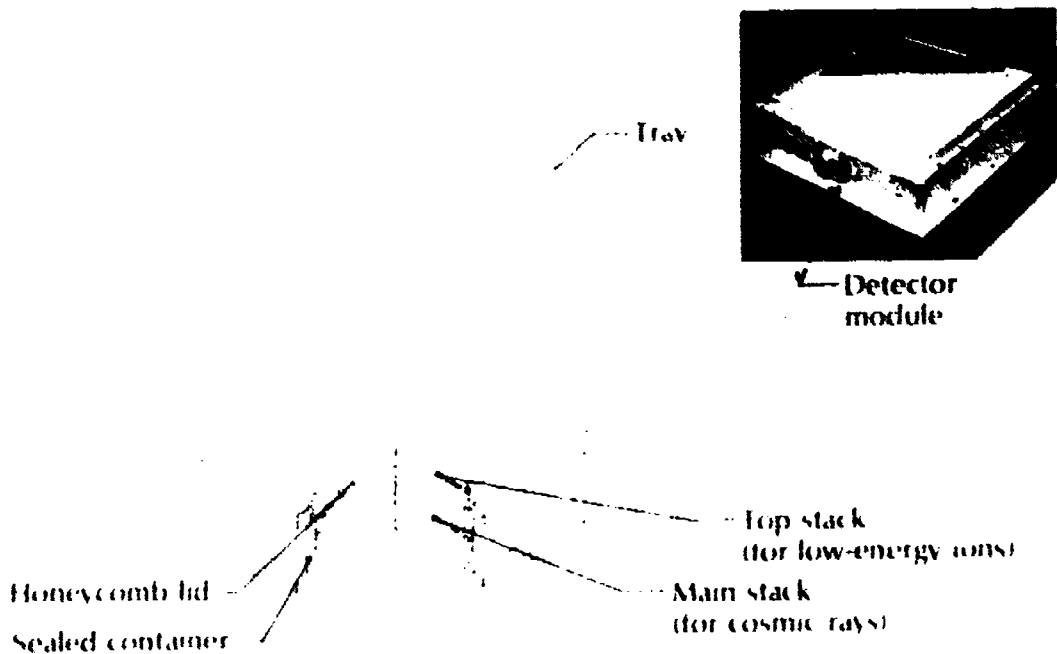
*Figure 48. Heavy ions in space experiment configuration.*

monitored by passive techniques. After recovery, processing and track measurements will be done at the Naval Research Laboratory.

Charge estimates are based on etch cone measurements. (The etching rate is calibrated as a function of the ionization density.) The charge resolution achievable with CR-39 is approximately 0.35 for nuclei at Z = 26. Calibrations will be carried out with laboratory beams of heavy ions.

It is apparent from existing measurements of the energy spectra of the various components at an orbit of 28° and from those outside the magnetosphere that if the anomalous component is observable (at the 28° orbit), then it should be clearly resolved from both the radiation belt and the galactic nuclei at kinetic energies of 100 to 200 MeV/u.

# Trapped-Proton Energy Spectrum Determination
# (M0002-1)

Frederick J. Rich and Irving Michael
Air Force Geophysics Laboratory
Hanscom Air Force Base, Massachusetts

Gerald J. Fishman
NASA George C. Marshall Space Flight Center
Huntsville, Alabama

Paul L. Segalyn
Army Materials and Mechanics Research Center
Watertown, Massachusetts

Peter J. McNulty
Clarkson College of Technology
Potsdam, New York

Y. V. Rao
Emmanuel College
Boston, Massachusetts

Christopher E. Laird
Eastern Kentucky University
Richmond, Kentucky

## Background

The purpose of this experiment is to quantify the flux of ions with energies greater than 1 MeV. The main experiment is sponsored by the Air Force Geophysics Laboratory for the purpose of measuring the energetic protons trapped in the Earth's magnetic field. A series of subexperiments are included which have different but related goals.

## Objective

The objective of this experiment is to measure the flux and energy spectrum of protons with energies of 1 to 10 MeV. These protons are trapped on the Earth's magnetic field lines as part of the inner radiation belt, or Van Allen zone. The proton will be encountered predominantly in the South Atlantic anomaly at a 90° pitch angle.

## Approach

The experiment consists of 18 stacks of passive plastic detectors (CR-39) arranged in portions of three LDEF trays. (See fig. 49.) The stacks are 1.49
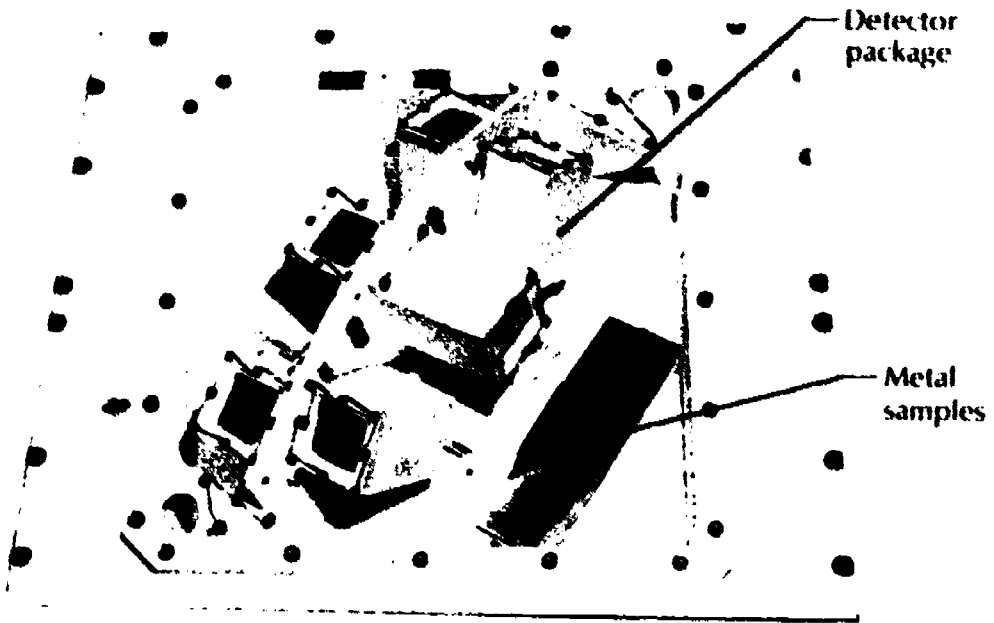


(a) Trays D3 and D9.
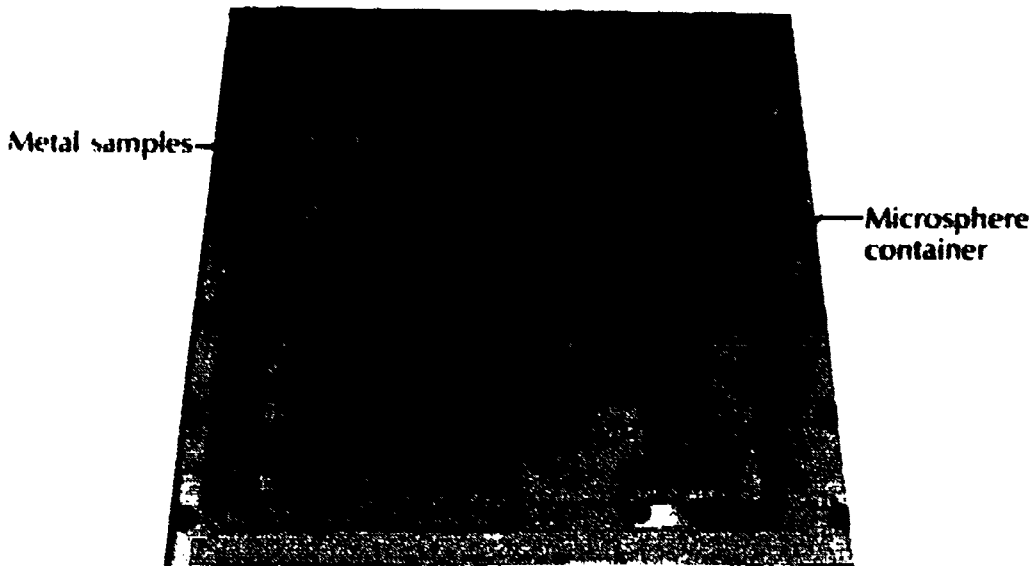


(b) Tray G12.

*Figure 49.—Trapped-proton energy spectrum determination experiment.*

in. square and 2.60 in. high. They are mounted in containers on a plate arranged in the trays to be normal to the Earth's magnetic field in the South Atlantic anomaly (SAA). The bottom half of each stack is composed of CR-39 without DOP and is 0.022 in. thick. The next 40 percent of the stack is CR-39 with DOP and is 0.022 in. thick. The top 10 percent of the stack is CR-39 with CHPC and is 0.011 in. thick. The stack is open to the vacuum of space. The top layer of plastic is directly exposed to space. A sheet of aluminum 0.001 in. thick separates each layer of plastic. Five of each six stacks are perpendicular to the magnetic field in the South Atlantic anomaly.

The three stacks of metal squares and the microsphere container which are visible in figure 49 are used in the three subexperiments described here.

### Neutron and Proton Activation on LDEF (NASA Marshall Space Flight Center and Eastern Kentucky University)

Radioactivity induced by protons and neutrons in the LDEF orbit will be determined by exposing metal samples to the ambient flux through the mission duration and measuring resulting gamma ray activation spectra in a low-level counting facility after recovery. In low Earth orbit, the main sources of activation will be primary cosmic rays, SAA protons, secondary neutrons, and atmospheric albedo neutrons. Induced radioactivity will be a major source of background radiation for certain classes of Shuttle-launched experiments. A quantitative determination of this activation during an early Shuttle mission is important to assess this source of background radiation. The metal samples that were chosen for flight have unique nuclear properties that make them suitable for these activation studies. One property is the relatively high probability that the sample will become radioactive following the passage of a neutron or proton. In addition, the sample will retain a measurable amount of radioactivity upon its return.

### Microsphere Dosimetry (Clarkson College of Technology)

Containers of small microspheres flown on LDEF will be used to record the energy deposited in volume elements with microscopic dimensions as a result of exposure to the natural radiation environment of space. The single-event-upset phenomena and hard errors in microelectronics, as well as the radiobiological effects in man, result from ionizations generated within sensitive volumes that have microscopic dimensions. Standard dosimetry measurements of the radiation environment of space are carried out using macroscopic sensitive volumes. Even a relatively small macroscopic dose can include order-of-magnitude differences in the number of ionizations in microscopic volume elements. Microspheres of different composition and diameter will be flown under identical conditions. Thermoluminescent dosimeters (TLD's) will be included to measure the macroscopic dose received

111

by each sample. Physical properties of the microspheres, such as changes in diameter after a period of postflight etching, will be measured to determine the dose received by each microsphere.

**Flux Measurement by Ion Trapping (Army Materials and Mechanics Research Center)**

Concentration profiles will be measured, primarily by secondary ion mass spectroscopy and Rutherford backscattering, for a wide variety of ions at different places on a series of metal plates directly exposed to space. The area under a profile and the profile shape give the total flux and energy distribution information. Sample materials include fused quartz ($SiO_2$), aluminum oxide ($Al_2O_3$), aluminum, copper, silicon, tantalum, tungsten, and zirconium.

# Measurement of Heavy Cosmic-Ray Nuclei on LDEF (M0002-2)

Rudolf Beaujean, Wolfgang Enge, and Georg Siegmon
Institute for Pure and Applied Nuclear Physics, University of Kiel
Kiel, Federal Republic of Germany

## Background

The long-duration flight on LDEF will provide the opportunity to collect a reasonable number of heavy cosmic-ray nuclei. A knowledge of the abundance of these nuclei is essential to any theory on the source, acceleration, propagation, confinement, and age of cosmic rays.

## Objective

The objective of this experiment is to measure the elemental and isotopic abundances of heavy cosmic-ray nuclei with nuclear charge Z equal to or greater than 3. The chemical and energy spectra will be measured for particles that have energies in the range from 20 to 1000 MeV per atomic mass unit. Two points of great interest are "geomagnetically forbidden" cosmic-ray particles and heavy ions of the trapped radiation.

## Approach

The experiment is passive and occupies one-sixth of a 3-in.-deep peripheral tray with several other experiments. The experiment package consists of visual track detectors that remain sensitive throughout the LDEF mission. (See fig. 50.) The scientific data are stored in latent tracks and can be revealed in the investigator's laboratory after recovery.

The detector stack consists of approximately 6.5 g/cm² of CR-39 plastic visual track detector sheets that have a well-established response. The detector stack is housed in an aluminum container that provides structural support and thermal contact to the LDEF structure. The top of the detector stack is covered by thin coated foils that provide thermal shielding and decoupling from deep space.

Heavy ions stopping in or passing through the plastic sheets of the stack produce latent tracks that can be revealed by chemical etching in the laboratory. Further analysis can be performed under optical and electron microscopes by measuring the shape and length of the etched cones. These parameters depend strongly on the energy loss along the trajectory of the incoming particle. The determination of nuclear charge and mass is based on the cone length versus residual range method. Plastic track detectors have registration

113

thresholds that make the detector system almost insensitive to electrons and protons except at low energies; therefore, they do not produce a disturbing background.
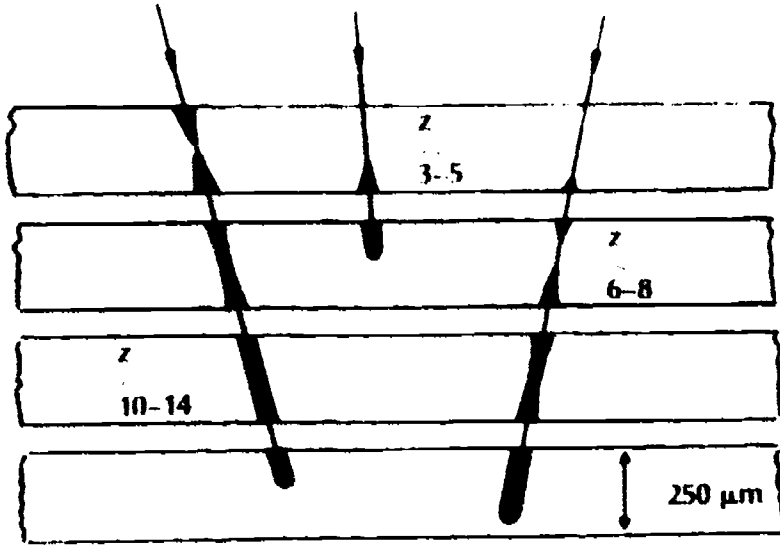


(a) Image of heavy nuclei impacts in plastic track detectors after etching. (Not to scale.)
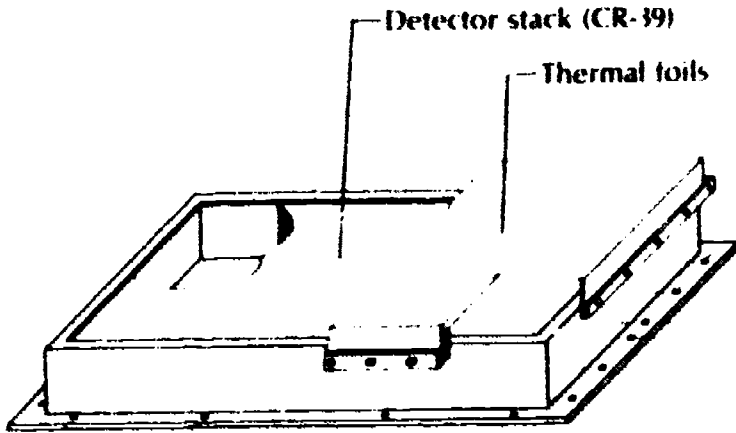


(b) Tray configuration.

*Figure 50.—Heavy cosmic-ray nuclei experiment configuration.*

**121**

# Linear Energy Transfer Spectrum Measurement Experiment
# (P0006)

Eugene V. Benton
University of San Francisco
San Francisco, California

Thomas A. Parnell
NASA George C. Marshall Space Flight Center
Huntsville, Alabama

## Background

The linear energy transfer (LET) is the energy deposited per unit path length of a charged particle traversing matter. For estimating the rate of damage from single-hit phenomena, the quantity that best combines the radiation environment, orbital situation, and spacecraft shielding is the linear energy transfer (LET) spectrum at the device location. To date, LET spectra measurements have been severely limited by statistics due to the short nature of STS missions. The designers of future long-life spacecraft such as a space station need LET spectra measurements for exposures of 1 year or more to establish shielding requirements and to select materials and devices that will not be adversely affected in space during the required operation life.

## Objectives

This experiment will measure the LET spectrum behind different shielding configurations for approximately 1 year. The shielding will be increased in increments of approximately 1 $g/cm^2$ up to a maximum shielding of 16 $g/cm^2$. In addition to providing critical information to future spacecraft designers, these measurements will also provide data that will be extremely valuable to other experiments on LDEF.

## Approach

A combination of thermal luminescence and track type detectors will be used to measure the LET. Aluminum will be used for the shielding. The passive detectors and shielding material will be placed in the canister shown in figure 51. The canister with detectors will be sealed with approximately 1 atm internal pressure. Control detectors identical to those to be flown will be used to establish the terrestrial background radiation to which the flight detectors are exposed prior to launch and after recovery.

115
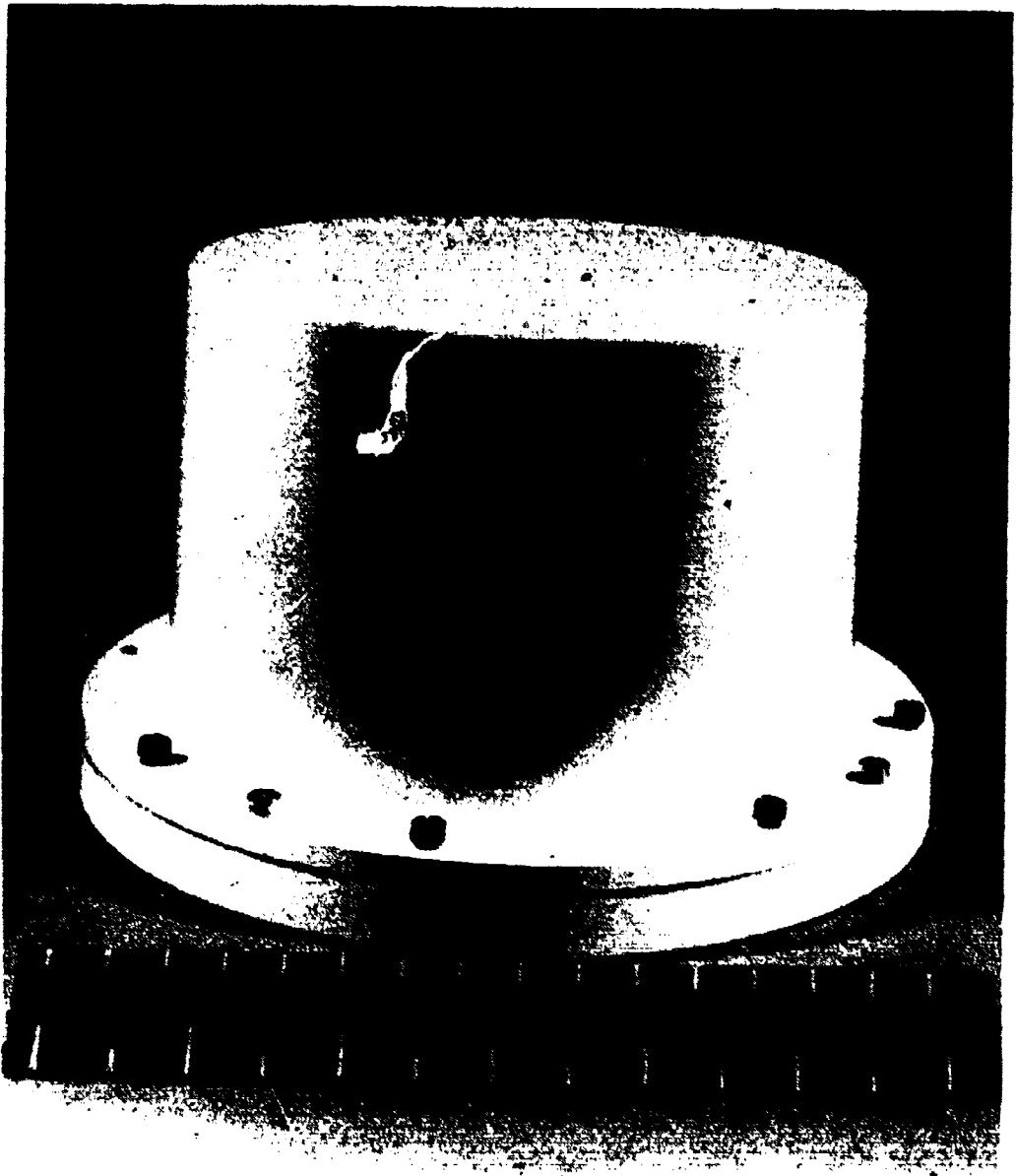
*Figure 51.—LET spectrum measurement canister.*

# Multiple-Foil Microabrasion Package
# (A0023)

J. A. M. McDonnell, D. G. Ashworth, W. C. Carey, R. P. Flavill,
and R. C. Jennison
University of Kent
Canterbury, Kent, United Kingdom

## Background

A number of the early Explorer satellites, the Ariel II, and three Pegasus satellites measured meteoroid penetrations in near-Earth space. These in-space penetration measurements, in addition to providing spacecraft design data, were used with existing ground-based radar and visual meteor data to extend size estimates of the near-Earth meteoroid environment to particles as small as approximately $10^{-10}$g.

Other early U.S. and Russian spacecraft used microphone type meteoroid detectors to measure small-particle impact fluxes. The microphone data indicated a small-particle population much greater than that indicated by the penetration measurements. The microphone data were, in fact, interpreted by some to indicate a dust belt around the Earth.

Difficulties in simulating meteoroid impacts in the laboratory created a number of uncertainties in interpreting both the microphone and penetration early measurements in terms of the near-Earth meteoroid environment.

Data on the near-Earth meteoroid environment have also resulted from analysis of the lunar-material samples obtained during the Apollo Program. The analysis of craters on the lunar material in terms of the meteoroid environment is limited by the facts that the craters occurred over a very long period of time ($10^5$ to $10^6$ years) and the exact exposure time is uncertain.

Taking advantage of the now recoverable and improved very sensitive thin-foil penetration detectors, this experiment will make a substantial step toward the elimination of a number of the remaining uncertainties in the estimates of the near-Earth micrometeoroid environment. In a very cost-effective way, the experiment will provide both design data regarding the erosion of spacecraft by microparticles and data on the near-Earth micro-meteoroid environment.

## Objectives

The specific scientific objectives of this experiment are to measure the spatial distribution, size, velocity, radiance, and composition of micro-particles in near-Earth space. The technological objectives are to measure erosion rates resulting from microparticle impacts and to evaluate thin-foil

117

meteor "bumpers." The combinations of sensitivity and reliability in this experiment will provide up to 1000 impacts per month for laboratory analysis and will extend current sensitivity limits by 5 orders of magnitude in mass.

## Approach

The experiment approach utilizes the well-established technique of thin-foil hypervelocity penetration supported by extensive investigations and calibrated in laboratory simulation to a high precision. Several of the different classes of impact events anticipated on encounter with such a thin-foil array are illustrated in figure 52. This range of classes indicates the potency of this technique compared to simple polished plates or single-foil penetrations. Deployment of such thin-foil detectors around LDEF will measure the spatial anisotropy of the impact flux. Microprobe analysis of penetration and spalla-tion areas after recovery will determine the particle elemental composition.

The detector design utilizes rolled aluminum foil down to a thickness of 1.5 μm (fig. 53). Bonding to etched grid supports achieves very rugged structures capable of withstanding vibrational levels and atmospheric pres-sure gradients typical of the LDEF-Shuttle environment.

The experiment will be located in one-third of each of four 3-in.-deep trays located at 90° intervals around the LDEF periphery and in about two-thirds of a 3-in.-deep end corner tray on the space-facing end of the LDEF.

118
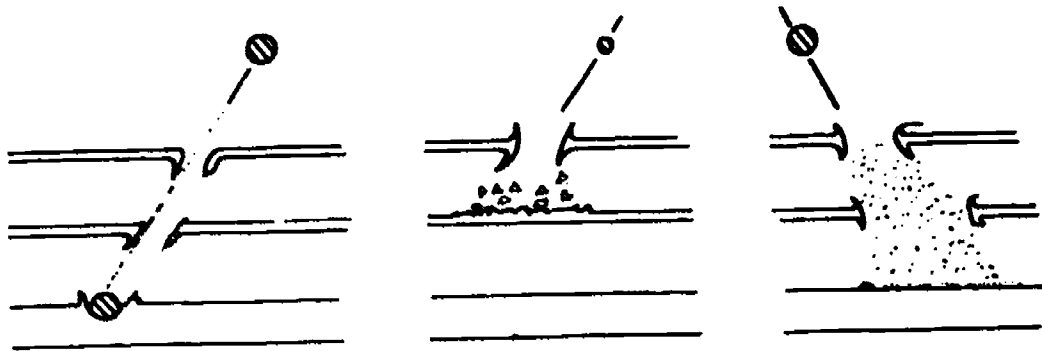
(a) Case 1—veloc-
ity: low; mass:
much greater than
critical; informa-
tion: radiance,
mass, approximate
velocity, composi-
tion (including re-
tention of particle
entity).

(b) Case 2—veloc-
ity: high; mass:
critical; informa-
tion: partial radi-
ance, mass and
velocity ($m^{1/3}$ $v^{2/3}$
dependence), com-
position (residual
traces, 5 percent).

(c) Case 3—veloc-
ity: high; mass:
much greater than
critical; informa-
tion: radiance,
mass, velocity,
composition (re-
sidual traces, 1 to
5 percent).



(d) Scope of investigation.
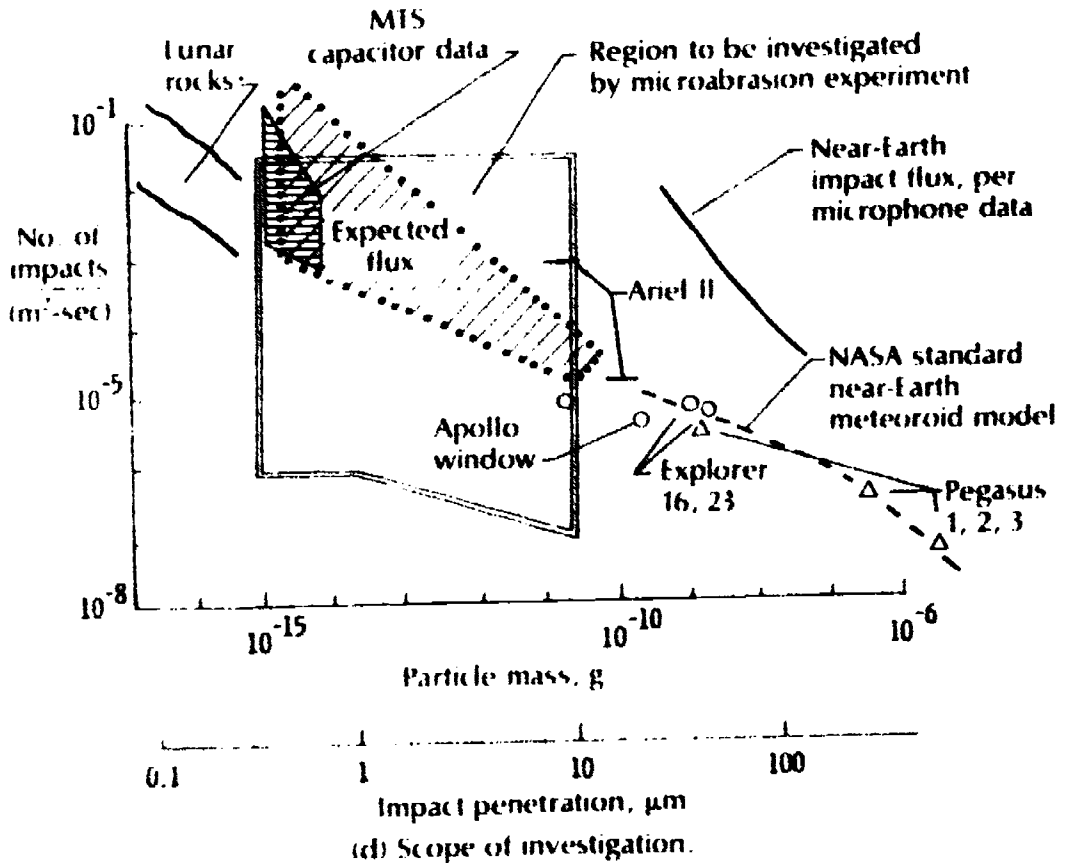
Figure 52. Illustration of impact events and scope of investigation.

Foil     Mesh

Diecast frame

Polished stop plate

← 42 cm →

Eight foil assemblies
per one-third tray

92 cm

1
2     3
4
5
6     7
8

← One-third tray →

← LDEF peripheral tray →
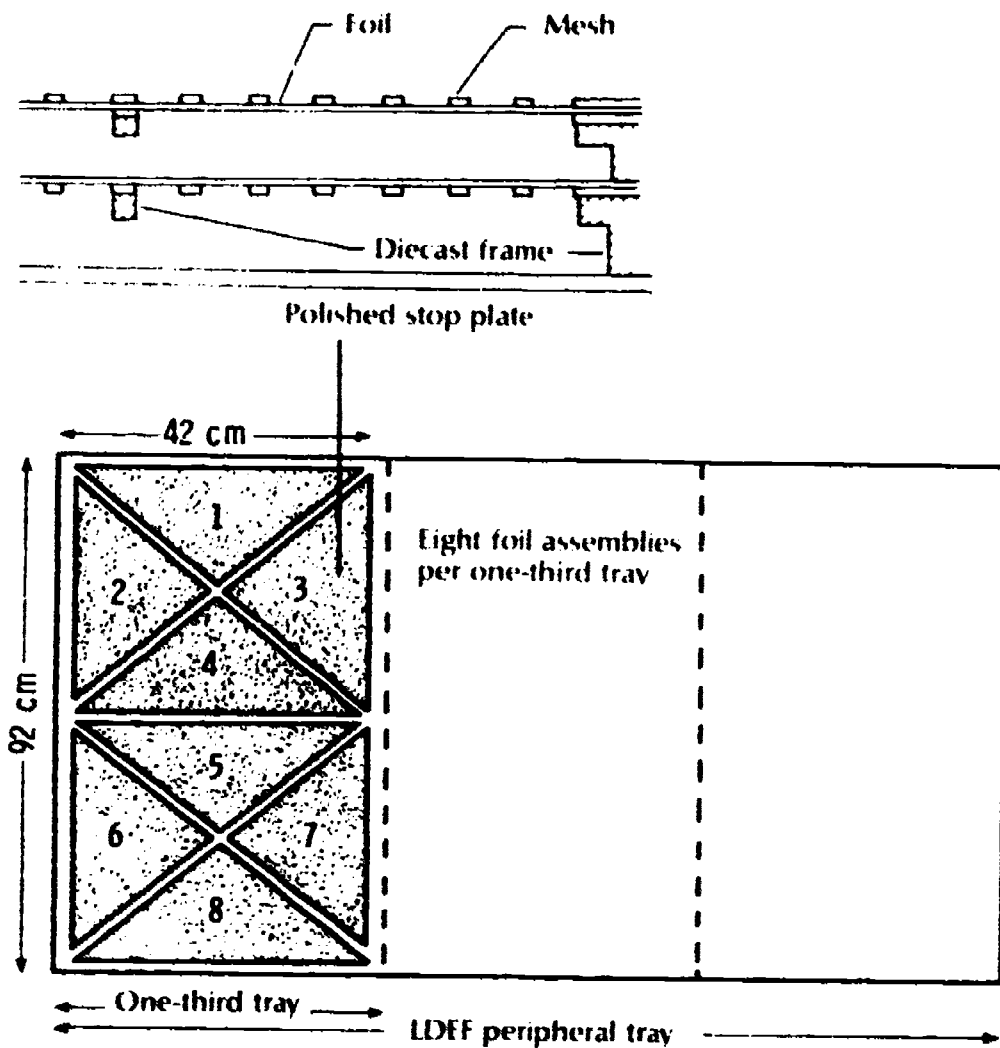
Figure 53.—Multiple-foil microabrasion package experiment.

# Study of Meteoroid Impact Craters on Various Materials (A0138-1)

J-C. Mandeville
CERT/ONERA-DERTS
Toulouse, France

## Background

Interplanetary dust particles (micrometeoroids) are expected to form well-defined craters upon impacting exposed material in space. Studying the frequency and features of these craters will provide data on the mass-flux distribution of micrometeoroids and, to a lesser extent, on the velocity magnitude and direction. Limited crater studies have been done in the past with materials retrieved after exposure in space on Surveyor 3, Apollo 4 and 11, Gemini 10 and 11, and Skylab. However, little has been learned regarding the composition of impacting particles. This experiment will focus on the determination of the composition of meteoroid material residues inside craters.

## Objectives

This experiment will study impact craters produced by micrometeoroids on selected materials (metals and glasses in the form of thick targets) to obtain valuable technological and scientific data. Specifically, the studies will focus on determining micrometeoroid composition and mass-flux distribution. Analyses will also be made on the distribution of impact velocity vectors.

## Approach

High-velocity impact effects on various materials have been studied extensively in the laboratory. It is, however, impossible to obtain velocities higher than 7 to 8 km/sec with relatively large particles ($>10^{-9}$ g). The LDEF can provide a unique opportunity to expose large-area targets for an extensive period of time and to recover them for subsequent analysis. Selected materials that act as impact detectors will be exposed to space. This method is entirely passive and consists of thick targets (compared to the dimensions of expected particles) of pure metals and glass. The collecting area ($\sim 750$ cm$^2$) is expected to record, with a high probability, impacts of micrometeoroids with a mass in the range of $10^{-14}$ to $10^{-7}$ g (corresponding to 0.2- to 35-$\mu$m particle diameters). The experiment is accommodated on an aluminum mounting plate (420 by 400 mm) located in one-sixth of a 12-in.-deep peripheral tray that contains nine other experiments from France. (See figs. 12 and 54.) Two types of samples will be used (table 12). Type I will be metallic surfaces (100

121

by 100 mm) bolted to an aluminum mounting plate (6 samples). Type II will be glass samples (25 mm in diameter) bolted to an aluminum mounting plate (27 samples). A set of similar samples will remain in the laboratory for subsequent comparison with space-exposed samples. A set of samples will also be retained to perform tests with a hypervelocity accelerator.

The first task after experiment retrieval will be a careful scanning of exposed material to search for impact microcraters. Usually, high-velocity craters produced in metals and in brittle materials have a distinctive mor-
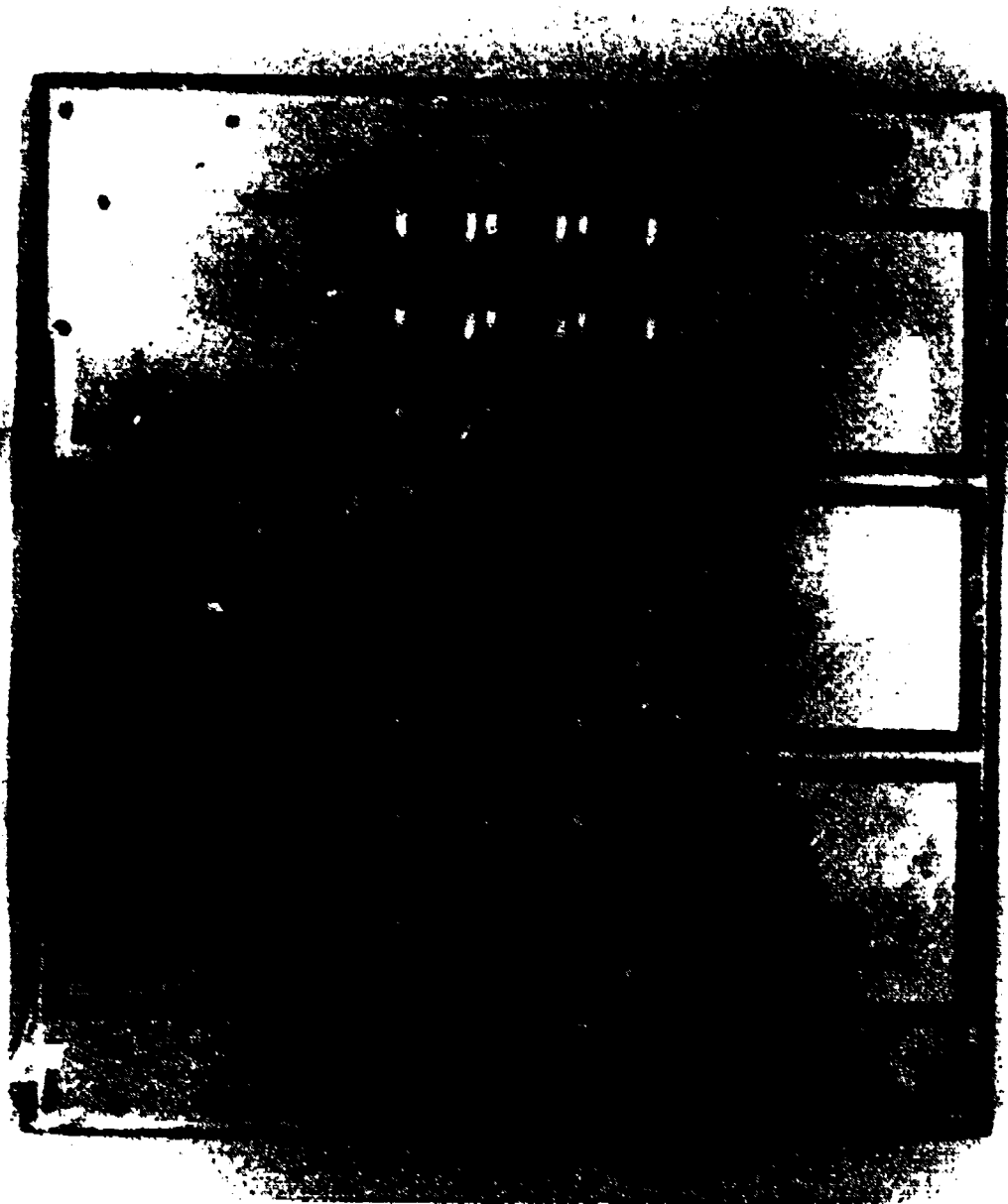


Figure 54. Arrangement of meteoroid impact targets.

122

phology and can be distinguished easily from other surface features. An optical microscope will be used to identify craters larger than about 10 μm, and such a crater is expected every 2 to 3 cm². The density of micrometer-sized craters will be higher (1 to 10 per cm²), but the necessary use of a scanning electron microscope (SEM) with 1000x magnification will limit the area to be scanned. (See table 13.)

Measurements made on craters will include diameter and depth measurements that, by comparison with experimental results, will give the mass and density of impacting particles. Velocity can be estimated from the morphology of craters produced on brittle materials. Impact direction can be evaluated by the shape of the craters. There is a close relationship between the circularity of craters and the angle of impact. The relationship between flux and mass will be derived from the areal density of microcraters.

For craters showing evidence of remnants of the projectile, chemical analysis will be made with X-ray microprobe and ion or Auger microprobe. If possible, atomic absorption spectrophotometry or neutron activation analysis will also be used.

**Table 12.—Experiment A0138-1 Samples**

| Sample | Material | Thickness, μm | Dimension, mm |
|---|---|---|---|
| A1 | Tungsten | 150 | 100 · 100 |
| A2 | Aluminum | 250 | 100 · 100 |
| A3 | Copper | 125 | 100 · 100 |
| A4 | Stainless steel | 250 | 100 · 10'' |
| A5 | Aluminum | 250 | 100 · 100 |
| A6 | Stainless steel | 250 | 100 · 100 |
| B1 to B2'' | Pyrex glass | 1.9 | 25 (diam.) |

**Table 13.— Examination Procedure***

| Instrument | Magnification | Minimum detectable crater diameter, μm | Average mass of micrometeoroid, g | Scanned area, cm² | Maximum number of expected craters for scanned area |
|---|---|---|---|---|---|
| Optical microscope | 20x | 25 - 40 | $10^{9}$ | 400 | 60 |
| | 40x | 10 - 20 | $10^{10}$ | 80 | 17 |
| | 80x | 5 - 10 | $10^{11}$ | 20 | 8 |
| SEM | 100x | 5 - 10 | $10^{11}$ | 4 | 2 |
| | 400x | 2 - 3 | $10^{12}$ | 1.4 | 1 |
| | 1000x | 1 - 2 | $10^{13}$ | 0.06 | 1 |
| | 5000x | 0.2 - 0.5 | $10^{14}$ | 0.006 | 1 |

*About 250 hours of SEM scanning time are expected.

123

# Attempt at Dust Debris Collection
# With Stacked Detectors
# (A0138-2)

J-C. Mandeville
CERT/ONERA-DERTS
Toulouse, France

## Background

Since the beginning of space exploration, a significant amount of data has been gathered on micrometeoroids. Flux-mass relationships, velocities, and orbits of the particles have been established with meteoroid impact and penetration detectors on satellites and space probes. Also, studies of impact craters on lunar samples and a few retrieved sample materials exposed to space have added data on micrometeoroids. However, these techniques have limitations that prevent the study of undisturbed particles.

To study undisturbed particles, cosmic-dust collectors have been flown on balloons and rockets, and more recently on high-altitude aircraft. These techniques for dust collection in the atmosphere are limited because of short exposure times and uncertainty in the discrimination between cosmic-dust particles and terrestrial contaminants.

## Objective

The primary objective of this experiment is to investigate the feasibility of future missions of multilayer thin-film detectors acting as energy sorters to collect micrometeoroids, if not in their original shape, at least as fragments suitable for chemical analysis. It is expected that this kind of particle collector will help in solving one of the most puzzling topics in cosmic-dust studies: the mineralogical and chemical composition of the particles. This is a matter of great interest in the study of the origin and evolution of the solar system.

## Approach

The experiment will consist of targets made of one or two thin metal foils placed in front of a thicker plate. The maximum sample thickness of 125 $\mu$m has been chosen to prevent foil perforation by particles with a mass in the range of $10^{-8}$ g. A particle penetrating the foil undergoes either a deceleration or a fragmentation, according to the thickness and nature of the foil. Thicknesses chosen for this experiment range from 0.75 to 5 $\mu$m of aluminum and are expected to slow down particles with diameters between 1 and 10 $\mu$m without complete destruction.

The experiment will include 31 samples with a sampling surface area of 240 cm². The samples will be mounted on a plate inside one of the FRECOPA boxes in a 12-in.-deep tray that contains nine other experiments from France. (See figs. 12 and 13.) The FRECOPA box will provide protection for the fragile thin metal films before and after space exposure. The description and list of samples are given in table 14. All samples will be mounted within aluminum frames (40 by 40 mm or 30 by 30 mm) which will hold the thick target and the thin foils in front. (See fig. 55.)

Measurements after flight exposure will be similar to those described for experiment A0138-1. Emphasis will be on the study of thin-film behavior during the cratering process and on the chemical analysis of projectile remnants.

**Table 14.—Dust Debris Targets**

| Sample | Material | Thickness, µm | Dimension, mm |
|---|---|---|---|
| D1 to D6 | Aluminum | 5 | 40 × 40 |
| | Aluminum | 125 | 40 × 40 |
| D7, D8 | Aluminum | 2 | 40 × 40 |
| | Aluminum | 5 | 40 × 40 |
| | Aluminum | 125 | 40 × 40 |
| D9, D10, D11 | Aluminum | 2 | 40 × 40 |
| | Aluminum | 125 | 40 × 40 |
| D12 | Aluminum | 125 | 40 × 40 |
| E1 to E6 | Aluminum | 2 | 30 × 30 |
| | Gold | 125 | 30 × 30 |
| E7, E8, E9 | Aluminum | 0.75 | 30 × 30 |
| | Aluminum | 125 | 30 × 30 |
| E10, E11, E12 | Aluminum | 0.75 | 30 × 30 |
| | Gold | 125 | 30 × 30 |
| E13 to E16 | Gold | 125 | 30 × 30 |
| E17 | Aluminum | 0.75 | 30 × 30 |
| | Aluminum | 2 | 30 × 30 |
| | Aluminum | 125 | 30 × 30 |
| E18 | Aluminum | 0.75 | 30 × 30 |
| | Gold | 125 | 30 × 30 |
| E19 | Aluminum | 0.75 | 30 × 30 |
| | Aluminum | 125 | 30 × 30 |
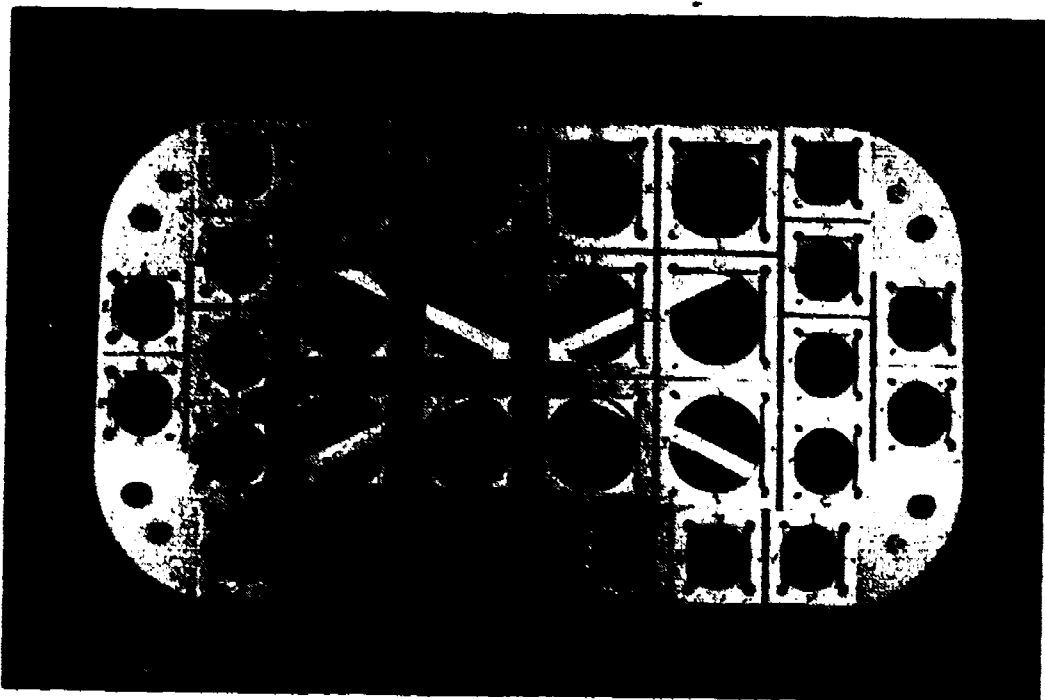
*Figure 55.—Arrangement of dust debris target within FRECOPA box.*

**133**

# The Chemistry of Micrometeoroids
## (A0187-1)

Friedrich Hörz, David S. McKay, and Donald A. Morrison
NASA Lyndon B. Johnson Space Center
Houston, Texas

Donald E. Brownlee
University of Washington
Seattle, Washington

Robert M. Housley
Rockwell International Science Center
Thousand Oaks, California

## Background

The mineralogy, petrography, and chemistry of both "primitive" and more evolved meteorites recovered on Earth are currently the subjects of intense laboratory studies. The purpose of these studies, in conjunction with our knowledge of terrestrial and lunar petrogenesis, is to establish an observational framework that can be used progressively to constrain and refine cosmochemical and mechanical-dynamic models of early solar-system evolutionary processes. Such modelling attempts include the nature and kinetics of nebular condensation and fractionation, the accretion of solid matter into planets, the differentiation and crustal evolution of planets, and the role of collisional processes in planetary formation and surface evolution. All of these processes are known to be highly complex.

Fine-grained interplanetary particles (micrometeoroids) of masses as little as $10^{16}$ g are, however, largely excluded from models of the early solar-system evolution because their mineralogic, petrographic, and geochemical nature is largely unknown. In comparison, however, their dynamics, orbital parameters, and total flux are reasonably well established, although still fragmentary in a quantitative sense. According to current (largely dynamical) hypotheses, a majority of these objects are derived from comets. This association affords a unique opportunity to study early solar-system processes at relatively large radial distances from the Sun (greater than approximately 20 AU). These cometary solids may reflect pressure and temperature conditions in the solar nebula which are not represented by any of the presently known meteorite classes, and therefore may offer potential insight into the formation of comets themselves.

## Objectives

The prime objective of this experiment is to obtain chemical analyses of a statistically significant number of micrometeoroids. These data will then be compared with the chemical composition of meteorites. Secondary objectives of the experiment relate to density, shape, mass frequency, and absolute flux of micrometeoroids as deduced from detailed crater geometries (depth, diameter, and plane shape) and number of total events observed.

## Approach

This experiment is designed to collect micrometeoroid residue in and around micrometeoroid impact craters that are produced by hypervelocity collisions of the natural particles with high-purity targets. After the return of these targets, the micrometeoroid residue will be chemically analyzed with a large array of state-of-the-art microanalytical tools (e.g., electron micro-probe, scanning electron microscope with energy-dispersive analyser, Auger and ESCA spectroscopy, and ion probe mass analyzer). In favorable cases, precision mass spectrometry may be possible. The experiment will involve both active and passive collection units.

### Active Unit

The principles of the "active" unit are described below. (See fig. 56.) A clam shell concept allows two sets of clam shells, housed in a 12-in.-deep
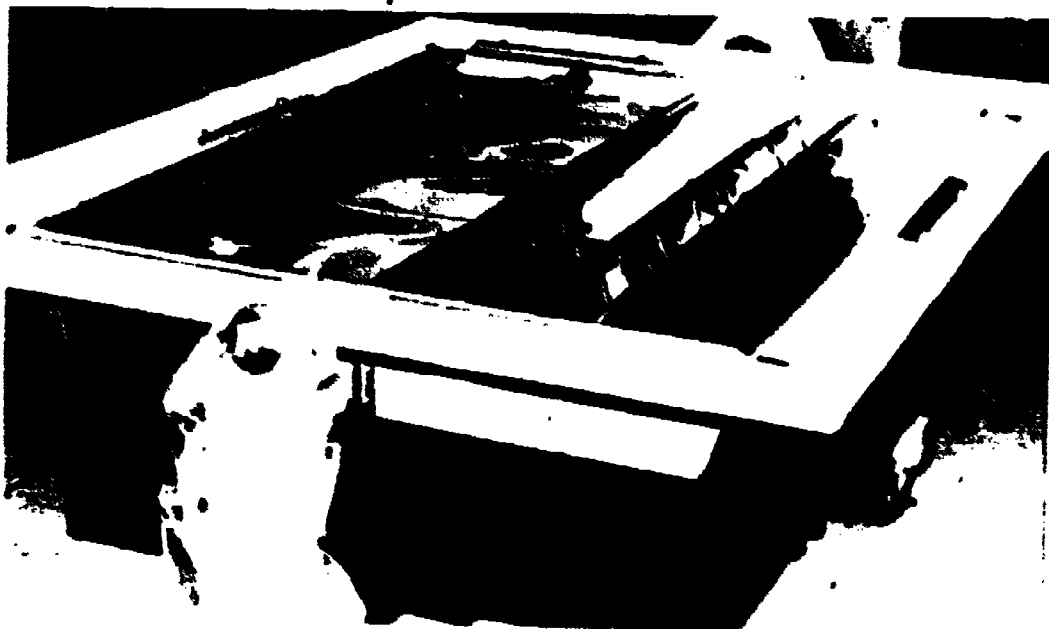


Figure 56    Active micrometeoroid detector unit.

peripheral tray, to be opened and closed. The figure shows one set of clam shells in the stowed (i.e., closed) mode and the other set in a deployed mode Due to the high sensitivity of the microanalytical tools and the extremely small masses of micrometeoroid residue to be analysed ($10^{-7}$ to $10^{-13}$ g), the stowed configuration will protect the collector surfaces from particulate contaminants during ground handling, launch, and LDEF deployment and retrieval sequences. The clam shells will be opened by a timed sequencer some 8 days after LDEF deployment and they will close at a similar time prior to redocking for retrieval of LDEF. The basic contamination barrier is a precision labyrinth seal.

The main collector surfaces are made of 99.99-percent pure gold sheets 0.5 mm thick and totaling some 0.85 $m^2$ total surface area. Two individual gold panels, each about 57 by 20.6 cm, will be fastened to each clam shell tray for a total of seven panels. A high-quality surface finish will be obtained by polishing, acid etching, and electroplating. The space for the eighth panel is taken up by a series of experimental collector materials (about 6.5 by 20.6 by 0.05 cm each) for the purpose of empirically determining collection efficiency and/or optimum chemical background (i.e., signal-to-noise ratio during the analytical phase). These auxiliary surfaces consist of Al (99.999 percent pure), Ti (99.9 percent pure), Be (99.9 percent pure), Zr (99.8 percent pure), C (99.999 percent pure), Kapton (a polyimide), and Teflon filters. There are three reasons for selecting gold as the main collector surface First, its behavior under hypervelocity impact conditions is reasonably well known, in contrast to that of some of the auxiliary surfaces. Second, gold is not an overly abundant constituent in meteorites, and third, it is a highly suitable substrate for many of the microanalytical techniques contemplated For a model exposure duration of 9 months, a fairly well established mass-frequency distribution, and a conservatively low flux estimate for micro meteoroids, the approximate numbers of micrometeorite craters expected on the gold collector are as follows: 165 craters larger than 5 $\mu$m, 52 craters larger than 10 $\mu$m, and 9 craters larger than 50 $\mu$m in diameter. Quantitative analysis is feasible only for craters larger than 20 $\mu$m in diameter (approximately 20 events), although an attempt will be made at qualitative analysis of smaller craters.

## Passive Unit

The experiment will use a "passive" collector unit that occupies a 3-in.-deep peripheral tray. (See fig. 57.) This unit will be covered by six Al (99.9 percent pure) panels (47 by 41 by 0.3 cm each). These surfaces have no special protection against contamination because they are rigidly bolted onto a structural framework which in turn is fastened to the LDEF tray. If contamination is not too significant, approximately another 25 events larger than 20 $\mu$m in diameter will be available for analysis. Furthermore, an

additional gold surface (approximately 12 by 2.3 by 0.05 cm) will be flown inside the experiment exposure control canister used in LDEF experiment S0010 (Exposure of Spacecraft Coatings) for optimum calibration of gaseous and particulate contamination.
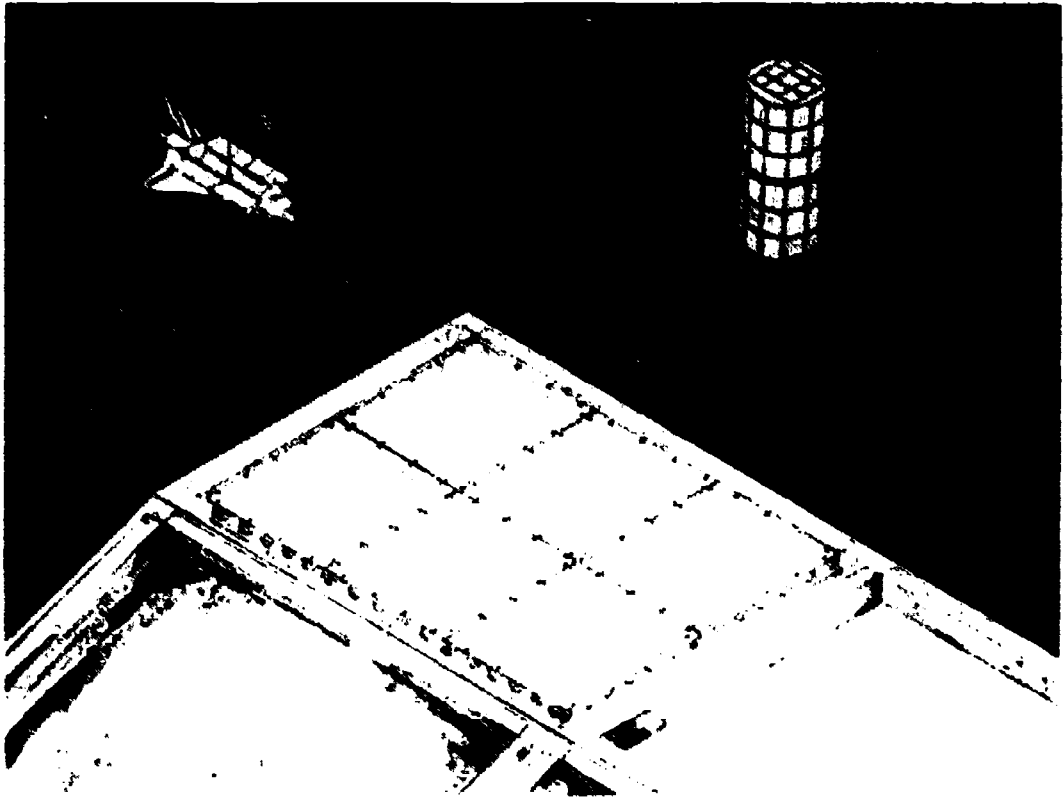


*Figure 57.--Passive micrometeoroid detector unit.*

137

# Chemical and Isotopic Measurements of Micrometeoroids by Secondary Ion Mass Spectrometry (A0187-2)

John H. Foote, Patrick D. Swan, Robert M. Walker, and Ernst K. Zinner
McDonnell Center for the Space Sciences
St. Louis, Missouri

Dieter Bahr, Hugo Fechtig, and Elmar Jessberger
Max-Planck Institute for Nuclear Physics
Heidelberg, Federal Republic of Germany

Eduard Igenbergs, Uwe Kreitmayr, and Heribert Kuczera
Munich Technical University
Munich, Federal Republic of Germany

Eberhard Schneider
Ernst-Mach Institute
Freiburg, Federal Republic of Germany

Norbert Pailer
Dornier System Manufacturing Co.
Friedrichshafen, Federal Republic of Germany

## Background

In the past, the study of interplanetary dust particles has been restricted mainly to measurements of their flux, mass and velocity distribution, and variation with direction and solar distance. Chemical and isotopic compositional information could be obtained from the Brownlee particles collected in the upper atmosphere. The launch of LDEF provides the first opportunity to collect micrometeoroid material in space which then can be subjected to isotopic analysis in the laboratory. Isotopic measurements of interplanetary dust are of great interest since at least part of the interplanetary dust is believed to be derived from comets. Because comets originate in the outer region of the solar system they probably have never been subjected to mixing of material during formation of the solar system, and thus they might have preserved presolar isotopic features.

Interplanetary dust particles are difficult to collect because of their high speed. Upon impact, much of the particle mass is evaporated and ejected from the target. This experiment utilizes a target covered with a thin foil to trap the ejected material.

## Objective

The objective of this experiment is to measure the chemical and isotopic composition of interplanetary dust particles of mass greater than $10^{-10}$ g for most of the major elements expected to be present.

## Approach

The experiment approach utilizes a passive Ge target which is covered with a thin metallized plastic foil. The foil is coated on the outer (i.e., space facing) surface with a Au-Pd film for thermal control and to protect the foil from erosion by atomic oxygen present in the residual atmosphere. The inner surface of the foil is coated with tantalum, which was selected in order to optimize the analysis of positive secondary ions by secondary ion mass spectroscopy (SIMS).

The experiment occupies a 3-in.-deep peripheral tray near the LDEF leading edge, one-third of a 6-in.-deep peripheral tray near the LDEF trailing edge, and two-thirds of a 6-in.-deep peripheral tray on the LDEF trailing edge. Figure 58 shows the one-third-tray experiment hardware and illustrates the micrometeoroid detection principle. An incoming meteoroid penetrates the foil before striking the target plate. Impact ejecta, consisting of a mixture of target and projectile material in the form of fragments, melt, and vapor, are collected on the underside of the film. The deposited interplanetary dust material can be anlayzed by a number of surface-sensitive techniques, among which SIMS is favored because of its high sensitivity and its isotopic analysis capability. Measurements are planned of the concentrations of Na, Mg, Al, Si, S, K, Ca, Fe, and Ni and the isotopic compositions of Mg, Si, Ca, and Fe (and possibly S and Ni) from particles greater than 10 $\mu$m in diameter. For an exposure of 12 months, approximately 60 impacts of particles of this size are expected for an area of 1 m². About 1 m² will be exposed on both the leading and the trailing edge. The leading edge has the advantage of receiving a higher flux because of the higher impact velocity (approximately 20 km/sec). On the trailing edge, impacts from terrestrial contaminants in orbit are excluded. In addition to chemical and isotopic measurements, information on particle mass, velocity, and density can be obtained from the study of the hole size and crater size and morphology.
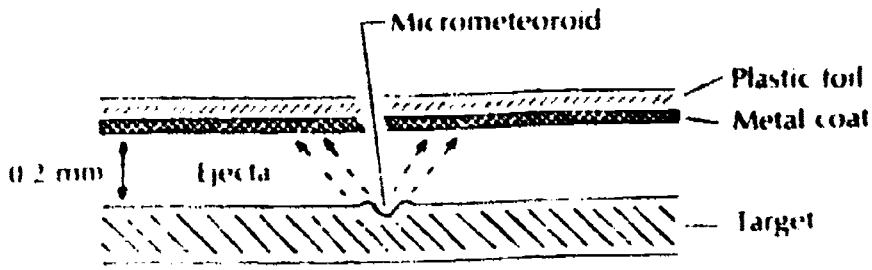
(a) Detection principle.
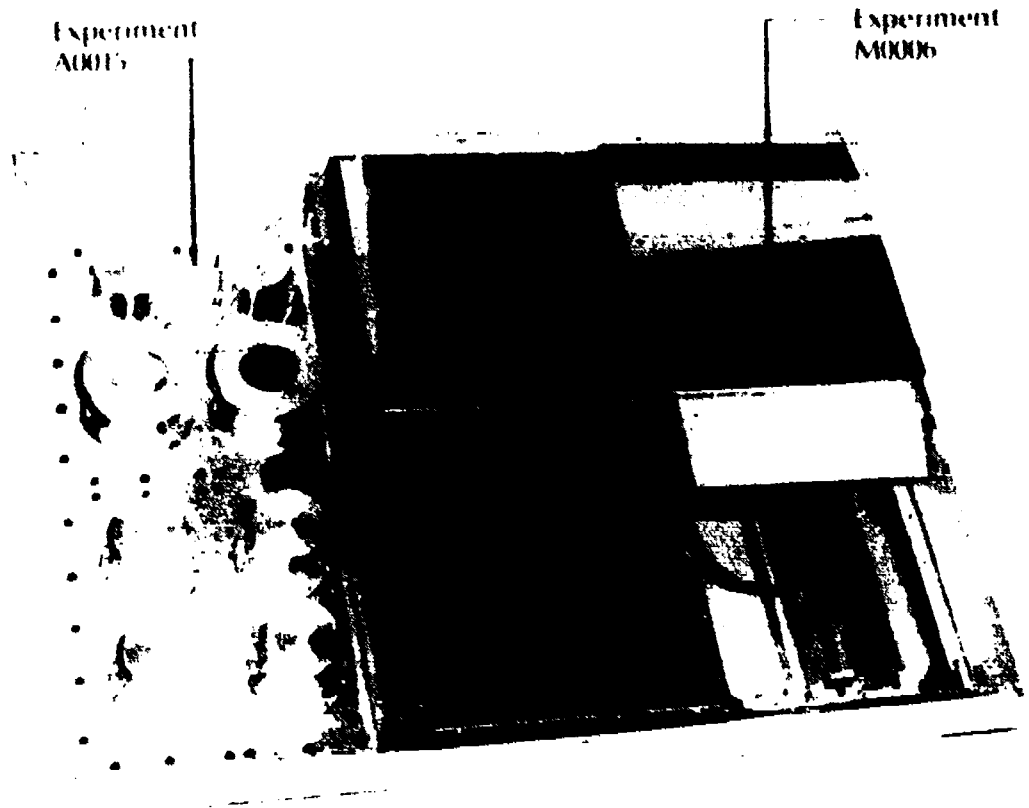


(b) Tray configuration.

Figure 58    Chemical and isotopic measurements of micrometeoroids
experiment

# Interplanetary Dust Experiment
## (A0201)

S. Fred Singer and John E. Stanley
University of Virginia
Charlottesville, Virginia

Philip C. Kassel, Jr.
NASA Langley Research Center
Hampton, Virginia

J. J. Wortman
North Carolina State University
Raleigh, North Carolina

## Background

The study of interplanetary dust historically has been plagued by the problem of low data rates and therefore statistically inadequate data analyses. The LDEF satellite will permit for the first time the flight of an experiment with a large effective area, yielding data with which excellent statistical confidence can be achieved. Additionally, it has been shown that a major source of the interplanetary micrometeoroid environment is comets. Confirmation and expansion of these results may give important insight into the cometary phenomenon.

## Objectives

The objective of this experiment is to study interplanetary dust, variously referred to as cosmic dust, cometary dust, zodiacal dust, or meteoric dust particles. Specific objectives are to obtain information regarding particle mass and velocity, and to undertake correlative analyses with other experiments, both on LDEF or near the time of the LDEF flight.

## Approach

The experiment will use metal-oxide-silicon (MOS) capacitor-type impact sensors with two different sensitivities. The total active area of the experiment will be about 1 m². Sixty percent of the sensors will have an oxide thickness of 0.4 μm, the higher sensitivity, and 40 percent will have a thickness of 1.0 μm.

The experiment will be located in four locations spaced at 90° intervals around the LDEF periphery and on the Earth-facing and space-facing ends. (See fig. 59.) Tray requirements include one 6-in.-deep tray, one-third each of three 3-in.-deep trays, one 3-in.-deep end corner tray on the Earth-facing

end, and about one-third of a 3-in.-deep end corner tray on the space-facing end. A one-third-tray location typically will contain 80 impact sensors and 1 Sun sensor.

Approximately every 2 hours, an experiment power and data system will record the status of all sensors and the recent experiment activity, which will include the time of occurrence of each impact and the total number of impacts for each sensitivity and tray location. The Sun sensors will be used to record the time from the most recent crossing of the dark-to-light terminator.

When the experiment is recovered, the recorded data and LDEF tracking data will be analyzed to determine the dust encountered as a function of mass, time, and velocity direction in geocentric coordinates. These data will then be correlated with theories and observations of other dust-related phenomena.



MOS detector

Experiment A0034

Experiment A0114
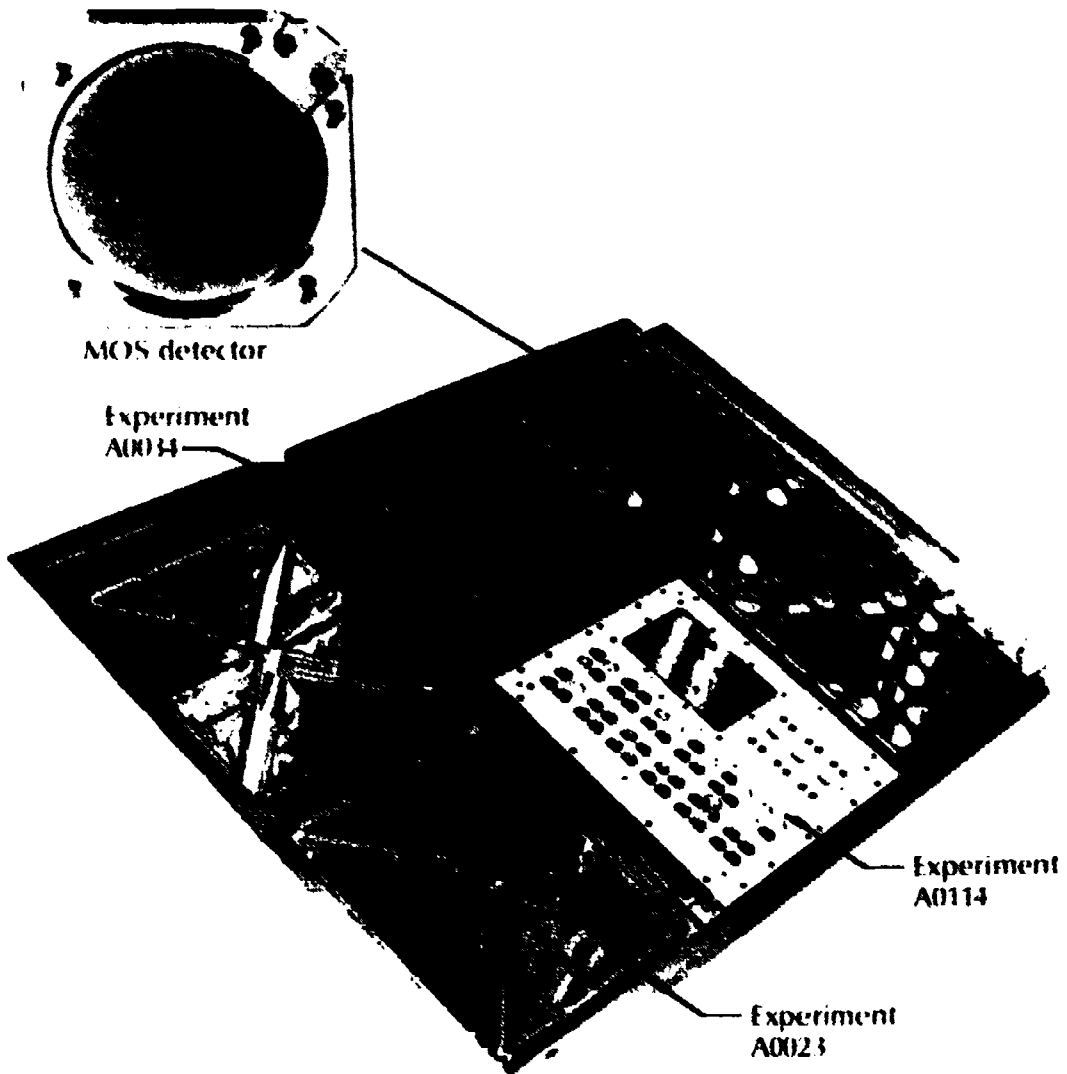
Experiment A0023

*Figure 59    Interplanetary dust experiment.*

135

# Space Debris Impact Experiment
# (S0001)

Donald H. Humes
NASA Langley Research Center
Hampton, Virginia

## Background

Current models of the near-Earth meteoroid environment are based on measurements by many different types of detectors, each measuring over its own narrow mass range with no overlapping of measurements. None of the detectors measures mass or size directly. As a consequence, an uncertain fitting together of the data has been used to estimate the population and size distribution of meteoroids near the Earth. This experiment will use the same detector, an aluminum plate, to detect meteoroids over a very large size range. A single factor that converts crater size to meteoroid mass can be applied to all the data. A much improved population and size distribution of meteoroids will be obtained.

Man-made debris may someday become a significant component of the space debris environment near the Earth. Future spacecraft explosions, whether accidental or intentional, can result in millions of fragments, each capable of inflicting substantial impact damage. Such fragments could remain in orbit for years. An estimate of the current man-made debris population will also be made with the experiment.

## Objectives

The specific objectives of this experiment are to establish the population and size distribution of meteoroids in the mass range from $10^{-10}$ to $10^{-3}$ g, to establish the current population of man-made debris in the same mass range, and to obtain data on the physical properties (composition and density) of meteoroids.

## Approach

The space debris impact experiment will expose large areas of thick aluminum plates to the space debris environment. The size distribution of the craters caused by meteoroids will be used to determine the population and size distribution of meteoroids. The size distribution of craters caused by man-made debris will be used to determine the population and size distribution of man-man debris. The shape of the craters, the impacting particle material found on the crater walls, and the location of the impacts on the spacecraft will

be used to distinguish between meteoroid craters and those caused by man-made debris.

This experiment occupies 19 3-in.-deep peripheral trays, two 3-in.-deep end corner trays on the Earth-facing end, and one 3-in.-deep end corner tray on the space-facing end of the LDEF. Additionally, several partial tray locations on the periphery will be utilized.

**144**

# Meteoroid Damage to Spacecraft
# (P0007)

Consortium of Investigators*

## Background

Observation of meteoroid impact damage to typical spacecraft components (i.e., solar cells, thermal control surfaces, and composite materials) can provide valuable information for the design of future spacecraft. A detailed inspection of LDEF and the LDEF experiments will probably reveal a number of examples of such damage. The LDEF will be the first large spacecraft to be exposed in space for an extended period of time and then recovered in such a manner that the external surfaces are not damaged by the recovery process. In addition, the experiments in the LDEF trays will expose examples of many typical spacecraft components to the space environment.

## Objective

The objective of this experiment is to obtain examples of meteoroid impact damage to typical spacecraft components, and by so doing to help establish design approaches to minimize meteoroid damage effects to future spacecraft. The results of the complete inspection of the LDEF will complement and extend the data obtained from specific meteoroid experiments flying in LDEF trays.

## Approach

All exposed external surfaces of LDEF and the experiments will be examined after retrieval before any experiment tray removal operations are begun. The locations of impact craters will be documented and the principal investigators of the trays containing impact craters will be requested to make the component containing the crater available to the consortium for study after evaluation of the item has been completed.

---

*Consortium members will be the investigators involved in the following meteoroid experiments: A0023, Multiple-Foil Microabrasion Package; A0138-1, Study of Meteoroid Impact Craters on Various Materials; A0138-2, Attempt at Dust Debris Collection With Stacked Detectors; A187-1, The Chemistry of Micrometeoroids; A0187-2, Chemical and Isotopic Measurements of Micrometeoroids by Secondary Ion Mass Spectrometry; A0201, Interplanetary Dust Experiment; and S0001, Space Debris Impact Experiment.

138

# Free-Flyer Biostack Experiment
## (A0015)

Horst Bücker
Institute for Flight Medicine, DFVLR
Cologne, Federal Republic of Germany

## Background

Studies on the biological effectiveness of HZE particles (particles of high atomic number Z and high energy) and stars are necessary to confirm ground-based work, as well as to assess the biological effects of HZE particles not currently available from accelerators on Earth. Spaceflight experiments are required to analyze and evaluate the biological effects of the different species of HZE particles prevalent in space.

In comparison with the Apollo lunar mission, the dosimetric data calculated for a 6-month flight of LDEF will yield an increase in total dose of approximately 360 percent, in HZE particle fluence of approximately 200 percent, and in stars of even 2700 percent. Thus LDEF will offer a unique opportunity to gather information on the effects of stars on biological matter.

## Objectives

The free-flyer biostack experiment is part of a radiobiological space research program that includes experiments in space as well as in accelerators on Earth. The program has been specially designed to increase knowledge concerning the importance, effectiveness, and hazards of the structured components of cosmic radiation to man and to any biological specimen in space. Up to now, our understanding of the ways in which HZE particles might affect biological matter is based on a few spaceflight experiments from the last Apollo missions (Biostack I and II, Biocore, and Apollo light flash investigations) and the Apollo Soyuz Test Project (Biostack III), and on the limited data available from heavy-ion irradiation from accelerators. In the near future, accelerators capable of accelerating particles up to higher atomic numbers and higher energies will promote increased activity in ground-based studies on biological effects of HZE particles. Comparison of data from such irradiation experiments on Earth with those from an actual spaceflight experiment will show any potential influence of the inevitably attendant spaceflight factors (e.g., weightlessness) on the radiobiological events. Further, the long duration of the LDEF flight will increase the chance of studying the biological effectiveness even of rare components of cosmic radiation, such as iron nuclei or superheavy particles of high energy, which are not yet available from ground-based facilities.

139

## Approach

The flight hardware used to achieve this objective consists of biological specimens and nuclear track detectors. Correlation of the biological and physical events was achieved by using a special sandwich construction of visual track detectors and monolayers of biological objects. Figure 60 shows a photograph of the experiment hardware and illustrates the detector unit construction.

The fluence of heavy particles and/or nuclear disintegration stars depends on the locations of the experiment on LDEF. Therefore, two experiment locations with different shielding against space are used. The experiment consists of 20 detector units, 12 units mounted in a 6-in. deep end corner tray on the Earth-facing end of LDEF, and 8 mounted in one-third of a 6-in. deep peripheral tray. Each unit weighs approximately 2 kg and does not require power. Knowledge of the temperature history around the single units is necessary. For all other orbital parameters needed for the experiment, normal tracking of the spacecraft will be sufficient. All experiment data analysis will be conducted at various experimenters' laboratories in Europe and the U.S. (See tables 15 and 16.)
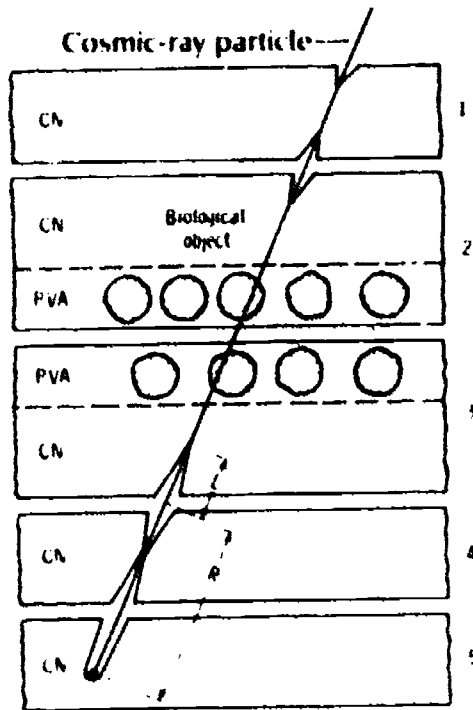
(a) Detector unit construction.
CN    cellulose nitrate; PVA
polyvinyl alcohol; I    cone
length; R    residual range.



(b) Tray configuration.

Figure 60.— Free-flyer biostack experiment.

**Table 15.—Biological Objects in Biostack Experiment**

| Biological object | Biological system | Track detectors | Effects under investigation | Investigator | Affiliation |
|---|---|---|---|---|---|
| Biomolecules | Rhodopsin | CN | Influence on the optical absorption | S. L. Bonting | University of Nijmegen, The Netherlands |
| Unicellular | Bacillus subtilis spores | CN, Lexan, AgCl | Influence on spore outgrowth, cell development, colony formation | R. Facius, G. Horneck, G. Reitz, M. Schafer, J.-U. Schott, K. Baltschukat | DLVR, FRG |
| Plant | Arabidopsis thaliana seeds | CN, Lexan, AgCl | Influence on germination, plant development, mutation induction | A. R. Kranz | University of Frankfurt, FRG |
| Plant | Sordaria fimicola ascospores | CN, Lexan, AgCl | Influence on germination, mycel growth, reproduction, mutation rate | J.-U. Schott | DLVR, FRG |
| Plant | Nicotiana tabaccum seeds | CN | Influence on germination, growth and development, mutation induction | M. Delpoux | University of Toulouse, France |
| Plant | Zea mays seeds | CN, Lexan | Influence on germination growth, differentiation and morphogenesis, mutation induction | C. A. Tobias, T. Yang, M. Freeling | University of California, Berkeley |

**149**

**Table 15.—Concluded**

| Biological object | Biological system | Track detectors | Effects under investigation | Investigator | Affiliation |
|---|---|---|---|---|---|
| Plant | Rice seeds | CN | Influence on germination, growth and development, mutation induction | M. Bay-onove | University of Monpellier, France |
| Animal | Artemia salina cysts | CN | Influence on early steps of development, metabolism (biochemical analysis), integrity of ultrastructure | G. Gasset, Y. Gaubin, H. Planel | University of Toulouse, France |
| Animal | Artemia salina cysts | CN | Influence on hatching, induction of development anomalies, histological anomalies | E. H. Graul, W. Ruther | University of Marburg, FRG |

**Table 16.—Radiation Detectors in Biostack Experiment**

| Cosmic radiation component | Detector | Range of information on Z and LET | Threshold | Tissue equivalence | Background noise | Time assignment | Investigator | Affiliation |
|---|---|---|---|---|---|---|---|---|
| Heavy ions | Nuclear emulsion | Very broad | No | No | High | No | H. Francois, R. Pfohl, G. Hedmann | CEA, France Centre Nucleaire Strasbourg, France |
| Heavy ions | Plastics: cellulosenitrate polycarbonate, CR-39 | Medium | Yes | Yes | Low | No | O. C. Allkoter, R. Beaujean, W. Enge, G. Sermund | University of Kiel, FRG |
| | | | | | | | W. Heinrich | University of Siegen, FRG |
| | | | | | | | R. Facius, G. Reitz, M. Schafer | DFVLR, FRG |
| | | | | | | | M. Debeauvais, R. Pfohl | Centre Nucleaire Strasbourg, France |
| | | | | | | | E. V. Benton | University of San Francisco |

**Table 16 —Concluded**

| Cosmic radiation component | Detector | Range of information on Z and LET | Threshold | Tissue equiv- alence | Background noise | Time as- signment | Investigator | Affiliation |
|---|---|---|---|---|---|---|---|---|
| Heavy ions | AgCl crys- tals | Broad | Yes | No | Medium to low | Yes | F. Schopper | University of Frank- furt, FRG. |
| | | | | | | | J.-U. Schott | DFVLR, FRG. |
| Gamma- rays, X- rays, pro- tons | Lif thermo- lumines- cence do- simeter | Integrating dosimeter | | — | | No | G. Portal, H. Francois | CEA, France |

152

# Seeds in Space Experiment
# (P0004-1)

George B. Park, Jr., and Jim A. Alston
George W. Park Seed Company, Inc.
Greenwood, South Carolina

## Background

Man, when exploring and developing terrestrial frontiers, has generally carried seed for crops to support his survival. In the foreseeable future, man will probably also transport seed in space as he explores and develops that new frontier. The space environment can be hostile to seed; therefore, data are needed on the effects of space on seed and on how seed should be packaged to survive in space. As a first step toward meeting this need, the George W. Park Seed Company, Inc., flew a Getaway Special seed experiment on STS-6 and found that seed can in fact survive a few days in low-altitude Earth orbits. The Seeds in Space Experiment for LDEF will investigate the effects on seed of exposure to space for 1 year.

## Objectives

The specific objectives of this experiment are to evaluate the effects of space radiation on the survivability of seed stored in space under sealed and vented conditions and to determine possible resulting mutants and changes in mutation rates.

## Approach

The basic concept for this experiment is to expose approximately two million seeds of many varieties to space for 1 year and then return them to Earth. The returned seed will be germinated along with control seed of each variety which has not been exposed in space, and the germination rates and development of the plants will be observed. The seed will be packaged in Dacron bags and stored in both sealed and vented containers mounted in a 6-in.-deep peripheral tray. Figure 61 shows photographs of the flight containers, which are painted white for thermal control. Most of the seed will be loaded into the large 12-in.-diameter sealed container to preserve pressure and sufficient moisture. This container has been constructed of aluminum with a thin dome, about 0.050 in. thick, to minimize shielding of space radiation to the top layer of seed. Layering of seed within the container provides increasing shielding to lower layers of seed. Radiation levels will be measured by thin dosimeters placed between layers of seed. Passive maximum-temperature indicators will also be placed inside the container. Another container, mounted on the bottom of the tray, will be painted black and will have a temperature range similar to the average internal temperature of the LDEF.

(a) Vented container.



(b) Sealed container.

Figure 6.    Seeds in Space Experiment

# Space-Exposed Experiment Developed for Students (SEEDS) (P0004-2)

Doris K. Grigsby[*]
NASA Headquarters
Washington. D.C.

## Background

This experiment. which is closely related to the Seeds in Space Experiment (P0004-1). will offer students the opportunity to evaluate the survivability of seeds stored in the space environment and to determine possible mutants and changes in the mutation rate which may occur.

## Objectives

The objectives of this experiment are to involve a very large number of students in a national project to generate interest in science and related disciplines; to offer students from the elementary through the university level an opportunity to participate in a first-hand experiment with materials flown in space; to permit active involvement in classroom experiment design, decision making. data gathering. and comparison of results; and to emphasize a multidisciplinary approach to the project involving subject areas other than science.

## Approach

Approximately 11 to 12 million tomato seeds will be stored in five sealed containers mounted in a 6-in.-deep peripheral tray. (See fig. 62.) Within each sealed container. the seeds will be packaged in four Dacron bags. Passive radiation detectors will be placed inside the canisters. Figure 63 shows the large sealed containers in the tray. without the top thermal cover. After approximately a 12-month exposure to the space environment. the seed will be returned to the George W. Park Seed Co.. Inc.. which will provide the seed kits. In addition to flight seed. an equivalent amount of control seed will be maintained in ground storage facilities. Both sets of seeds will b    aluated postflight to determine germination rates.

After the first LDEF mission is completed. participating student groups will be provided with kits containing samples of both exposed and control seeds. The students will design and conduct their own classroom experiments. Information gathered and evaluated by the students will be made available to the public. NASA. and the Park Seed Co.

[*]Experiment Coordinator

148

Figure 6.2 — Photographs of a sealed container shown with and without bags of flight seed.
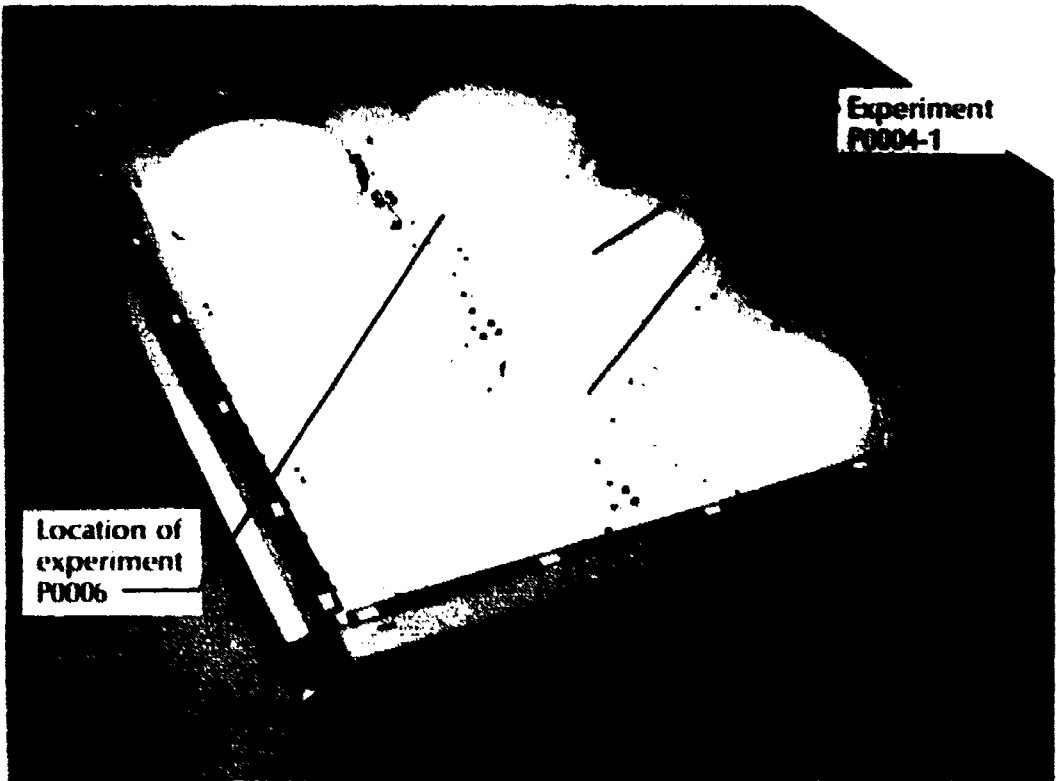
Figure 63.- SEEDS experiment shown integrated with Seeds in Space Experiment (P0004-1) and Linear Energy Transfer Spectrum Measurement Experiment (P0006)

157

*Electronics and Optics*

# Holographic Data Storage Crystals for LDEF (A0044)

W. Russell Callen and Thomas K. Gaylord
Georgia Institute of Technology
Atlanta, Georgia

## Background

A compact high-bit-capacity recorder (on the order of $10^{11}$ bits) and memory system does not exist at the present time. However, electro-optic holographic recording systems are being developed and appear to be extremely promising.

## Objective

The objective of this experiment is to test the spaceworthiness of electro-optic crystals for use in ultrahigh-capacity space data storage and retrieval systems.

## Approach

The experiment approach is to passively expose four holographic data storage crystals, each 10 by 10 by 2 mm in size, to the space environment. Three of the iron-doped lithium niobate crystals contain recorded holograms and one is unrecorded (control sample). Crystal 1 is heat treated for maximum sensitivity and is blank. Crystal 2 contains a plane wave hologram written with a helium-neon laser ($\lambda = 632.8$ nm). Crystal 3 contains a plane wave hologram written with an argon laser ($\lambda = 514.5$ nm), and crystal 4 contains a spoke pattern hologram written with an argon laser ($\lambda = 514.5$ nm). The crystals containing the holograms were fixed in an atmosphere of lithium carbonate to extend the lifetime of the holograms.

This spectrum of crystals will assure determination of the most suitable crystal treatment for space use. A glass control sample will also be flown.

In crystals 2, 3 and 4, the data will be protected by charge neutrality of combined ion and electron patterns, and the holograms should be directly recoverable upon reexposure to uniform illumination. Two control crystals will remain on the ground, one containing a helium-neon laser hologram and one containing an argon laser hologram.

The crystals for this experiment will be included with the various electro-optical components of LDEF experiment S0050, Investigation of the Effects of Long-Duration Exposure on Active Optical System Components, and will be located in the same experiment tray. Figure 64 illustrates the concept of data storage in an optical-phase holographic memory.
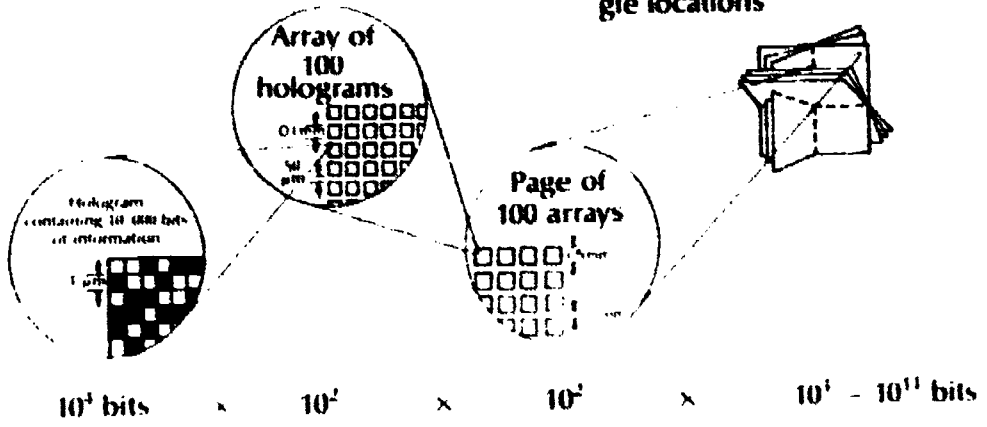
Figure 64. Data storage concept for an optical-phase holographic memory.

# Exposure to Space Radiation of High-Performance Infrared Multilayer Filters and Materials Technology Experiments (A0056)

John S. Seeley, R. Hunneman, and A. Whatley
Department of Cybernetics, University of Reading
Reading, Berks, United Kingdom

Derek R. Lipscombe
British Aerospace Corporation
Stevenage, Hartfordshire, United Kingdom

## Background

Infrared multilayer interface filters have been used extensively in satellite radiometers for about 15 years. Filters manufactured by the University of Reading have been used in Nimbus 5, 6, and 7, TIROS N, and the Pioneer Venus orbiter. The ability of the filters to withstand the space environment in these applications is critical; if degradation takes place, the effects would range from worsening of signal-to-noise performance to complete system failure. An experiment on the LDEF will enable the filters, for the first time, to be subjected to authoritative spectral measurements following space exposure to ascertain their suitability for spacecraft use and to permit an understanding of degradation mechanisms.

Additionally, the understanding of the effects of prolonged space exposure on spacecraft materials, surface finishes, and adhesive systems is of great interest to the spacecraft designer. Thus, a series of materials technology experiments will be included with the experiment on infrared multilayer filters.

## Objectives

The objective of the multilayer filters experiment is to expose high-performance infrared multilayer filters to the space environment and recover them for subsequent analysis and comparison with laboratory control samples. Semiconductors such as PbTe, Si, and Ge will be examined to see if excess free carriers have been generated by exposure, and for evidence of surface contamination or degradation and/or decomposition. ZnS and other dielectrics will be examined for evidence of bulk degradation, such as enhanced absorption, color center excess, and reststrahl abnormalities.

The objectives of the materials technology experiments are to evaluate the degradation of spacecraft surface finishes, the outgassing of spacecraft

surface finishes. the effect of thermal paints on carbon-fiber-reinforced plastic (CFRP) sheet and the thermal differentiation of expansion between base material and thermal coating. the strength of adhesive-bonded joints (lap shear). the effect of CFRP strength stiffness and interlaminar strength. the dimensions of CFRP curvature. and the effect on bond strength between CFRP-aluminum alloy skins and honeycomb core.

## Approach

The experiment will utilize one-sixth of a 3-in.-deep peripheral tray and one-fourth of a 3-in.-deep end center tray on the Earth-facing end of the LDEF. Figure 65 illustrates the arrangement of the filters and materials samples.

The infrared filters being considered for the experiment are listed in table 17. The samples will be measured on an infrared spectrometer with particular reference to any critical parts of their spectrum (e.g., peak transmission and center wave number of bandpass filters. edge position and steepness in edge filters. and transmission in longwave filters) prior to assembly into the experimental structure. At the same time. the samples will be visually inspected and photographed. and any other testing (for example, adhesion tests) will be carried out. Upon retrieval. the samples will be visually inspected prior to shipment back to the laboratory for postflight testing.

**162**

Material samples

Infrared filters

Substrate bearing infrared filter and coatings

Substrate holder

Lead washers

Plate

Backing disk

Disk springs

Snap rings
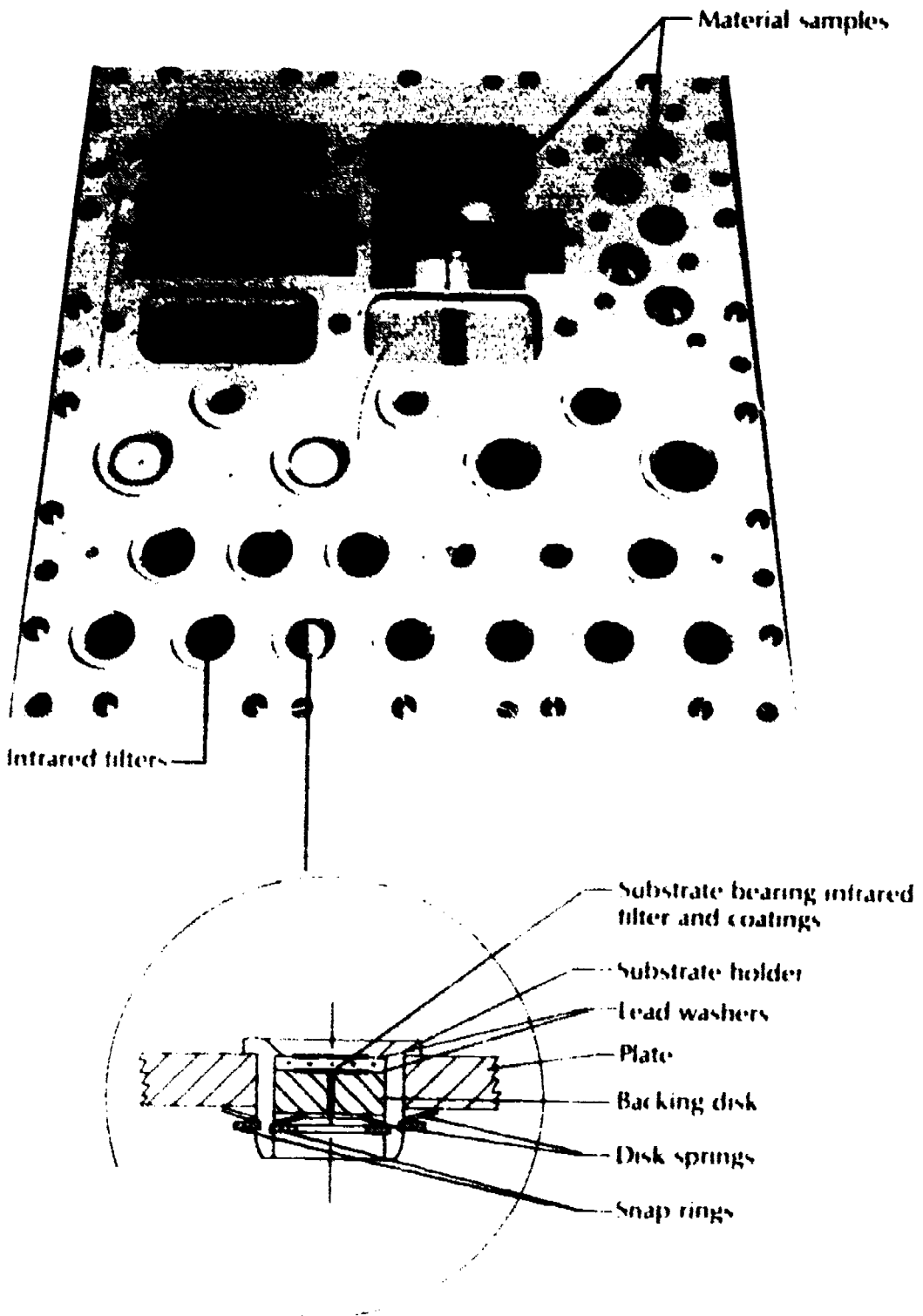
Figure 65   Arrangement of infrared multilayer filter and materials technology experiments.

**163**

**Table 17.—High-Performance Infrared Filters**

| Sample type | Materials (substrate layers) | Function |
|---|---|---|
| Substrate | CdTe | Longwave blocker |
| Substrate | Quartz | Shortwave blocker for longwave filter |
| Substrate | BaF$_2$ | Longwave blocker |
| Substrate | KRS5 (TlBrI) | Longwave blocker |
| Substrate | KRS6 (TlClBr) | Longwave blocker |
| Substrate + coating | Germanium with ZnS/PbTe multilayer | Broadband antireflection coating |
| Substrate + coating | Germanium with ZnS/PbTe, photoresist or PbF$_2$ | Broadband antireflection coating |
| Substrate + coating | Silicon with photoresist | Antireflection coating |
| Substrates + coatings | Silicon with ZnS, silicon with ZnSe, silicon with CdSe | Longwave reststrahl blockers used in Venus, Pioneer probe |
| Substrates + coatings | Germanium with ZnS PbTe multilayers | Bandpass filter on two substrates, 15-μm CO$_2$ band comprising two full blocker edge filters, used in TIROS N Stratospheric Sounding Unit |
| Substrate + coatings | Silicon with CdSe PbTe multilayers | Longwave edge filter at 23 μm, fully blocked to shortwave |
| Substrate + coatings | Germanium with ZnS/PbTe multilayers | 10.6-μm narrowband filter, fully blocked to shortwave |
| Substrate + coatings | Germanium with ZnS PbTe | 15-μm narrowband filter for CO$_2$ band, similar to filters used in Nimbus 5 |
| Substrates + coatings | TlClBr with ZnSe/TlClBr multilayers + photoresist antireflection coating | Longwave edge for Jupiter missions |
| Substrate + coatings | Silicon with ZnSe/TlClBr multilayer | Longwave edge for Jupiter missions |
| Substrate + coatings | Silicon with CdTe/TlBrI multilayer | Longwave edge for Jupiter missions |
| Substrate + coatings | Germanium with ZnS/PbTe multilayer | 10.6-μm narrowband filter, fully blocked to shortwave, ZnS spaced |
| Substrate + coatings | Germanium with ZnS/PbTe multilayer with photoresist antireflection layers | Steep-edge filter at approximately 11.5-μm |
| Mesh filters | Melinex + evaporated Au films | Far-infrared mesh filters |

# Effect of Space Exposure on Pyroelectric Infrared Detectors (A0135)

James B. Robertson, Ivan O. Clark, and Roger K. Crouch
NASA Langley Research Center
Hampton, Virginia

## Background

NASA's commitment to air pollution monitoring and thermal mapping of the Earth, which includes the remote sensing of aerosols and limb scanning infrared radiometer projects, requires photodetection in the 6- to 20-$\mu$m region of the spectrum. The Hg-Cd-Te detectors that are presently used in these wavelengths must be cooled to 50 to 80 K. The cryogenic systems required to achieve these temperatures are large, complex, and expensive.

Pyroelectric detectors can detect radiation in the 1- to 100-$\mu$m region while operating at room temperature. This makes the pyroelectric detector a prime candidate to fill NASA's thermal infrared detector requirements.

## Objective

The objective of this experiment is to determine the effects of long-duration space exposure and launch environment on the performance of pyroelectric detectors. This information will be valuable to potential users of pyroelectrics for predicting performance degradation, setting exposure limits, or determining shielding requirements.

## Approach

In brief, the approach is to measure important detector parameters on a number of detectors before and after flight on the LDEF. Commercially available detectors will be purchased for the experiment. Performance parameters to be measured are responsivity, detectivity, and spectral response. Material properties to be measured are pyroelectric coefficient and dielectric-loss tangent.

After the detectors are returned to the laboratory, all tests and measurements will be repeated to determine the amount and type of damage suffered during launch and exposure.

The detectors for this experiment will be included with the various electro-optical components of experiment S0050, Investigation of the Effects of Long-Duration Exposure on Active Optical System Components, and will be located in the same experiment tray.

158

# Thin Metal Film and Multilayers Experiment (A0138-3)

J. P. Delaboudiniere and J. M. Berset
CNRS/LPSP
Verrieres le Buisson, France

## Background

It is well known that ultraviolet (UV) and extreme ultraviolet (EUV) experiments suffer degradations during space missions of even 1 month duration. It is believed that the degradation is due mainly to condensation of outgassing products, followed by solar-induced polymerization. However, penetrating charged particles are also known to produce volume effects. On the other hand, degradation may start immediately after manufacturing of the component due to oxidation, moisture, or chemical corrosion by atmospheric constituents such as $CO_2$ and $SO_2$. Finally, when the filters are used as windows for gas absorption cells or gas filters, or when they define the instrumental bandwidth by themselves (as in photometers and colorimeters), the effects of mechanical degradation by thermal cycling and or dust impact may be dramatic.

## Objectives

The objectives of this experiment are to investigate the sources of degradation of both state-of-the-art and newly developed components and to test the usefulness of the concept of storing experiment samples in dry nitrogen under launch and space vacuum conditions during reentry mission phases.

## Approach

The experimental approach is to passively expose EUV thin films and UV filters to the space environment for postflight measurement and comparison with preflight measurements. The experiment will be located in one of the three FRECOPA boxes in a 12-in.-deep peripheral tray that contains nine other experiments from France. (See figs. 12 and 13.) The FRECOPA box will provide protection for the experiment samples during the launch and reentry phases of the LDEF mission.

All samples will be manufactured at LPSP according to carefully controlled techniques and will be separated into two exactly similar lots, one of which will serve as control samples and will be stored under vacuum conditions in the laboratory. The flight lot will also be divided into two half-lots. One will be mounted in the FRECOPA box to see solar illumination and the other will be protected from solar illumination. After LDEF de-

ployment, the FRECOPA boxes will be automatically opened to permit exposure and will be closed prior to LDEF retrieval. After the flight samples are retrieved, their optical properties and the optical properties of the control lot will be remeasured. The control lot will be remeasured to account for intrinsic aging.

Each half-lot of the flight samples will contain 12 EUV free-standing "single-layer" thin films (set $S_1$), 24 EUV "single-layer" thin films (set $S_2$), 12 multilayers deposited on glass substrates (set $S_3$), and 4 UV crystals (set $S_4$).

The filters in sets $S_1$ and $S_2$ are thin (1500 to 3000 A) films of selected metals. Under such thickness, good optical transmission is obtained in wavelength bands approximately 100 A wide. Selected materials that provide bands in the extreme ultraviolet include Al, Al + C, Sn, and In.

The metallic multilayers in set $S_3$ are new optical components for the EUV region. Interference effects within a stack of alternatively absorbing and transparent materials of appropriate thickness are used to increase the reflecting efficiency within a narrow wavelength range. The number of periods is on the order of 10 to 40. Layers of Si/W and C/W are scheduled to be included if available.

The UV crystal filters in set $S_4$ are relatively thick (2 mm) crystal windows of LiF and MgF, and are of general use in the far UV range.

For the preflight test program, fabrication controls and preliminary EUV bandpass measurements will be made with a grazing incidence mono-chromator. The full bandwidth of free-standing filters and multilayers will be measured with a synchrotron light source in several wavelength intervals from 40 to 2000 A, with emphasis on the interval from 100 to 1000 A. Optical constants will be measured from deposits on glass substrates.

Preflight measurements will be repeated for the postflight test program, and surface physical and chemical analyses will be made using the samples deposited on glass substrates and some of the free-standing films in cases where drifts have been observed. This will be possible because several filters of each kind will be used (i.e., destructive testing is possible).

# Vacuum-Deposited Optical Coatings Experiment (A0138-4)

A. Malherbe
Optical Division, Matra S.A.
Rueil Malmaison, France

## Background

In the past, the Matra Optical Division has developed a wide range of optical component manufactured by vacuum deposition, such as metallic and multidielectric reflective coatings in the UV range, metal-dielectric interference filters in the UV (down to 1100 A) and IR ranges, narrow-bandpass filters in the near-UV and visible ranges, selective metallic mirrors in the range from 1500 to 2500 A, antireflective and reflective IR coatings, beam splitters in the visible and IR ranges, and optical surface reflection (OSR) coatings. Many of these components, some of which were the first of this type to be manufactured in the world (e.g., interference filters at Lyman α), have been incorporated into scientific and technical experiments flown on balloons and rockets as well as on Symphonie, Meteosat, OTS, D2-B, TIROS N, and others. These components appear to have operated successfully in flight, but detailed information concerning their long-term behavior is not available.

## Objective

The objective of this experiment is to analyze the stability of various vacuum deposited optical coatings exposed to the space environment.

## Approach

The experimental approach is to passively expose samples of the optical coatings of interest. (See table 18.) Preflight and postflight optical measurements, including visual and microscopic inspections, will be compared to determine the effects of space environment exposure.

The experiment will be located with nine other experiments from France in a 12-in.-deep peripheral tray. The optical coating samples will be located in one of the three FRECOPA boxes located in the tray. (See fig. 12.) The FRECOPA box (fig. 13) will provide protection from contamination for the samples during the launch and reentry phases of the LDEF mission.

Preflight and postflight measurements will include visual and micro-scopic examination and spectrophotometric analysis. For samples that show changes, microphysical analyses will be performed by experienced laboratories.

**Table 18.– Optical Coatings Used in Experiment A0138-4**

| Sample | Performance[a] | Application |
|---|---|---|
| Metallic interference filter made in ultrahigh vacuum, λ = 121.6 nm | T = 10 percent Δλ near 10 nm | Scientific |
| Metallic interference filter made in classical vacuum λ = 121.6 nm | T = 8 percent Δλ near 12 nm | Scientific |
| Metallic interference filter, λ = 130 nm | T = 12 percent Δλ near 15 nm | Scientific |
| Dielectric interference filter, λ = 500 nm | T = 50 percent Δλ near 5 nm | Scientific |
| Bandpass infrared filter, λ = 15 μm | T = 50 percent Δλ near 2 μm | Telecommunication, Earth observation |
| Al + MgF₂ metallic mirror on glass substrate | R = 80 percent at λ = 121 nm | Scientific |
| Al + MgF₂ metallic mirror on Kanigen substrate | R = 75 percent at λ = 121 nm | Scientific |
| Al + LiF metallic mirror on glass substrate | R = 55 percent at λ = 102 nm | Scientific |
| Al + LiF metallic mirror on Kanigen substrate | R = 50 percent at λ = 102 nm | Scientific |
| Platinum mirror | R = 20 percent at λ = 121 nm | Scientific |
| Au mirror | R = 20 percent at λ = 121 nm | Scientific |
| Ag + ThF₄ metallic mirror on glass substrate | R = 95 percent at λ = 450 nm | Earth observation |
| Ag + ThF₄ metallic mirror on Kanigen substrate | R = 95 percent at λ = 450 nm | Earth observation |
| Dielectric mirror at λ = 250 nm | R = 95 percent at λ = 250 nm | Scientific |
| Dielectric mirror at λ = 170 nm | R = 95 percent at λ = 170 nm | Scientific |
| Metallic selective mirror at λ = 170 nm | R = 80 percent at λ = 200 nm and R = 20 percent at λ = 300 nm | Scientific |
| SiO₂-TiO₂ dielectric mirrors | R = 95 percent in visible | Earth observation |
| Antireflection coating in 14- to 16-μm region | T = 94 percent at 15 μm | Telecommunication |
| Antireflection coating in 8- to 13-μm region | T = 94 percent at 10 μm | Earth observation, meteorology |
| Dichrometric separation in visible and infrared region | R = 90 percent in visible, T = 80 percent at 10 μm | Earth observation |

[a] T = transmission, R = reflectance.

# Ruled and Holographic Gratings Experiment (A0138–5)

Gilbert Moreau
Jobin-Yvon Division, Instruments S.A.
Longjumeau, France

## Background

In the past, several ruled and holographic gratings from Jobin-Yvon with various coatings were successfully flown on rocket experiments from LPSP and other organizations as well as satellites D2-A, D2-B, OSO-I, and some from the U.S. Future utilizations of such gratings are being considered for the Space Telescope and for various Spacelab projects being developed by France, Germany, Belgium, and other countries.

The technique used to replicate gratings can also be used to obtain a wide range of lightweight optical components, including sophisticated aspherical, highly polished mirrors.

## Objectives

The objective of this experiment is to test the behavior of ruled and holographic gratings with various coatings after extended exposure to the space environments. Specific objectives include examining the coatings for possible changes and differentiating between the influences of vacuum and solar illumination.

## Approach

The experimental approach is to passively expose samples of the gratings and coatings of interest. Preflight and postflight examination to characterize the optical quality of the gratings will include measurement of wavefront flatness, reflection efficiency, and stray-light level.

The experiment will be located with nine other experiments from France in a 12-in.-deep peripheral tray. The grating samples will be located in one of the three FRECOPA boxes located in the tray. (See fig. 12.) The FRECOPA box (fig. 13) will provide protection for the samples from contamination during the launch and reentry phases of the LDEF mission.

The following is a list of the samples to be used in this experiment with a description of each. Type "G" is a replica of a grooved grating with 1200 grooves/mm blazed at 2500 A (aluminum-coated blank pyrex). Type "H" is an original holographic grating with 3600 grooves/mm and a spectral range of 500 to 1500 A (platinum-coated blank pyrex). Type "HU" is an ion-etched blazed grating with 1200 grooves/mm blazed at 2500 A (aluminum-coated

163

blank pyrex). Type "W" is a control mirror on blank pyrex. One half is coated with aluminum and the other half with platinum. Samples will be located on both sides of the mounting plate within the FRECOPA box and will have the shape of a parallelepiped with dimensions 34 by 34 by 10 mm. A set of control samples will also be stored in the laboratory for comparison with those retrieved from space.

Preflight and postflight measurements to be made include the following parameters.

1. Wave surface flatness. - This will separate changes introduced by groove distortion and blank distortion and will be measured on an order of zero for types H, G, and W, and on an order of one for types G, H, and HU. The measurement will be made by photography using a Michelson interferometer.

2. Reflection efficiency. - This is measured with a photogoniometer from 2200 to 6000 A for types G, HU, and W and with a vacuum photogoniometer from 584 to 1216 A for types H and W.

3. Stray light level. - For types G and HU, measurements will be made using a continuum spectrum (deuterium lamp) near 2000 A on a monochromator with a liquid filter. For type HU, measurements will be made using a laser line (6328 A) on a monochromator. These measurements will help define the limits of utilization for each type of grating. Comparison of the different measurements before and after space exposure will help define the space environment elements that cause degradation of grating optical qualities and the grating components which are damaged by those elements.

171

# Optical Fibers and Components Experiment
# (A0138-7)

J. Bourrieau
CERT/ONERA-DERTS
Toulouse, France

## Background

Fiber optics are becoming important components in communication systems, optoelectronic circuits, and data links. Space applications are now available with various advantages: weight and size reduction, data transmission rate increase (10 to $10^7$ Mbits), and reduction of electromagnetic susceptibility and power requirements. High sensitivity to ionizing radiations, however, may be a restriction for optic-fiber use on satellites. Presently, in-flight observations of optic-fiber damages are not available, but an increasing number of laboratories are carrying out irradiation tests on these components using neutrons, gamma rays, and X-rays. Radiation damage on optical materials, however, is strongly linked to the test conditions (temperature, dose rate, energy, and nature of the incident particles), and laboratory tests are not as representative as actual space environment exposure.

## Objectives

The main objective of this experiment is the comparison of fiber optics permanent damages induced by ionizing radiation after a long exposure in space and after laboratory tests. Specific objectives are to validate irradiation tests performed with radioactive sources ($Sr^{90}-Y^{90}$), to verify computer codes used for the fluence and dose profiles, to determine the performance of fiber optics waveguides in a low-altitude orbit (doses between 10 and 100 Gy are expected), and to determine the origin of transmission losses (e.g., color centers and index variations) in the material.

## Approach

The experimental approach is to passively expose two optic-fiber waveguides (one step index and one graded index) of some 60 cm in length with connectors. (See fig. 66.) Preflight and postflight measurements of optical properties will be compared to determine the effects of space environment exposure.

The experiment will be located with nine other experiments from France in a 12-in.-deep peripheral tray. The optical fibers will be located in one of the three FRECOPA boxes in the tray. (See fig. 12.) The FRECOPA box (fig. 13)

will provide protection for the optical-fiber waveguides from contamination during launch and reentry phases of the LDEF mission. The in-flight absorbed dose profile will be measured with five thermoluminescent dosimeters shielded by various aluminum thicknesses.

Irradiation of the selected optic fiber waveguides will be carried out in the laboratory with an $Sr^{90}$–$Y^{90}$ beta ray source in order to simulate the in-flight dose. Before and after flight and laboratory simulation, measurements of the optic-fiber waveguide light transmission will be made with a spectrophotometer. Four sets of samples will be manufactured, one for ground test and the others for control, flight, and space flight sets.
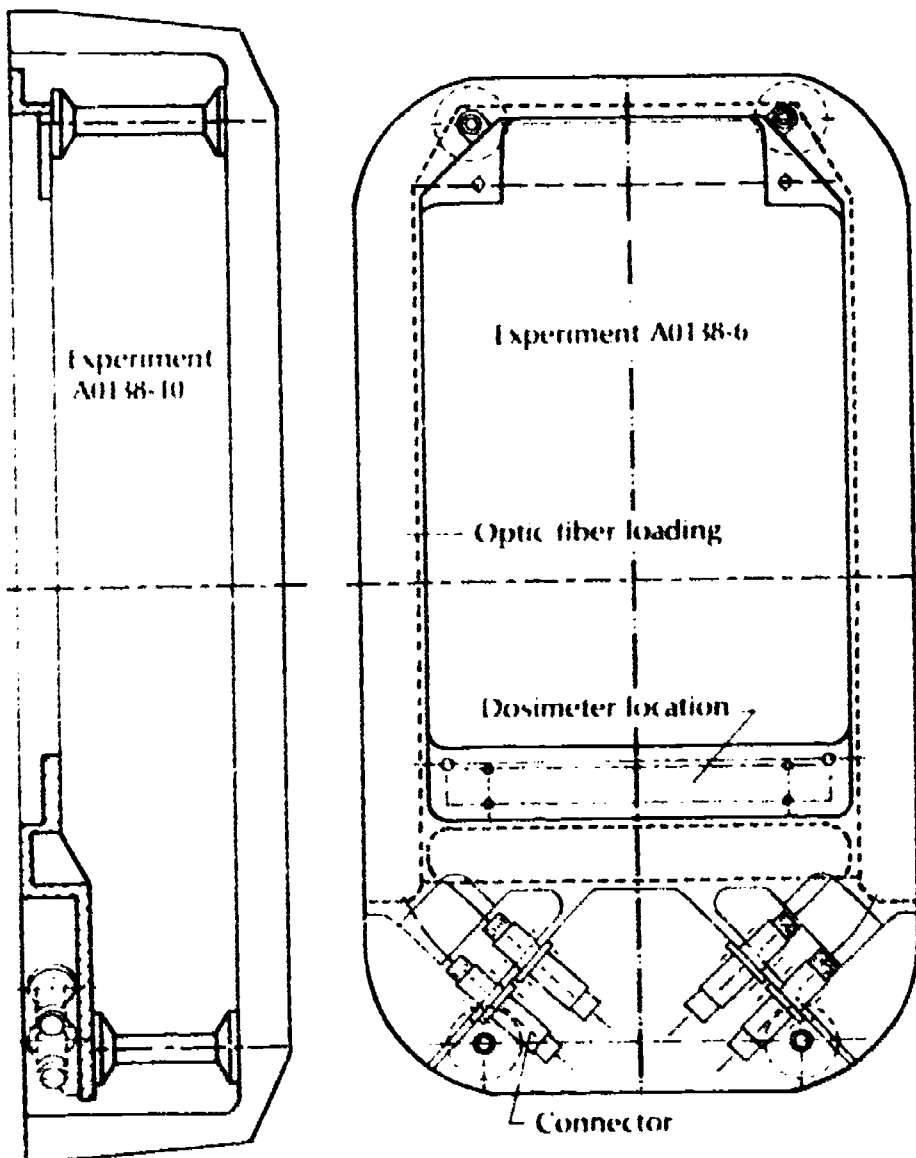


Figure 66. –Optical-fibers experiment configuration.

173

# Passive Exposure of Earth Radiation Budget Experiment Components (A0147)

John R. Hickey and Francis J. Griffin
The Eppley Laboratory, Inc.
Newport, Rhode Island

## Background

Earth Radiation Budget (ERB) experiments require accuracies on the order of fractional percentages in the measurement of solar and Earth flux radiation. In order to assure that these high-accuracy devices are indeed measuring real variations and are not responding to changes induced by the space environment, it is desirable to test such devices radiometrically after exposure to the best approximation of the orbital environment.

## Objective

Since the Earth Radiation Budget experiment was operational on Nimbus 6 and is operational on Nimbus 7, and since in-flight calibration is difficult for the solar and Earth flux channels, the objective of this experiment is to expose ERB channel components to the space environment and then retrieve them and resubmit them to radiometric calibration after exposure. Subsequently, corrections may be applied to ERB results and information will be obtained to aid in the selection of components for future operational solar and Earth radiation budget experiments.

## Approach

Passive exposure of solar and Earth flux channel components of the ERB radiometer is the basis of the approach. Three Earth flux channel types of ERB will be mounted in one-fourth of a 3-in.-deep end center tray on the Earth-viewing end of the LDEF. (See fig. 67.) Prior to delivery, these channels will undergo complete radiometric and spectrophotometric examination. These tests will be repeated after retrieval to evaluate changes in orbit. The solar-channel components will be mounted in one-sixth of a 3-in.-deep peripheral tray near the leading edge of the LDEF (in the direction of the velocity vector) to view the Sun in the manner most like the ERB experiment on Nimbus. Solar-channel components to be tested include thermopiles, interference filters, and fused silica optical windows. (See fig. 68.) Additionally, some state-of-the-art vacuum-deposited interference fil-
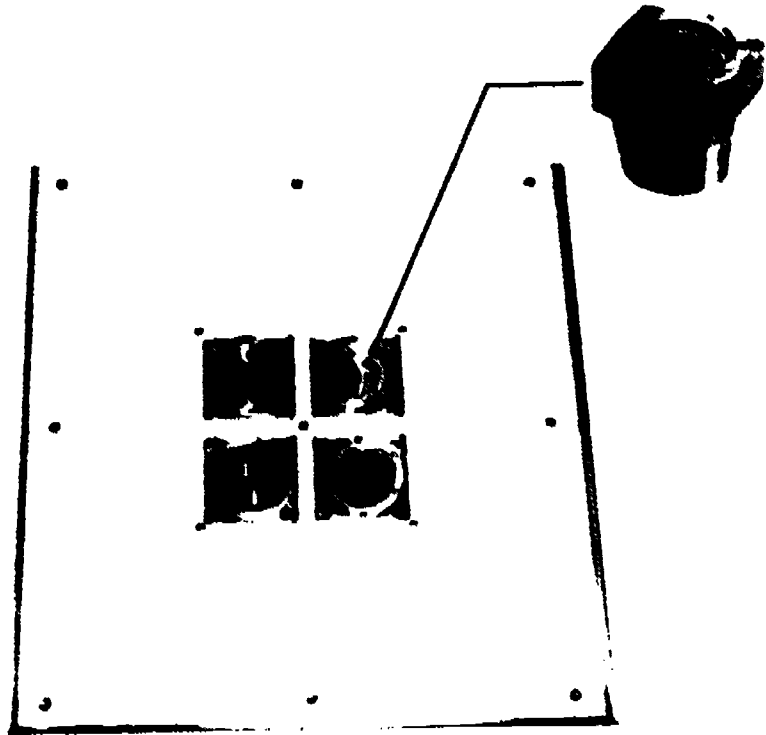
Figure 67.   Earth flux channel components.



Thermopiles, interference
filters, and fused
silica optical windows

Interference
filters
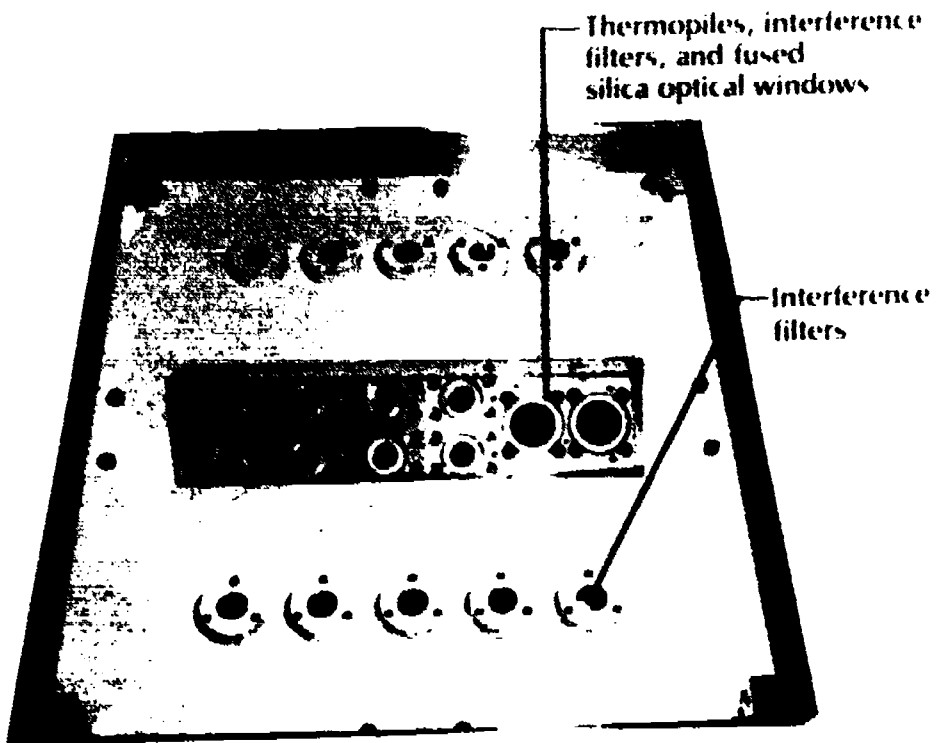
Figure 68.—Solar-channel components.

175

ters have been included to examine space environment effects on these components. The two thermopiles will have different black paint on the receivers. The cavity unit will be similar to that proposed for future solar-constant measurement missions. Vacuum bakeout will be performed on all elements as prescribed and performed for Nimbus prior to delivery. Radio-metric testing and weighing will be performed on the thermopile and cavity devices. Spectrophotometric testing will be performed on filters and fused silica components.

169

# Effects of Solar Radiation on Glasses
# (A0172)

Ronald L. Nichols
NASA George C. Marshall Space Flight Center
Huntsville, Alabama

Donald L. Kinser
Vanderbilt University
Nashville, Tennessee

## Background

The deterioration of glass when subjected to solar radiation has been scientifically observed. Since the molecular structure of glass is considered to be in a metastable state, this lack of stability is not an unexpected event; the glass would achieve a lower state of energy if its atoms were rearranged in a long-range repetitious lattice structure. Changes in the properties of a glass are commonly associated with exposure to solar radiation. Because of insufficient test data for glasses exposed to actual space radiation, the materials engineer must attempt to extrapolate from data for artificial solar radiation exposure in order to select glasses for use in hardware that will be exposed to the space environment for long periods of time. This limitation severely degrades the confidence level for the performance of glasses utilized in space.

## Objective

The objective of this experiment is to determine the effects of solar radiation and space environment on glasses in space flight by exposing glass specimens to the space environment and analyzing the optical, mechanical, and chemical property changes that occur. The property changes of samples receiving differing cumulative solar radiation exposure will be compared.

## Approach

This experiment will be conducted by passively exposing glass samples to the space environment. Glass samples occupying one-sixth of a 3-in.-deep tray will be located near the trailing edge of the LDEF so that they will be exposed to a maximum amount of incident solar radiation. This location will contain 68 cylindrical disc samples 1.25 in. in diameter. (See fig. 69.) Another group of 52 samples occupying one-fourth of a 3-in.-deep tray will be located on the Earth-facing end of the LDEF and will receive minimum exposure to solar radiation. The properties of each sample will be measured
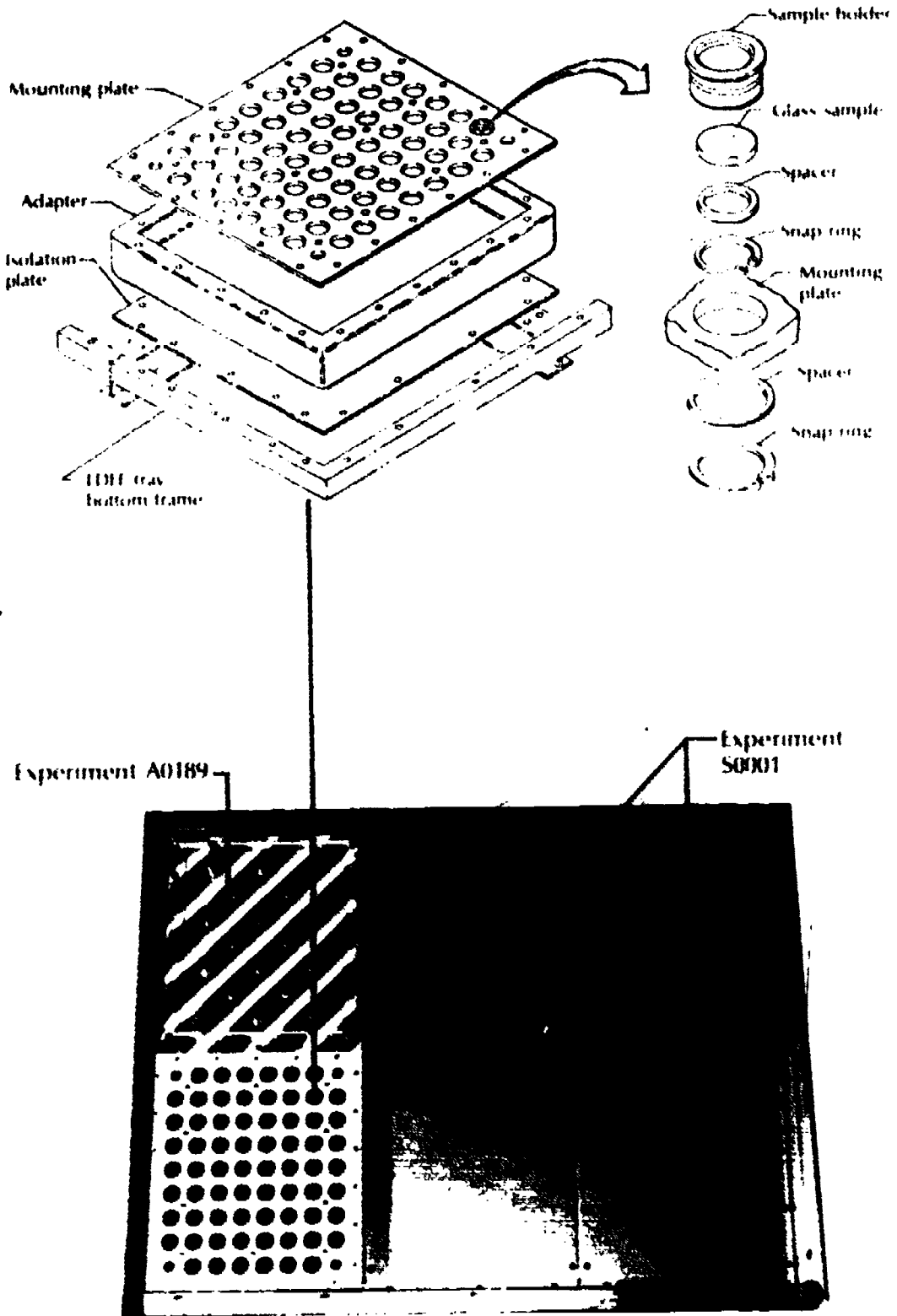
Figure 69. Solar radiation on glasses experiment.

171

prior and subsequent to exposure to the space environment. Several samples of each glass composition selected for flight will be evaluated to allow a statistical analysis of the data obtained. Candidate compositions include aluminosilicates, fused silica, titanium silicate, lead silicates, borosilicates, soda potash lime, potash borosilicate, and soda lime silica glasses

# Study of Factors Determining the Radiation Sensitivity of Quartz Crystal Oscillators (A0189)

John D. Venables and John S. Ahearn
Martin Marietta Laboratories
Baltimore, Maryland

## Background

It has long been known that radiation increases the acoustic absorption of quartz crystal oscillators and produces shifts in their resonant frequency which may be as large as 400 parts per million. The need for high-precision quartz oscillator clocks (and filters) in communication satellites, missiles, and space probes makes it necessary to improve the radiation stability of materials used for these applications.

Experiments performed at Martin Marietta Laboratories demonstrate that the technique of transmission electron microscopy (TEM) provides a powerful method for studying the effect of radiation on crystalline quartz. When suitably thin samples of $\alpha$-quartz are examined by TEM, it is observed that defect clusters form at a rapid rate within the material even when the incident electron energy is as low as 40 keV. Studies of this phenomenon indicate that the clusters are formed from atoms that have been displaced by electrons in the incident beam, that the clusters nucleate at impurities (because the cluster concentration appears to be impurity dependent), and that the clusters induce large strain fields in the lattice surrounding them, as evidenced by their paired black-dot images, which are characteristic of "strain field contrast."

Two factors suggest that the observed clusters may be responsible for the radiation-induced frequency drift and acoustic-absorption effects associated with irradiated quartz resonators. First, the clusters are expected to be very effective in modifying the piezoelectric properties of quartz because of the large strain fields associated with them. Second, both phenomena appear to be sensitive to the impurity concentration. If this conclusion is valid, it suggests that TEM can be used to classify grades of quartz according to their suitability for use in radiation-hard resonators. Moreover, using this technique it may be possible to identify the impurities that are responsible and thereby effect an improvement in the stability of quartz oscillators.

## Objective

The objective of this experiment is to determine whether there is a correlation between defect cluster concentrations observed for different

grades of quartz examined by TEM and the electrical stability of quartz resonators exposed to the complex radiation associated with an orbital LDEF environment.

## Approach

To accomplish the objectives, several grades of single-crystal α-quartz containing a wide range of impurity concentrations have been examined by TEM to determine differences in their susceptibility to cluster formation during electron irradiation. Based on the sensitivity of the quartz materials to radiation as determined by TEM, two grades of quartz have been selected for fabrication into resonators. The selection has been made to maximize the differences in radiation sensitivity of the chosen materials. The electrical properties of the resonators are being established by measuring their resonant frequency as a function of time to establish the natural frequency drift of the resonators before insertion into orbit. After exposure to the LDEF environment, a second series of electrical measurements will be made on the resonators to determine variations from the preflight data. Changes in the electrical data will then be compared with TEM results to determine whether TEM observations are relevant to the study of the stability of quartz resonators in an outer-space environment.

The experiment hardware consists of one-sixth of a 3-in.-deep peripheral tray with 14 5-MHz fifth-overtone, AT-cut resonators mounted on an aluminum plate, as shown in figure 70. The resonators have been fabricated from two materials (synthetic swept premium Q and Brazilian natural quartz) selected because the TEM technique indicates large differences in their radiation sensitivity. Four resonators (two from each grade of material) will be used as controls and shielded from radiation. The remaining ten resonators (five from each grade) will be exposed to the space radiation. In addition, two resonators (one from each grade) will be kept in the laboratory as additional controls. By determining the frequency drift of the resonators before and after the LDEF flight, as well as the frequency offset occurring during the flight, it will be possible to separate the natural frequency drift from that induced by the space radiation and to determine whether the radiation damage observed by TEM correlates with the space radiation environment of an orbital LDEF flight

174

—Holddown cage—

—O-ring—

—Resonator case (glass)—

—Holddown screws
(helicoils)

—Mounting plate—

—O-ring—

—Electrical leads

Control
resonator
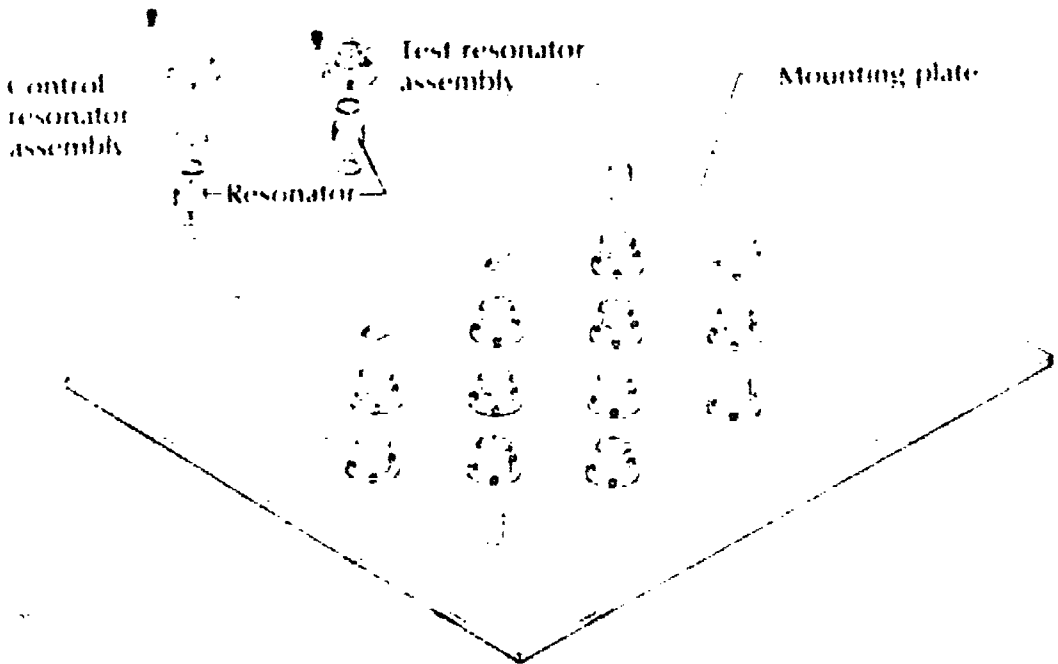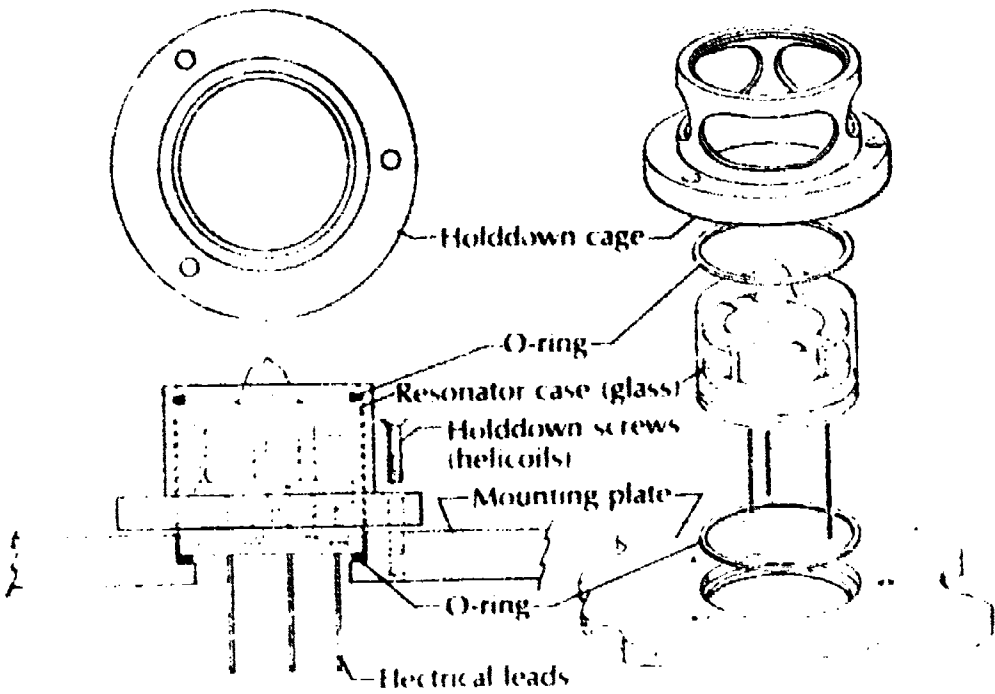assembly

Test resonator
assembly

Mounting plate

—Resonator—

Figure 70. Quartz crystal oscillator experiment.

# Investigation of the Effects of Long-Duration Exposure on Active Optical System Components (S0050)

M. Donald Blue, James J. Gallagher, and R. G. Shackelford
Engineering Experiment Station, Georgia Institute of Technology
Atlanta, Georgia

## Background

In the future, electro-optical systems will find increasing applications in space-based systems. The successful flights of interplanetary probes dating back to Mariner II in 1962 have demonstrated the ability of optical systems to operate in the interplanetary space environment over periods of many months. Current and planned Earth resources and meteorological satellites are indicative of the complexity being achieved in such systems, and the planned laser intersatellite communication links show a new level of sophistication being developed for future electro-optical systems.

The environmental hazards peculiar to space include radiation-induced discoloration, electrically active flaws, and changes in index of refraction. These problems may arise from sublimation, outgassing, and decomposition effects as well as from deposition of such products and other debris onto component surfaces. Other hazards are abrasion or cratering of surfaces, which are caused by meteoroids and cosmic dust.

Optical and electro-optical components must survive this environment. Assurance of survival is typically provided by ground-based testing to simulate those aspects of the space environment which are considered most serious. The availability of the LDEF permits exposure of electro-optical components to a true space environment at a reasonable cost.

## Objectives

The objectives of this experiment are to determine quantitatively the effects of long-duration space exposure on the relevant performance parameters of lasers, radiation detectors, and selected optical components, to evaluate the results and implications of the measurements indicating real or suspected degradation mechanisms, and to establish guidelines, based on these results, for selection and use of components for space electro-optical systems.

## Approach

The experiment includes a representative sample of sources, detectors, and passive components typical of basic elements in electro-optical systems.

These components are mounted in a 6 in. deep peripheral tray in a manner that simulates their likely surroundings in an operational system. Figure 71 shows the construction and assembled appearance of one of the six subtray panels making up the experiment. Careful attention to surface coatings is required to maintain component temperatures below levels at which deterioration can occur. The arrangement shown in the figure uses a sunscreen, black paint, and anodized coatings to achieve a temperature range of —50 to 68 C
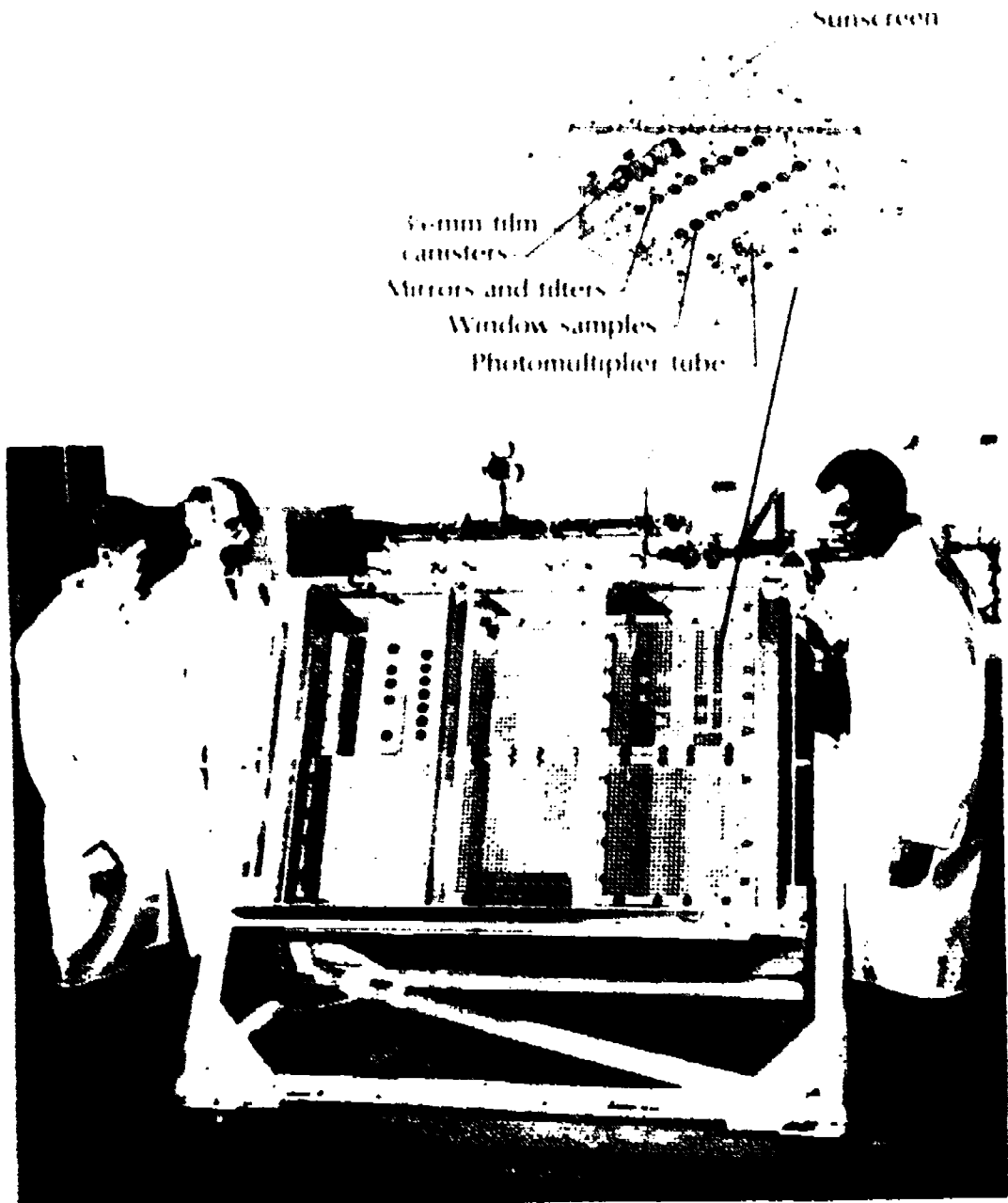


Figure 71. —Active optical system components experiment.

A total of 171 components have been acquired, of which 136 will be mounted in the tray and 35 will be maintained in the laboratory as controls. A brief listing of these components is presented in table 19.

The analysis procedure involves careful measurement of the operational characteristics of the components before and after space flight. It may be necessary to analyze surface debris or coatings of condensed materials on optical surfaces, although the extent and nature of such effects cannot be anticipated at this time. The analysis techniques available include scanning electron microscopy, electron and X ray fluorescence spectroscopy, and X-ray diffraction.

Duplicate components will be stored in a laboratory environment and will be available for comparison purposes in most cases. The experiment will be passive and no electrical power will be employed. Components normally operated at cryogenic temperatures will not be cooled. For this reason, the

Table 19. — Electro-Optical Components

| Passive components | Active components | Detectors |
|---|---|---|
| Black paint, EccoSorb CR-110 | Modulator, ammonium dihydrogen phosphate | Silicon PIN |
| Black paint, 3M black 401 C10 | Channeltron array | Silicon photovoltaic |
| Black paint, HTRI bone black D-111 | Laser diode, Al$_x$Ga$_x$As | Silicon gamma ray detector |
| Black paint, 3M CR-110 on EccoSorb | Laser diode array | PbSnTe photovoltaic planar arrays |
| Black paint, Chemglaze Z-306 flat | GaAs LED | GaAsSb photovoltaic |
| Neutral-density filter | YAG, Nd rod | InSb photovoltaic |
| Narrowband filters | CO$_2$ waveguide laser | PbS photoconductive |
| Hot mirror | HeNe laser | PbSe photoconductive |
| Dielectric mirrors | Holographic crystals | HgCdTe photoconductive |
| Optical glasses | Flash lamps | HgCdTe photovoltaic |
| Window, MgF | | Pyroelectric LiTaO$_3$ |
| Window, Al$_2$O | | Ultraviolet photomultiplier tube |
| Window, CaF$_2$ | | UV Si |
| Window, LiF | | Pyroelectric, Strontium barium niobate Triglycine sulfate LiTaO$_3$ |
| Window, SiO$_2$ | | |
| Mirror, Al + MgF$_2$ | | |
| Mirror, UV laser | | |
| Filter, Lyman α | | |
| Filter, 1600 Å | | |
| 35-mm canister shortwave radiation film | | |
| Black polyethylene | | |

experiment will serve to establish a baseline for the effects of degradation of components at ambient temperature. Future experiments on the effects of exposure at normal cryogenic operating temperatures can be combined with the ambient-temperature data to separate degradation effects that are specifically temperature related.

# Fiber Optic Data Transmission Experiment
# (S0109)

Alan R. Johnston and Larry A. Bergman
Jet Propulsion Laboratory
Pasadena, California

## Background

Application of fiber optic technology to data transmission on a space-craft will yield several benefits in comparison to conventional copper wire transmission. Probably the most important advantage is that fiber links are inherently insensitive to pickup, electromagnetic interference, and ground loops. Also, fibers are roughly two orders of magnitude smaller and lighter than their copper wire equivalent, and ultimately it is anticipated that a fiber link will become cheaper than copper. The same components, once installed, could handle the wide range of signal bandwidths, from telephone rates (tens of kilobits) up to tens of megabits. In addition, there is a largely unexplored relationship with the developing microcircuit technology, suggesting other applications that are presently unknown. Therefore, early verification of fiber optic technology in the spacecraft environment should have a broad-based interest in the future, and this experiment will provide an opportunity to test representative types of fiber links in an actual space environment.

## Objective

The objective of this experiment is to test fiber optic components in the space environment to determine their ability to operate over long periods of time without degradation of performance.

## Approach

The experiment occupies a 6-in.-deep peripheral tray and consists of approximately 10 state-of-the-art fiber cable samples and three candidate connector types which will be passively exposed to the space environment. Figure 72 shows the flight hardware.

Four fiber cable samples will be mounted in a planar helix coil on thermally isolated mounting plates attached at the tray surface. Six or more additional cable samples will be mounted on the bottom surface of the tray. Each of the cable samples will be terminated in connectors mounted on brackets. These will be located on the back surface of the upper plates, or on the base plates for the internally mounted samples.
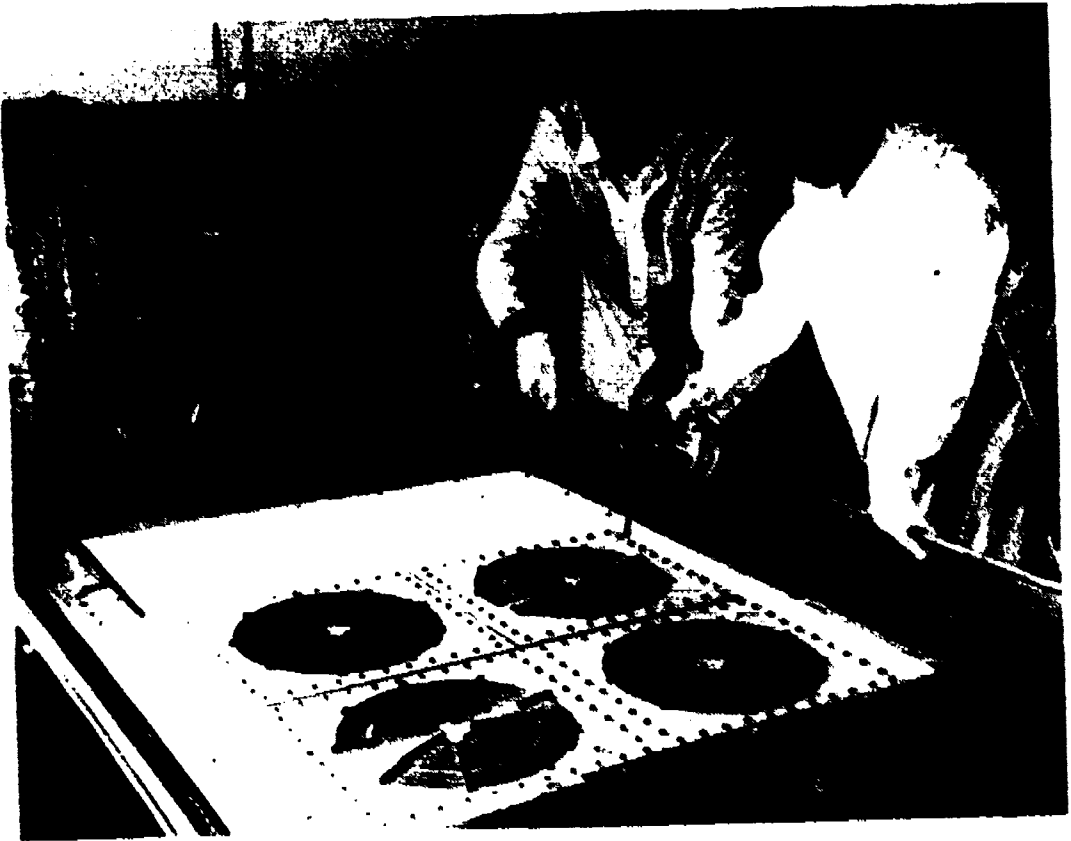
Figure 72. Fiber optic data transmission experiment shown during receipt and inspection activity

181

# Space Environment Effects on Fiber Optics Systems (M0004)

Edward W. Taylor
Air Force Weapons Laboratory, Kirtland Air Force Base
Albuquerque, New Mexico

## Background

Although the application of fiber optic technology in ground-based data links is becoming commonplace, the technology advancement for aerospace military application has not yet developed to the extent that full utilization is a reality. Although fiber optic technology offers advantages such as reduction of system susceptibility to electromagnetic pulse (EMP), electromagnetic interference (EMI), system-generated EMP (SGEMP), ground loop, and inadvertent discharge phenomena, the undesirable response of optical fibers exposed to ionizing radiation is presently of concern to military aerospace system designers. Functional improvements, such as weight and power reductions, realized through the use of fiber optic technology certainly appear attractive at this time, particularly in aerospace communication systems. However, since optical waveguide electro-optic technology has yet to be used in space-borne applications, issues such as link life expectancies, power consumption, sensitivity, and radiation hardening are of primary concern.

Space qualification of materials unique to fiber optic technology (i.e., bonding and potting agents) over a typical temperature range from $-65°C$ to $125°C$ under vacuum conditions is an immediate need for satellite applications. In essence, then, fiber optic space application must begin with early spaceflight assessment of the influence of launch and orbital extremes. This Air Force Weapons Laboratory (AFWL) investigation, although primarily concerned with the survivability and vulnerability of fiber optic systems exposed to the space radiation environment, is also cognizant of the entire space qualification requirement.

## Objectives

The objectives of this experiment are to assess the performance survivability of hardened fiber optic data link design for application in future spacecraft systems and to collect, analyze, and document the effects of space environmental conditions on link performance. Particular attention will be directed toward the integration and operation of new fiber optic link components exhibiting increased hardening to radiation environments. The opportunity to expose operational fiber optic data links to an actual space environment for 6 months or longer and to retrieve the data links for analysis

82

is expected to impact future Air Force design of space-qualified fiber optic systems. Data from the experiment, along with data from previous AFWL material and component radiation response studies, will be used to form reliable design criteria for future spacecraft applications, particularly relative to the long-term low-dose space radiation effects as a function of temperature.

## Approach

This investigation is composed of nine distinct experiments consisting of both active and passive data links or components. Certain links or components will be preirradiated in order to assess the effects of the long-term low-dose space radiation environment on link performance. The data rate for the active fiber optic links was selected to be 10 Mbits/sec. Shown in figure 73 is a photograph of the fiber optics systems experiment, which will be installed in a 6-in.-deep peripheral tray. In all instances, emitters, detectors, and all connectors, couplers, and electronic components are tray shielded. Experimental measurements to be performed and recorded on magnetic tape will include bit error loss (BER) burst errors and fiber attenuation losses for the data links, in addition to fiber temperature and tray volume temperature.
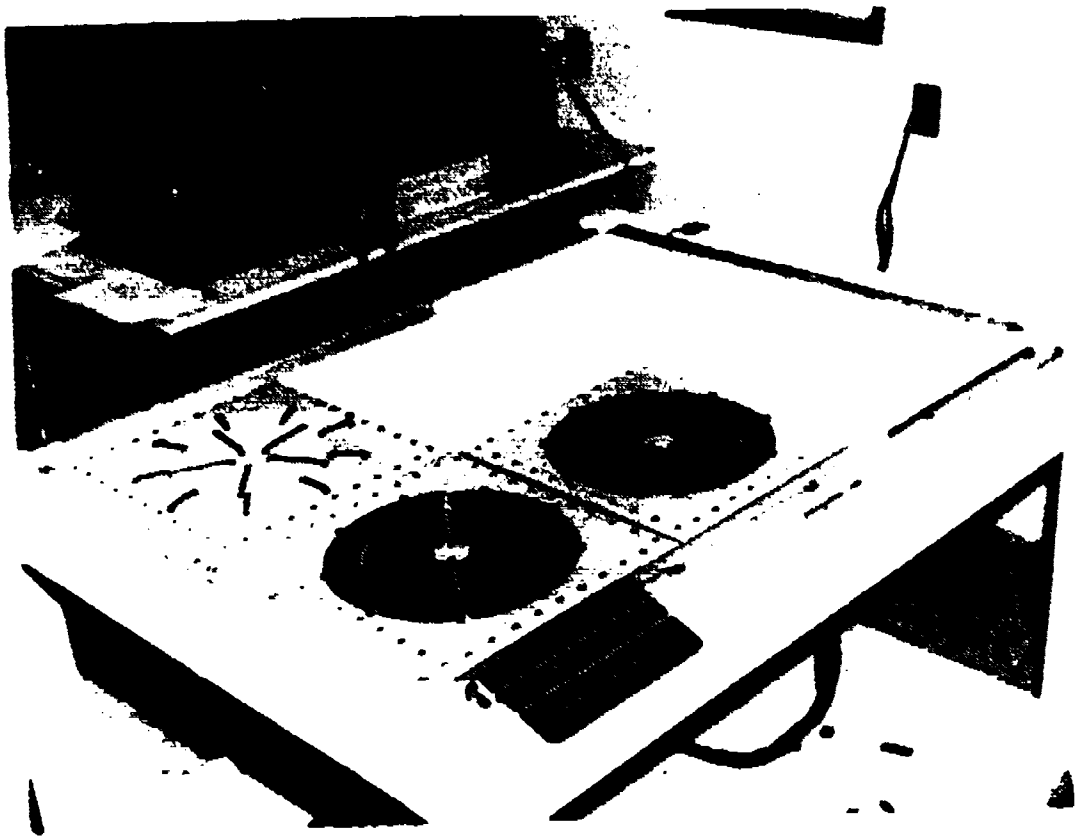


Figure 73 — Fiber optics systems experiment.

183

Thermoluminescent devices will be used within the tray volume in order to measure incident radiation. An experiment power and data system (EPDS) will be used to satisfy the data recording requirements.

## Active Experiments

*Active data links.* — Four active links will be exposed to space. One of these links will consist of 45 m of cabled glass fiber incorporating a hermetically sealed emitter and detector operating at a wavelength of 1.3 μm. The remaining active links will consist of three cabled plastic-coated silica fiber links using LED's and PIN photodiodes operating at a wavelength of 830 nm. Two of these links will be 20 m long and the remaining link will be 48 m long. Optical waveguides, connectors, and other experimental equipment will consist of components selected according to recent results of Air Force studies.

*One-m temperature data link.* — A 1-m optical data link will be used for recording the relative temperature of the tray inner volume.

## Passive Experiments

*Ten-m data links.* — Three 10-m data links will be located within the tray volume. The links have been preirradiated and will be evaluated upon LDEF retrieval for increased radiation damage. These links will serve primarily as comparison links and will be evaluated upon LDEF retrieval for comparison to the active-link experiments.

*Components experiment.* — This experiment will contain preirradiated and nonirradiated LED's and photodiodes rigidly mounted within a section of the tray volume. As in the case of the active and passive links previously discussed, each component will be characterized prior to launch and will be tested functionally upon mission completion in order to assess any degradation effects from the launch or orbit conditions.

# Space Environment Effects
## (M0006)

Joseph A. Angelo, Jr., and Richard G. Madonna
Air Force Technical Applications Center
Patrick Air Force Base, Florida

Lynn P. Altadonna
Perkin-Elmer
Danbury, Connecticut

Michael D. D'Agostino and Joseph Y. Chang
Grumman Aerospace Corp.
Bethpage, New York

Robert R. Alfano and Van L. Caplan
The City College
New York, New York

## Objectives

The primary purpose of this experiment is to examine the effects of long-term exposure to the near-Earth space environment on advanced electro-optical and radiation sensor components. A secondary objective involves an exobiology experiment to observe the effect of long-duration spaceflight on the germination rate of selected terrestrial plant seeds.

## Approach

The approach of the main experiment is to measure the optical and electrical properties of the electro-optical and radiation sensor components before and after exposure to the space environment. The selected components being tested are hard mounted in an experiment exposure control canister (EECC) which occupies one-third of a 6-in.-deep tray, which is then sealed. (See fig. 74.) The sealed EECC prevents contamination of the test components during ground transportation to and from the launch site, payload processing at the launch complex, and launch and landing. The EECC is programmed to open 2 weeks after deployment and close 1 week prior to anticipated retrieval. The EECC will not be reopened until the experiment has been returned after the flight to the investigator's laboratory.

The electro-optical and radiation sensor components include a variety of semiconductor materials (e.g., CdSe, p-GaAs, n-GaAs, and GaAs), mirrors (including fused silica and beryllium), a Nd⁺:glass laser rod, a fiber optics cable, and a variety of polymeric materials.

Seed container

Fiber optics
cable

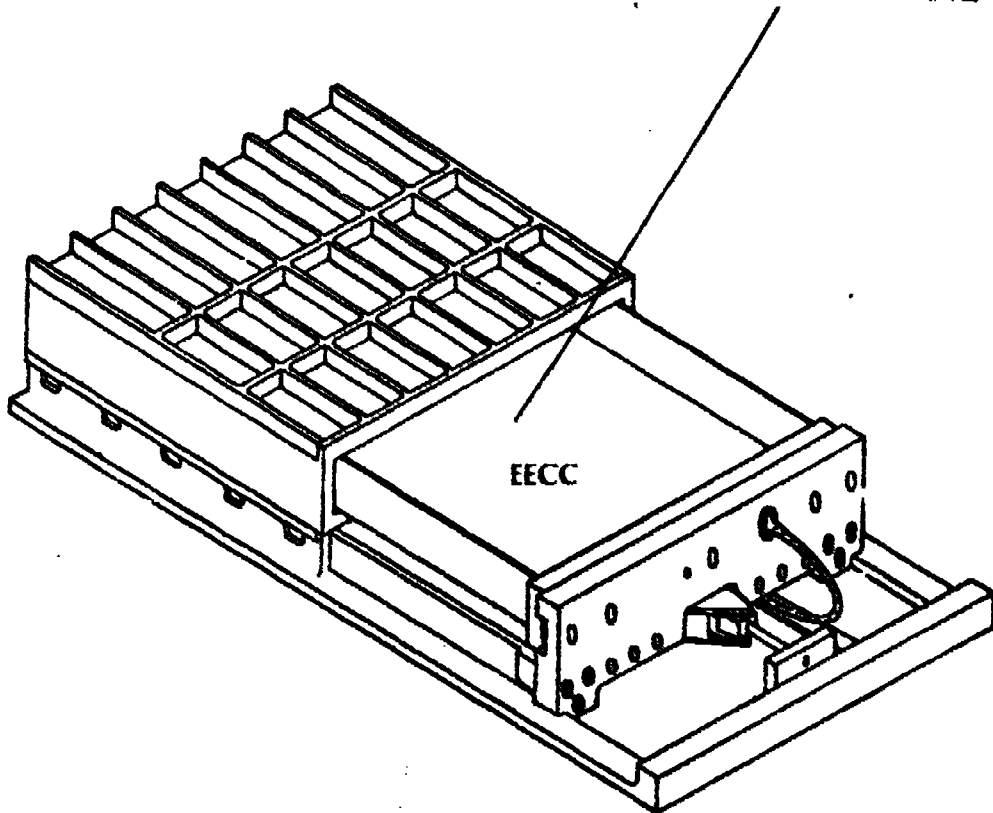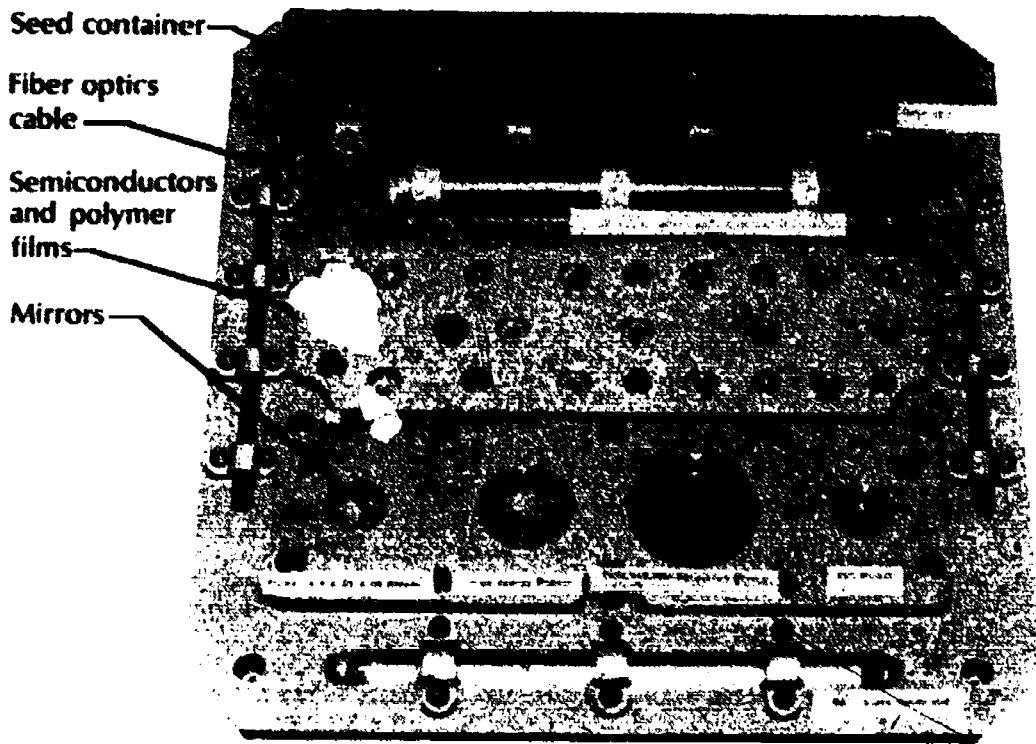Semiconductors
and polymer
films

Mirrors

EECC

*Figure 74.—Space environment effects experiment.*

The secondary exobiology experiment involves a variety of terrestrial plant seeds enclosed in a benign environment (dry air) aluminum alloy tube. Postflight germination rates of these seeds will be compared to the germination rates of control seed samples kept on Earth. Lithium fluoride (LiF) radiation dosimeters are also included in the seed capsule to provide an approximate measure of total space radiation exposure within the capsule. The experiment is housed in an aluminum alloy tube and involves seeds of hybrid 3358 corn, sugar pumpkin, giant gray-striped sunflower, garden bean (Tennessee green pod and bush Romano #14), Henderson's bush lima bean, and Alaska pea.

# Symbols and Abbreviations

| | |
|---|---|
| AFWAL | Air Force Wright Aeronautical Laboratory |
| AFWL | Air Force Weapons Laboratory |
| AR | antireflectance |
| AU | astronomical units |
| BER | bit error loss |
| CERT | Centre d'Etudes et de Recherches de Toulouse |
| CFRP | carbon-fiber-reinforced plastic |
| CHPC | dicyclohexyl peroxydicarbonate |
| CNES | Centre National d'Etudes Spatiales |
| CNRS | Centre National de la Recherche Scientifique |
| CST | Centre Spatial de Toulouse |
| CVCHP | cascade variable–conductance heat pipe |
| DERTS | Direction d'Etudes et de Recherches et Techniques Spatiales |
| DFVLR | Deutsche Forschungs– und Versuchsanstalt für Luft– und Raumfahrt |
| DOD | Department of Defense |
| DOP | di-octyl phthalate |
| EAROM | erasable read-only memory |
| EECC | experiment exposure control canister |
| EMI | electromagnetic interference |
| EMP | electromagnetic pulse |
| EPDS | experiment power and data system |
| ESCA | electron spectroscopy for chemical analyses |
| ESTEC | European Space Research and Technology Center |
| EUV | extreme ultraviolet |
| FRECOPA | French cooperative payload |
| HEPP | heat pipe experiment package |
| IITRI | Illinois Institute of Technology Research Institute |
| IR | infrared |
| JSC | Johnson Space Center |
| KSC | Kennedy Space Center |
| LDEF | Long Duration Exposure Facility |
| LED | light-emitting diode |
| LPSP | Laboratoire de Physique Stellaire et Planetaire |
| MBB | Messerschmitt–Bölkow–Blohm GmbH |
| MOS | metal oxide silicon |
| OCLI | Optical Coating Laboratory, Inc. |
| ONERA | Office National d'Etudes et de Recherches Aérospatiales |

| | |
|---|---|
| OSR | optical surface reflection |
| PCM | phase change material |
| PIN | refers to structure of device |
| QCM | quartz crystal microbalance |
| RMS | remote manipulator system |
| SAA | South Atlantic anomaly |
| SEM | scanning electron microscopy |
| SGEMP | system-generated electromagnetic pulse |
| SH | superheavy |
| SIMS | secondary ion mass spectroscopy |
| STS | Space Transportation System |
| TLD | thermoluminescent dosimeter |
| TEM | transmission electron microscopy |
| THERM | thermal measurement system |
| TTF–TCNQ | tetrathiofulvalene tetracyanoquilodiaethane |
| u | ratio of total kinetic energy of particle, MeV, to atomic mass of particle |
| UV | ultraviolet |
| VCHP | variable-conductance heat pipe |
| Z | nuclear charge |
| $\beta$ | ratio of particle velocity to speed of light |

| 1. Report No. NASA SP–473 | 2. Government Accession No. | 3. Recipient's Catalog No. | | |
|---|---|---|---|---|
| 4. Title and Subtitle LONG DURATION EXPOSURE FACILITY (LDEF) MISSION 1 EXPERIMENTS | | 5. Report Date February 1984 | | |
| | | 6. Performing Organization Code 542–04–13–02 | | |
| 7. Author(s) Lenwood G. Clark, William H. Kinard, David L. Carter, Jr., and James L. Jones, Jr. | | 8. Performing Organization Report No. L–15230 | | |
| | | 10. Work Unit No | | |
| 9. Performing Organization Name and Address NASA Langley Research Center Hampton, Virginia 23665 | | 11. Contract or Grant No | | |
| | | 13. Type of Report and Period Covered Special Publication | | |
| 12. Sponsoring Agency Name and Address National Aeronautics and Space Administration Washington, DC 20546 | | 14. Sponsoring Agency Code | | |
| 15. Supplementary Notes | | | | |

16. Abstract

The experiments on the first mission of the Long Duration Exposure Facility are described. The LDEF launch is currently scheduled for STS-13 in early April 1984 with retrieval approximately 12 months later on a subsequent Shuttle flight. The LDEF has been designed to provide a large number of economical opportunities for science and technology experiments which require modest electrical power and data processing while in space and which benefit from postflight investigations with the retrieved hardware. In fact, many of the experiments are completely passive and depend on postflight laboratory investigations for the experiment results. The experiment complement on the first LDEF mission includes 57 experiments from the United States and eight other countries. The experiment disciplines covered include materials, coatings, thermal systems, power, propulsion, astrophysics, lunar and planetary sciences, life sciences, electronics, and optics.

| 17. Key Words (Suggested by Author(s)) Long-Duration Exposure Facility LDEF Space Shuttle Space experiments | 18. Distribution Statement Unclassified–Unlimited Subject Category 15 |
|---|---|

| 19. Security Classif. (of this report) Unclassified | 20. Security Classif. (of this page) Unclassified | 21. No. of Pages 197 | 22. Price<sup>a</sup> A09 |
|---|---|---|---|